INFORMATION TO USERS

This manuscript has been reproduced from the microfilm master. UMI films the text directly from the original or copy submitted. Thus, some thesis and dissertation copies are in typewriter face, while others may be from any type of computer printer.

The quality of this reproduction is dependent upon the quality of the copy submitted. Broken or indistinct print, colored or poor quality illustrations and photographs, print bleedthrough, substandard margins, and improper alignment can adversely affect reproduction.

In the unlikely event that the author did not send UMI a complete manuscript and there are missing pages, these will be noted. Also, if unauthorized copyright material had to be removed, a note will indicate the deletion.

Oversize materials (e.g., maps, drawings, charts) are reproduced by sectioning the original, beginning at the upper left-hand corner and continuing from left to right in equal sections with small overlaps.

Photographs included in the original manuscript have been reproduced xerographically in this copy. Higher quality 6" x 9" black and white photographic prints are available for any photographs or illustrations appearing in this copy for an additional charge. Contact UMI directly to order.

ProQuest Information and Learning
300 North Zeeb Road, Ann Arbor, MI 48106-1346 USA
800-521-0600

UMI®

Université d'Ottawa · University of Ottawa

REMOVAL OF ORGANICS FROM WATER/WASTEWATER BY MEMBRANE AIR STRIPPING

Hassan Mahmud

A thesis submitted to the School of Graduate Studies and Research
in partial fulfillment of the requirements for the
degree of
DOCTOR OF PHILOSOPHY
in
Chemical Engineering
(Specialization: Environmental Engineering)
in the Department of Chemical Engineering
University of Ottawa

August, 2001

To my late father and mother Dr. J. Buksh and Mrs. Zuhura Khatoon.

ABSTRACT

Removal and recovery of volatile organic compounds (VOCs) from industrial wastewater and groundwater has become increasingly important due to stringent environmental regulations. Membrane air-stripping (MAS), using microporous polypropylene hollow fiber membrane modules, is one of the most promising processes for this purpose. The mass transfer of water and VOCs in MAS was studied using such a module, with air-flow on the lumen side and liquid cross-flow on the shell side. Chloroform, toluene and their mixture were used as model VOCs.

Water transport experiments showed that mass transport was significantly decreased when the membrane had been in contact with water for prolonged periods. It was hypothesized the increased mass transfer resistance was due to water condensation in a fraction of the membrane pores. MAS of chloroform from aqueous solutions confirmed the additional mass transfer resistance with prior exposure to water. It was concluded that membrane pores were completely air-filled at the start and became partially wetted with water after prolonged period during the MAS process. The currently existing models are able to predict the performance only for either completely air-filled or liquid-filled pores. A modification of an existing model was proposed to take into account diffusion through the partially water-filled pores, as well as the partially air-filled pores. It was found that the model predictions agreed well with the experimental data. This hypothesis also provided a plausible explanation for the conflicting literature values of the membrane mass transfer resistance. It was also found that the membrane mass transfer resistance of the partially water-filled pores was two orders of magnitude higher than that of air-filled pores.

Lévéque's (1928) correlation overestimates the local mass transfer coefficient in a cylindrical tube at low velocities. A modification of this correlation has been proposed to predict the local air film mass transfer coefficient at low air velocities. The proposed correlation predictions matches well with the experimental data.

The overall mass transfer coefficients of chloroform obtained in this work for liquid cross-flow on the shell side were up to twice as high as those reported in the literature, even though our experiments were carried out at much lower water and air velocities. However, the air pressure drop on the lumen side was significantly higher than that for system with air flow on the shell side. The overall mass transfer coefficients did not change when the initial chloroform concentration in the feed ranged from 81 to 908 ppm. MAS process was found effective in concentrating chloroform to more than 90% from a feed aqueous solution of ppm levels.

The adsorption of toluene had strong detrimental impact on the performance of the polypropylene hollow fiber module. It is hypothesized that the toluene sorption resulted in swelling of the polypropylene fibers causing a reduction of the effective pore diameter and as a result of this, the toluene transport was substantially lower than expected. Due to this effect, the presence of toluene in the binary aqueous solution with chloroform significantly reduced the mass transport of chloroform compared to that with only chloroform.

Henry's law constants were determined for individual chloroform and toluene as well as for their mixtures at 23°C and are reported. The effect of initial chloroform concentrations on Henry's law constant was experimentally examined.

RÉSUMÉ

L'enlèvement ainsi que la récupération de composés organiques volatiles (COV) des eaux usées de provenance industrielle ou sous-terraine est en importante croissance en raison des lois environnementales de plus en plus contraignantes. Un procédé des plus prometteur pour cette application est le "membrane air-stripping" (MAS), utilisant des modules composés de membranes en fibre creuses de polypropylène. Le transfert de masse de l'eau et des COV dans le MAS a été étudié à l'aide de ces modules avec le débit d'air du côté du "lumen" et le débit d'eau du côté de la coquille. Le chloroforme, le toluène et leurs mélanges ont été utilisés comme modèles de COV.

Des expériences menées sur le transport de l'eau ont démontré une baisse significative du transport de la masse après que la membrane ait été en contact avec de l'eau pour des périodes prolongées. L'hypothèse a été avancée que la résistance au transfert de masse soit due à la condensation dans une fraction des pores de la membrane. Le MAS du chloroforme en solution aqueuse a confirmé la résistance additionelle au transfert de masse suite à une exposition préalable à l'eau. Nous en avons conclu que les pores de la membrane étaient complètement remplis d'air au départ et sont devenus partiellement mouillés avec de l'eau durant le précédé MAS. Les modèles présentement existants ne sont capables de prédire la performance des pores que lorsqu'ils sont entièrement et uniquement remplis soit d'eau ou d'air. Une modification d'un des modèles existants a été proposée pour tenir compte de la diffusion au travers de pores partièlement remplis aussi bien d'eau que d'air. Nous avons établi que les prédictions de ce modèle sont en accord avec les résultats obtenus expérimentalement. Cette hypothèse a aussi fourni une explication plausible quant aux valeurs conflictuelles relevées dans la littérature concernant la résistance au transfert de masse. Nous avons également déterminé que la résistance de la membrane au transfert de masse était de deux fois supérieure dans le cas de pores partièllement remplis d'eau en comparaison à l'air.

La corrélation établie par Lévéque (1928) surestime le coefficient de transfert de masse local à basse vitesse dans un tube cylindrique. Une modification apportée à cette

correlation est proposée pour prédire le coefficient de transfert de masse local air film à basses vitesses de l'air. Les prédictions de corrélation proposées correspondent bien aux résultats expérimentaux obtenus.

Les coefficients de transfert de masse globaux obtenus pour le chloroforme dans le cadre de nos travaux sur le débit de liquide du côté coquille étaient de deux fois supérieurs à ceux rapportés dans la littérature scientifique et celà même si nos expériences étaient pratiquées à des vitesses de l'air et de l'eau beaucoup plus basses. Cependant, la baisse de pression du côté "lumen" était significativement supérieure à celle d'un système avec débit d'air du coté coquille. Les coéfficients de transfert de masse n'ont pas changé, quand les concentrations initiales de chloroforme dans la solution d'alimentation variaient de 81 à 908 ppm. Le procédé MAS a été trouvé efficace pour concentrer le chloroform à plus de 90% de la solution aqueuse de départ et celà à des niveaux de ppm.

L'adsorption du toluène a eu un impact très néfaste sur la performance du module de filtration avec fibre de polypropylène. Une hypothèse a été émise que l'adsorption du toluène a entraîné le gonflement des fibres de polypropylène causant ainsi une réduction du diamètre des pores et, en consequence, conduisant à une baisse plus importante que prévue du transport de toluène. En raison de cet effet causé par le toluène, le transport de chloroforme dans un système binaire chloroforme-toluène s'en est trouvé également affecté à la baisse comparativement à un système uniquement composé de chloroforme.

Les constantes de la loi de Henry ont été déterminées pour le chloroforme, le toluène ainsi que leurs mélanges et celà à 23°C. L'effet des concentrations initiales de chloroforme sur la constante de Henry a été étudié expérimentalement.

ACKNOWLEDGMENTS

I would like to thank the Almighty, the Creator of the Universe, Who knows everything that we know till now and we do not know yet. He has given me the strength and patience to complete this research.

I wish to express my sincere appreciation and gratitude to my supervisors Prof. Takeshi Matsuura, Department of Chemical Engineering and Prof. Roberto M. Narbaitz, Department of Civil Engineering, University of Ottawa, and Dr. Ashwani Kumar, Group Leader, Institute of Chemical Process and Environmental Technology (ICPET), National Research Council of Canada (NRC), Ottawa, for their invaluable guidance, constructive criticism and continued encouragement throughout the course of this study and in the preparation of this thesis. Thanks are also due to Mauro Dal-Cin, Research Officer, ICPET, NRC for his invaluable advice from time to time. I am grateful to Serge Croteau, Carolyn Lick and Steven Argue, Technical Officers, ICPET, and Peter L'Abbe, Technical Officer, Optics, Institute of National Measurement and Standard, NRC, Ottawa, for their help during this study.

Finally, I should thank my wife and lovely daughters for their patience.

I also wish to thank ICPET, NRC for the partial financial support. The financial support in the form of Ontario Graduate Scholarships from the Government of Ontario and Excellence Scholarships and Teaching/Research Assistantships from the University of Ottawa are gratefully acknowledged.

PUBLICATIONS

- Mahmud, H., A. Kumar, R. M. Narbaitz and T. Matsuura, (2000), "A Study of Mass Transfer in the Membrane Air-Stripping Process Using Microporous Polypropylene Hollow Fibers", *J. Membrane Science*, vol. 179, No. 1-2, pp. 29-41.

- Mahmud, H., A. Kumar, R. M. Narbaitz and T. Matsuura, (1998), "Membrane Air Stripping: A Process for Removal of Organics from Aqueous Solutions", *Separation Science and Technology*, vol. 33, No. 14, pp. 2241-2255.

NOMENCLATURE

List of symbols

a = surface to volume ratio, m^2/m^3
A = empirical constant
B = empirical constant
B_0 = empirical constant
B_1 = empirical constant
BAT = best available technology
C = concentration of the component of concern in the liquid phase at distance z, ppm
C^* = liquid phase concentration that would be in equilibrium with the air phase concentration, g/m^3 or ppm.
C_{aa} = concentration of the VOC in the system after adsorption, ppm
C_{ba} = concentration of the VOC in the reservoir before adsorption, ppm
C_f = final concentration of the loss test after 24 hours, ppm
C_i = initial concentration of the loss test, ppm
C_{in} = concentration in the aqueous influent ($z = 0$), ppm
C_o = estimated initial concentration of the VOC in the liquid phase after loss, ppm
C_{out} = concentration in the aqueous effluent ($z = L$), ppm
C_t = VOC concentration in the reservoir at time t, ppm
C_0 = VOC concentration in the reservoir at time 0, ppm
C_1 = measured initial concentration, ppm
C.I. = confidence interval
CLASP= closed loop air-stripping process
d_i = inner diameter of the hollow fiber, m
d_o = outer diameter of the hollow fiber, m
d_p = pore diameter, m
D_w = diffusion coefficient of compound in water, m^2/s
D_c = continuum diffusion coefficient of compound in air phase, m^2/s
D_c^w = continuum diffusion coefficient of water in air phase, m^2/s
D_{eff}^w = effective diffusion coefficient of water in air, m^2/s
D_{eff} = effective diffusion coefficient of compound in air, m^2/s
D_{Kn} = Knudsen diffusion coefficient of compound in air, m^2/s
GAC = granular activated carbon
GC(P&T) = gas chromatograph (Purge & Trap)
GC6890= gas chromatograph (HP 6890 series)
Gr = Graetz number ($\frac{Pe.d_i}{L}$)
H = dimensionless Henry's Law constant
H_d = dimensional Henry's law constant, atm
ΔH^0 = enthalpy change due to dissolution of component in water ($joules.mol^{-1}$)

h = length of the hollow fiber module compartment (0.5 L), m
HLC = Henry's law constant
IC = inorganic carbon
J = empirical constant
K_L = overall liquid-phase based mass transfer coefficient, m/s
K_G^w = overall gas-phase based mass transfer coefficient for water, m/s
k = rate constant, min^{-1}
k_m^w = mass transfer coefficient due to membrane for water, m/s
k_a = local air-phase mass transfer coefficient, m/s
$\bar{k}_a$ = average local air-phase mass transfer coefficient, m/s
k_a^w = local air-phase mass transfer coefficient for water, m/s
k_L = local liquid-phase mass transfer coefficient, m/s
$\bar{k}_L$ = average local liquid-phase mass transfer coefficient, m/s
k_m = membrane mass transfer coefficient, m/s
$K_L a$ = overall volume specific mass transfer coefficient, h^{-1}
L = hollow fiber length, m
MAS = membrane air-stripping
MW_1 = molecular weights of the compound, g/mole
MW_2 = molecular weights of air, g/mole
n = number of fibers
n_s = number of samples
Pe = Peclet number ($d_i v^w / D_w$)
p_p = partial pressure of the component, atm
PP = polypropylene
P_T = total pressure, atm
PTFE = polytetrafluoroethylene
p_v = vapor pressure of the component, atm
ΔP = breakthrough pressure, kPa
ppb = parts per billion
ppm = parts per million
PTA = packed-tower aeration
Q_a = air flow rate, m^3/s
Q_w = water flow rate, m^3/s
q = exponent
R = stripping factor = $Q_w/Q_a H$
R_c = universal gas constant, (8.314 4 abs. Joules.deg^{-1}.mol^{-1})
Re = Reynolds number ($d_o v^w / \nu$)
r = pore radius, m
r_c = module radial position ($r_{in} < r_c < r_{out}$, in Fig. 5.2), m
r_{in} = outer radius of the center tube, m
r_{out} = inner radius of the membrane module, m
S = dimensionless Raoult's law constant for water
Sh = Sherwood number ($\frac{k d_o}{D_w}$)

$\overline{Sh}$ = average Sherwood number

Sc = Schmidt number ($\frac{\nu}{D_w}$)

t = time, s

T = temperature in Kelvin, °K

TC = total carbon

TOC = total organic carbon

TCE = trichloroethylene

u^a = air velocity outside the hollow fiber, m/s

u^w = aqueous solution velocity outside the hollow fiber, m/s

u' = average velocity within the module without hollow fibers, m/s

V_a = volume of the air, m^3

V_L = volume of the liquid, m3

V_T = total volume of solution in the system, m^3

V_w = reservoir volume, m^3

V_{il} = diffusion volumes of the parts of compound, cm^3/mole

$\sum V_{il}$ = diffusion volumes of the compound, cm^3/mole

$\sum V_{i2}$ = diffusion volumes of air, cm^3/mole

v^a = air velocity inside the hollow fiber, m/s

v^w = aqueous solution velocity inside the hollow fiber, m/s

VOC = volatile organic compound

X = mass concentration of the component in the air phase, g/m^3 or ppm

X_{in} = organic concentration in incoming air at $z = L$, ppm

$\frac{dX^w}{dz}$ = water vapor concentration gradient along length of fiber lumen, ppm/m

X^w = water vapor concentration in the air phase at distance z, ppm

X_L^w = water concentration in the stripping air at the exit of the membrane module, ppm

X_{sat}^w = saturated water vapor concentration, ppm

x = fraction of the pore filled with air

$1-x$ = fraction of the pore filled with water

Y = mole fraction of the component in the gas phase, mole/mole

Y^* = mole fraction of the component in the liquid phase in equilibrium with the gas phase, mole/mole.

z = distance from hollow fiber inlet, m

Greek Letters

γ_c = critical surface tension of a solid, N/m

γ_d = surface tension at detachment, N/m

γ_L = surface tension of a liquid, N/m

δ = pore length, m

ε = fiber porosity (dimensionless)

θ = contact angle, degree

μ = micro
ν = kinematic viscosity of air/water, m^2/s
τ = pore tortuosity (dimensionless)
ω = coefficient of variation for the fiber radius measurements

TABLE OF CONTENTS

LIST OF TABLES

LIST OF FIGURES

CHAPTER 1

Introduction

1.1 MOTIVATION

An estimated 1.6 to 5.0 billion kg of volatile organic compounds (VOCs) enter the environment each year in U.S.A. only (Ehrenfeld and Ong, 1986) and cause a significant pollution burden. These VOCs mainly contaminate groundwater and industrial wastewater. Contamination of water supplies by VOCs is a recognized problem (Clark et al., 1984; Dyksen and Hess, 1982). This contamination could be attributed to one or more of the following sources: improper disposal of common industrial solvents, leaking storage tanks, municipal or industrial landfill leachates and others. Although contaminated groundwater normally contains parts per billion (ppb) levels of VOCs, even these levels render them unfit for human consumption. Cleanup of these contaminated groundwater aquifers is difficult, expensive and very slow. Additionally, contamination of drinking water by halogenated hydrocarbons, produced as by-products of chlorination is a concern. There are many different types of industrial wastewater that contain ppb to ppm levels of VOCs. These VOCs are wasted resources that could be recovered for reuse. Furthermore, removal and recovery of VOCs from industrial wastewater and groundwater has become increasingly important due to stringent environmental regulations. Conventional treatment methods have some limitations (Goethaert et al., 1993). Membrane air-stripping (MAS) is a relatively new and developing technology for such

applications. Although MAS has been studied only at bench scale so far, it has shown great potential to minimize the pollution caused by VOCs (Mahmud et al., 1998). MAS research had focussed mainly on microporous polypropylene hollow fiber membrane modules, wherein the contaminated aqueous solution was pumped through the lumen side while the stripping air was allowed to flow on the shell side (Mahmud et al., 1998). Furthermore, most of these studies were concentrated on the removal of halogenated aliphatic hydrocarbons normally encountered in contaminated ground/drinking water at parts per billion (ppb) concentration levels.

In the MAS process, the membrane is used to provide a contact between the contaminated water and stripping air at the interface of air-filled pores on the liquid side without direct mixing. Water would not normally wet the air-filled pores of the hydrophobic membrane (Kiani et al., 1984; Semmens et al., 1989). Mass transfer (diffusion) of the VOCs occurs across the membrane barrier from the liquid to the air and the VOCs are swept away by stripping air. In the MAS process mass transfer comprises of three sequential steps (Semmens et al. 1989; Yang and Cussler, 1986) involving VOC diffusion from the bulk solution across the liquid boundary layer to the membrane surface, diffusion through the air-filled pores and finally diffusion through the air boundary layer outside the membrane pore into the stripping air. The overall liquid-phase based mass transfer coefficient (K_L) observed for MAS is usually lower than that for conventional air-stripping processes probably due to the mass transfer resistance ($\frac{1}{k_m H}$) created by the membrane itself (Kiani et al., 1984; and Yang and Cussler, 1986). There are also conflicting views

regarding the role of membrane mass transfer resistance for air-filled pores (Yang and Cussler, 1986; Semmens et al. 1989; Kreulen et al., 1993; Qi and Cussler, 1985c).

1.2 OBJECTIVES OF THIS RESEARCH

Objectives of this research were determined based on the research needs identified after a critical review of the literature. This review revealed that:

- A more thorough investigation of MAS systems with the stripping air-flow through the lumen side and aqueous solution flow through the shell side is required, as opposed to the conventional reverse operation.
- Further studies are also needed with other VOCs of alicyclic and aromatic groups for their importance as pollutants.
- Furthermore, the use of these membranes for treatment of wastewater containing higher VOC concentration levels also needs investigation.
- The transport mechanism of the VOCs from the aqueous phase to the air phase through the membrane pores requires an in-depth investigation to gain a better understanding of the solute transport mechanism to address current contradictory views regarding the role of membrane mass transfer resistance for air filled pores.
- Predictability of the existing local mass transfer correlations needs further verification for this system.

The results of these investigations may provide a new approach for the treatment of VOCs laden industrial wastewater streams. The specific objectives of this study are:

1. To investigate the performance of microporous polypropylene hollow fiber membrane modules for the removal of VOCs from aqueous solution, by changing the air flow from the shell side to the lumen side and liquid flow from the lumen side to the shell side in order to determine its effect on the overall mass transfer coefficient and on the air side pressure drop.
2. Determine the contribution of mass transfer resistance due to the membrane.
3. Investigate membrane air-stripping of two VOCs from the aqueous phase to the air phase, with VOC concentrations in the aqueous solution in the range of 50 to 1050 ppm (as is usually found in industrial wastewater).
4. Study membrane air-stripping of a binary aqueous mixture of VOCs.
5. Verify the applicability of the existing mass transfer correlations.
6. Determine the Henry's law constants for the individual compounds as well as of mixtures at the temperature of the experiments.

1.3 ORIGINALITY OF THE RESEARCH

The salient points addressed in the thesis are summarized below:

- MAS of water was tested to investigate the role of membrane mass transfer resistance for polypropylene hollow fiber membranes for the first time.
- Investigations were conducted for the first time on removal/recovery of VOCs at the ppm range of concentration from the aqueous solutions; this concentration was 1000 times higher than that conventionally studied and reported so far for these membranes.

- Detailed investigations were conducted on MAS of toluene at ppm concentration levels from the aqueous solutions for the first time.
- Investigations were conducted on MAS of a mixture of chloroform and toluene from the aqueous solutions at ppm concentration levels to ascertain the effect of the presence of one compound on other compound during MAS. Such data were not found in the literature.
- A model was developed to predict diffusion through the partially water-filled pores, as well as the partially air-filled pores.
- A model has been proposed to predict the local mass transfer resistance at low air/gas velocities in cylindrical tubes. No model specific to this range was found in the literature.
- A new economical laboratory-scale batch system was designed to operate without headspace to avoid error during experiments with VOC laden water/wastewater.

1.4 CONTRIBUTION TO SCIENCE AND TECHNOLOGY

The contributions to the field of chemical engineering, membrane separation science technology and environmental engineering are expected to be as follows:

- The findings of this study will provide a better understanding of the role of membrane mass transfer resistance in MAS applications using polypropylene hollow fiber modules.
- The effect of operating period will elucidate and explain the wide discrepancies among MAS mass transfer coefficients reported in the literature.

- Demonstration of the effect of adsorption/swelling of toluene on the mass transfer performance of polypropylene hollow fibers will be of great use during MAS design.
- The correlation developed for the prediction of membrane mass transfer resistance for diffusion of VOC through the partially water-filled pores, as well as the partially air-filled pores will provide better tools for design.
- Modification of Lévéque's (1928) correlation for the prediction of local air-phase mass transfer resistance at low air velocities in a cylindrical tube will better describe the experimental data.
- The knowledge base of MAS will be expanded by demonstrating the impact of changing the flow of air from the shell side to the lumen side, compared to the conventional approach of having the VOC laden aqueous solution on the lumen side.
- Demonstration of the feasibility of recovering VOC in a relatively pure and concentrated form from dilute aqueous solutions by MAS will benefit many industries.
- Development of a new economical laboratory-scale batch system capable to operate without headspace will provide researchers with an easy tool for investigation of VOC laden water/wastewater.
- The results from the investigation on the effect of chloroform concentration in the range of 20 to 900 ppm on the Henry's law constant will expand the viability of the applicability of Henry's law constant at a wider range of concentration.

CHAPTER 2

Literature Review: Technological Options

This chapter compares the conventional technologies for removal/recovery of VOC from aqueous solution with the proposed technology (MAS). It also outlines the advantages and disadvantages of each technology. After a critical review of the literature, the research needs in the area of the proposed technology are also identified in this chapter.

2.1 CURRENT TECHNOLOGIES FOR VOC REMOVAL FROM AQUEOUS SOLUTIONS

Conventional treatment methods for removal and recovery of volatile organics include air stripping, adsorption, advanced oxidation, anaerobic/aerobic biological methods and distillation. All these techniques, in general, have at least one major disadvantage (Goethaert et al., 1993). Liquid-phase adsorption is economical only at low VOC concentrations due to the high cost of adsorbent replacement and/or regeneration; as well as possibly the need to dispose of the spent adsorbent, which may be considered a hazardous waste. On the other hand, distillation is economical only at higher VOC concentrations. The effectiveness of advanced oxidation is compound dependent and it can form new products that could be more harmful than the original ones. Some of these techniques also result in release of gaseous VOC emissions thereby transferring the contaminants to another phase only (Brewer, 1991). Among conventional techniques, packed-tower aeration (PTA) is the most economical and hence the most widely used

process for removal of ppb levels of VOCs from water. The US Environmental Protection Agency (USEPA, 1990) considered it the best available technology (BAT) for removal of VOCs from drinking water. However, the contaminants are simply transferred from the water to the air phase during the stripping process and the exhaust air may require further treatment before being released to the atmosphere. When local regulations require off-gas treatment, gas-phase granular activated carbon (GAC) adsorption is generally employed to control the gas phase emissions from PTA. Gas phase GAC adsorption of off-gases has several limitations. The contaminants are once again transferred from the gas to the solid phase only. The presence of moisture in exhaust stripper air competes with VOCs for adsorption sites on the GAC, thus reducing their effective adsorption capacity for VOCs and increasing GAC usage. The regeneration or disposal of the contaminated GAC is costly and adds significantly to the overall cost of VOC removal from contaminated water (Kosuko et al., 1988; McGregor et al., 1988). Although air stripping with off-gas treatment is much more expensive than air stripping alone, their combined cost is comparable to those of liquid-phase GAC adsorption (Dvorak et al., 1993). As the contaminated sites are often located in urban centers, tall PTA towers are sometimes considered aesthetically undesirable and more compact alternative technologies are selected.

Aerobic biological processes are also gaining importance for removal of organics from contaminated water; however, a part of the VOCs is air stripped during the biodegradation process (Freitas dos Santos, 1995). The end products of this process are

mainly carbon dioxide and biomass. As a result, carbon dioxide increases in the atmosphere and contributes to global warming, which is of great concern.

2.2 MEMBRANE AIR-STRIPPING PROCESS

Separation of VOCs from liquid streams by membrane air-stripping (MAS) is being considered as an alternative that may overcome some of the shortfalls of PTA. Although, like PTA, membrane air-stripping transfers contaminants from one phase to another phase, treatment of the stripped air is much easier (Bhowmick and Semmens, 1994), because it uses significantly less air (Zander et al., 1989a). Membrane air-stripping may be used over a wide range of VOC concentration levels. MAS could be useful for water pollution reduction and groundwater cleanup.

The MAS process is characterized by the imposition of a hydrophobic microporous membrane between contaminated water and a stripping air phase. In this process, the membrane is used only to provide intimate contact between the two phases at the interface of the air-filled membrane pores without direct mixing. No selective characteristics are required for the membrane except high surface hydrophobicity. Due to the latter characteristic, water would not normally wet the membrane pores and consequently, the pores would be filled with air (Kiani et al., 1984; Semmens et al., 1989). Hydrophobicity is further discussed in Section 2.2.3. A MAS system, consisting of one or more membrane module(s), is used in conjunction with contaminated water and stripping air supply systems. The contaminated water is pumped across one side of the membrane while clean stripping air is blown counter or co-currently on the other side of

the membrane. Mass transfer of the contaminants occurs across the membrane barrier from the liquid side to the air side and is removed by the stripping air flow. The pressure of the aqueous (non-wetting) phase needs to be higher than that of the air (wetting) phase to prevent air coming into the aqueous phase.

In packed-tower air stripping, mass transfer of VOCs from the liquid phase to the air phase takes place through intimate direct contact between the two phases, while in membrane air stripping, mass transfer occurs at the interface of the mouth of the air-filled membrane pores at the liquid side. The concentration gradient between the two phases acts as the driving force for this transfer. The concentration gradient is maintained by constantly sweeping away the VOCs crossing the barrier into the stripping air, thereby maintaining an essentially near zero VOC concentration on the stripping side.

2.2.1 Advantages and Disadvantages

Some advantages of membrane air stripping over conventional packed tower air stripping are (Reed et al., 1995): a) higher surface to volume ratio resulting in more compact installations; b) no loading and flooding limitations; c) no channeling; and d) reduction of dispersed phase back mixing. In addition to the above operational advantages, the modular nature of membrane air stripping drastically reduces technical scale-up problems (Guha et al., 1993).

A major disadvantage of the MAS systems is that the overall mass transfer coefficient (K_L) for membrane air-stripping is usually lower than that for conventional processes

due to the mass transfer resistance created by the membrane (Yang and Cussler, 1986; Kiani et al., 1984). However, the membrane modules, especially hollow fiber configurations, provide much higher effective surface to volume ratios (a) than packed towers. They are as high as 8,000 m^2/m^3 (Matson et al., 1983) compared to maximum of 800 m^2/m^3 for bubble columns, sieve trays or packed beds (Laurent and Charpentier, 1974). As a result, the value of $K_L a$ (overall volume specific mass transfer coefficient) is much higher for membrane systems than that for conventional processes. Thus, the overall volume specific rate of stripping (mass of contaminants removed per unit time per unit volume of process equipment) for a membrane unit is likely to be several times larger than that for conventional PTA treatment systems. Zander et al. (1989a) have reported that the value of $K_L a$ measured for hollow fiber membrane air stripping systems were at least one order of magnitude greater than those for packed towers. In addition to higher overall mass transfer resistance, a high air pressure drop on the shell side in the hollow fiber module may increase the energy cost for a full-scale system (Zander et al., 1989a). It should be noted that the modules tested by Zander et al. (1989a) were designed primarily for medical purposes and their design had not been optimized for industrial use. Although the modular nature of the membrane makes scale-up technically easy, the economics of scale-up are not as attractive as those for other technologies.

2.2.2 Membrane Materials, Membranes and Module Configurations

The choice of microporous membranes for certain processes are made mainly based on their pore sizes. However, this approach may not be adequate for MAS and require consideration of the membrane materials. There is very little information in the literature

on possible materials that can be used in the preparation of membranes for membrane air stripping of organics from aqueous solutions. Only a few types of polymeric membranes have been tested for the purpose. Matson (1992) stated that 1) polymeric membranes of silicone rubber and its various copolymers e.g., the block polymer formed from polydimethylsiloxane and polycarbonate; or 2) microporous membranes prepared from low surface energy polymers such as polytetrafluoroethylene (PTFE) and polypropylene (PP) should be suitable for membrane air-stripping. Microporous membranes made from polymers of highly hydrophobic surface that provide non water-wettable pores, should be effective in VOCs removal from aqueous solutions. The choice of hydrophobic materials will also depend on the characteristics of the organic solutions and their interaction with or damaging capabilities to the membrane material (Kiani et al., 1984).

Two types of membrane configurations have been tested so far for membrane air stripping: a) microporous flat membrane in plate and frame modules and b) microporous hollow fiber membrane modules. Both configurations have some advantages and disadvantages. However, membrane efficacy requires a large contact surface area (Kesting, 1971; Matsuura, 1993). Given the higher surface to volume ratio of the hollow fiber membrane configuration and its compactness, it is a better choice. The membrane geometry does influence the rate of mass transfer through its porosity and thickness (Kiani et al., 1984). Mass transfer coefficients for polypropylene hollow fibers have been reported as being inversely proportional to the membrane thickness for liquid-filled pores (Qi and Cussler, 1985c).

Due to their surface hydrophobicity, high chemical resistivity and low cost (Kroschwitz, 1985), polypropylene or silicon coated polypropylene hollow fiber membranes have been widely investigated and become membranes of choice for the removal of VOCs from water by membrane air-stripping (Semmens et al., 1989; Zander et al., 1989a; Bhowmick and Semmens, 1993, 1994; and Castro and Zander, 1995).

2.2.3 Membrane Surface Hydrophobicity and Its Role in Membrane Air-Stripping Process

Hydrophobicity of a solid material is usually expressed in terms of a contact angle (θ) or a critical surface tension (Keurentjes et al., 1989). The most widely used method for determination of the contact angle of a liquid on a surface is a direct measurement of θ using a sessile drop of the liquid on the surface. The critical surface tension of a solid (γ_c) is defined as the surface tension (γ_L) at which the contact angle of a liquid just vanishes on that solid (Fox and Zisman, 1950; Zisman, 1964):

$$\gamma_c = lim\,(\theta \rightarrow 0)\,\gamma_L \qquad (2.1)$$

where:
γ_c = critical surface tension of a solid, N/m
θ = contact angle, degrees
γ_L = surface tension of a liquid, N/m

Usually, θ is measured on a surface using different liquids or mixtures of two liquids having different surface tensions. If $\cos\theta$ versus the surface tension of the liquid is plotted (Zisman plot), extrapolation to $\cos\theta = 1$ gives the critical surface tension γ_c (Zisman, 1964).

In order to measure θ accurately, a homogenous and ideally smooth surface of a dense film of the material is required. Due to the surface roughness and capillary forces due to the presence of pores in a membrane, the observed contact angle may differ significantly from the real contact angle. Keurentjes et al. (1989) developed a sticking bubble technique for the measurement of membrane hydrophobicity and partially overcame these limitations. The surface tension measured by this method is expected to be less affected by the presence of pores. The membrane is submerged in liquids of different surface tensions. Air bubbles are attached to the membrane and the reference surface tension at detachment (γ_d) for the membrane is the one at which the air bubble detaches from the membrane with a 50% probability. Keurentjes et al. (1989) found γ_d and γ_c (reported critical surface tension for the polymer) were in good agreement for polypropylene microporous membranes.

In the MAS process, hydrophobicity of the membrane surface plays a very important role. Due to this characteristic, the pores are not wetted by the dilute aqueous solution of VOCs and therefore should be filled with air. The aqueous phase requires a certain minimum pressure (breakthrough pressure) to force itself into and through the membrane pores. The breakthrough pressure for a membrane depends on the pore-size, the surface tension of the liquid and the contact angle of the non-wetting phase on the membrane (Tirmizi et al., 1996) and can easily be determined by the following Young-Laplace equation:

$$\Delta P = -\frac{2\gamma_L \cos\theta}{r} \qquad (2.2)$$

where:
ΔP = breakthrough pressure, kPa
r = pore radius, μm

Using this equation, the characteristics of a membrane for MAS process can be predetermined. Tirmizi et al. (1996) investigated applicability of the Young-Laplace equation to polypropylene hollow fibers having pore sizes of 0.05, 0.1 and 0.2 μm. They observed a linear relationship between breakthrough pressure and $-\gamma_L \cos\theta$ up to a certain pressure. It was also reported that this linear relationship held up to 100 kPa for pore radius of 0.2 μm and the slope of this plot successfully predicted the pore size of the membrane (as 0.203 μm) using the Young-Laplace equation. In order to prevent the membrane from getting wet, the pressure of the aqueous (non-wetting) phase needs to be lower than the breakthrough pressure (Kim and Harriott, 1987; Sirkar, 1992). On the other hand, the aqueous (non-wetting) phase pressure needs to be higher than that of the air (wetting) phase to prevent air from entering the aqueous phase.

2.2.4 Effect of pH, Ozone and Chlorine on Polypropylene Membranes

The effect of pH, ozone and free chlorine on microporous polypropylene hollow fiber membranes has been investigated by Castro and Zander (1995) using an aqueous mixture of chloroform, bromoform, bromodichloromethane and dibromochloromethane as feed. They showed that these membranes were compatible with waters with a below neutral pH (pH 5 to 7) and low chlorine concentration but not with waters with a higher pH (>7) or high chlorine (≥15 ppm) concentrations. At high pH, these membranes exhibited a marked reduction in performance, lower membrane bubble pressures and a reduction in

pore area. Water with high pH requires pretreatment prior to use with these membranes. At high chlorine concentrations, there was no substantial reduction in performance but a reduction in pore area and damage to the epoxy potting material were reported. These membranes were also found not to be suitable for treating waters containing ozone.

2.2.5 Influence of Packing Density

Zander et al. (1989a) observed that the air pressure drop at the shell side across hollow fiber membrane modules was much higher than that for packed towers. The packing density of the hollow fiber in the modules was thought to be the cause for this high pressure drop. Based on data obtained from three hollow fiber modules with different packing densities, Schwarz et al. (1991) concluded that packing density might not be the only cause for this pressure drop. Proper design of the bundle to prevent fiber blockage at the exit port and eliminating major headloss across the air ports may help reduce the pressure drop. The influence of packing density on the removal of 1,1,2-trichloroethane, trichloroethylene and carbon tetrachloride from aqueous mixtures has been studied using modules with three different fiber densities (Schwarz et al., 1991). The authors could not come to any conclusion as to the variation in removal rates for the three different packing densities because the differences were within the limit of experimental error. This aspect needs to be investigated in more detail.

2.2.6 Fouling of Polypropylene Hollow Fiber Membrane

Four types of fouling are considered important when hollow fiber membranes are used in water treatment applications (Schwarz et al., 1991):

1) Suspended solids accumulation

Suspended solids in the water can quickly plug the membrane modules in pressure driven membrane processes. In the concentration driven air-stripping process, no solids accumulate at the membrane wall since no water crosses the membrane; thus, it is not a problem for this process. However, the ends of the hollow fibers can become plugged by influent solids and pre-treatment may be necessary.

2) Biological fouling and slime development

Growth of bacteria on the surface may or may not be a problem depending on the water characteristics and the type of material being stripped.

3) Calcium carbonate deposition

During CO_2 stripping from groundwater, $CaCO_3$ may deposit on the fiber surface if the pH is high. Most groundwater treatment applications acidify the water to a pH of approximately 4 to minimize fouling problems.

4) Deposition of iron oxidation products

Reduced iron found in groundwater is oxidized and precipitates as $Fe(OH)_3$ as oxygen permeates from the sweeping air to the aqueous side of the membrane. Some of the ferric hydroxide formed may deposit on the walls of the membrane and some will be carried out with the water stream. This oxidation is strongly dependent on the pH and the ferric ion concentration in the water.

Iron fouling of hollow fiber membranes has been investigated by Schwarz et al. (1991). They conducted two separate studies: a) long-term field study to evaluate the effect of iron fouling on performance and b) laboratory study to characterize the kinetics of iron

fouling. The first study was conducted for 75 days with a commercially available microporous polypropylene hollow fiber membrane module with an effective surface area of 3.4 m^2 and pores of 0.03 μm diameter covering 40 percent of the membrane surface. It was stated that iron fouling was the main problem during this field study from the evidence of release of a high concentration of iron from the membrane during its regeneration with acid after 75 days. The iron concentration in the feed was not reported. This type of fouling increases the membrane resistance to mass transfer. Although Yang and Cussler (1986) stated in an earlier study that membrane resistance for gas filled pores is a negligible factor and that the overall resistance is governed mainly by liquid film diffusion during removal of VOCs by air stripping, however in practice, as the membrane becomes fouled, its resistance does become increasingly significant (Schwarz et al., 1991).

The second study was conducted to evaluate the factors influencing the rate of iron fouling of polypropylene hollow fibers under controlled conditions (Schwarz et al., 1991). These tests were conducted with deoxygenated water with ferrous sulfate concentrations of 5 to 20 ppm. It was reported that the velocity of the feed in the hollow fiber plays a greater role in ferric hydroxide accumulation than the ferric ion concentration in the feed. It was also reported that not all the ferric hydroxide formed accumulates on the fiber but that a portion remains in the aqueous system as a precipitate and is transferred to the next module(s). Thus, in an industrial MAS application involving several modules in series, the second and subsequent modules would be more prone to particulate fouling and fiber plugging by the ferric hydroxide formed upstream.

Pre-acidification of water or intermediate filtration between modules must be planned to avoid this potential problem.

2.2.7 Membrane Air Stripping Applications

Membrane air stripping has been investigated for removal of VOCs from low concentration aqueous solutions in recent years (Semmens et al., 1989; Zander et al., 1989a; Bhowmick and Semmens, 1994; Boswell and Vaccari, 1994; Castro and Zander, 1995). It has been reported by these researchers that VOCs, such as chloroform, 1,1,2-trichloroethane, trichloroethylene, tetrachloroethylene, carbon tetrachloride, bromoform and bromodichloromethane have been effectively removed from aqueous mixtures using polypropylene membranes.

A detailed comparison was conducted by Zander et al. (1989a) on the removal of chloroform, bromoform, bromodichloromethane, trichloroethylene, tetrachloroethylene, carbon tetrachloride using conventional packed air stripping towers and polypropylene hollow fiber membrane air stripping modules. It was reported that although the active length of the membrane was 0.55 m compared to a packed tower length of 3.66 m, the removal of VOCs for the membrane system ranged from 5 to 95 percent compared to 20 to 98 percent for packed towers. A direct comparison was not possible due to size differences; hence a comparison was made based on mass transfer coefficients. It was reported that the overall volume specific mass transfer coefficient for the membrane system was generally more than an order of magnitude greater than those measured for a packed tower air stripping system.

2.2.8 Treatment of Air Stripping Off Gas

The organic contaminants in the stripped air can be vented to the atmosphere, collected by condensation or be subjected to further treatment prior to release. Bhowmick and Semmens (1993, 1994) and Bhowmick (1992) have conducted studies to evaluate the possibilities of treating VOCs contaminated stripped air from a hollow fiber MAS process by UV photooxidation in an attempt to develop the closed loop air stripping process (CLASP). In this process, air used in a hollow fiber MAS system treating a synthetic aqueous mixture of five VOCs (chloroform, 1,1,2-trichloroethane, trichloroethylene, tetrachloroethylene and carbon tetrachloride) was irradiated with ultraviolet light in a photooxidation chamber. The VOCs in the air were destroyed by photolysis and oxidation processes occurring in the gas phase. In this system, the production and fate of intermediates were of great interest. It was reported that phosgene, chloroacetylchloride and chloroacetaldehyde were formed in low concentrations. There was no problem of ozone formation in large quantities (Bhowmick and Semmens, 1994) as reported in an earlier study by Bhowmick and Semmens (1993). It was reported that phosgene, which was produced in the greatest amount compared to other by-products, was readily photooxidized by radiation at 185 nm (Bhowmick and Semmens, 1994). It was also suggested that a part of these intermediates might be diverted back to the stripper before being photooxidized. The effect of this reverse stripping (the impurities in the stripping gas being adsorbed in the water) should be investigated in detail. The fate of the intermediates is then dictated by their stability. Phosgene hydrolyzes instantaneously to HCl and CO_2 (Greenwood and Earnshaw, 1984). This process appears to offer a number of potential advantages over conventional air stripping with off-gas

treatment: no gaseous VOCs emissions; the VOCs are oxidized to harmless end-products; no adsorber is required; and no adsorbent regeneration or disposal costs are incurred.

This process can be used for PTA also, but as the PTA process uses a much higher air to water ratio during the stripping process than that of membrane air stripping (Zander et al., 1989a), thus a much larger CLASP will be required. An effective oxidation process needs a low air flow rate while effective air stripping in PTA requires a high air flow rate (Bhowmick and Semmens, 1994). Given this inherent conflict in operational parameters, the closed loop configuration for a packed tower air stripping/photooxidation process may not be technically and commercially feasible. The second alternative is to recover the organics through condensation. The recovered organics can be reused to avoid the gas phase emissions problem.

2.3 COMPARATIVE ECONOMICS

A cost comparison between the packed tower and hollow fiber membrane air-stripping was conducted by Schwarz et al. (1991) for 99.9 % removal of 1500 ppb trichloroethylene (TCE) from aqueous mixture. The authors collected the capital cost information for the packed tower and hollow fiber membrane systems from Peters and Timmerhaus (1980) and Rutledge (1990), respectively. For this comparison, the design of the hollow fiber membrane system was chosen to minimize membrane and pumping costs. Modules of 0.305 m diameter were used. The packed tower design was based on the mass transfer correlations developed by Onda et al. (1968). It was reported that the packed tower method of air stripping remains the least expensive option at the time of the

study at $0.26/m^3 treated compared to $0.36/m^3 for the hollow fiber membrane method. The stripped air treatment cost was not included in these costs. It was also stated that at the time of their study, a fair cost comparison between the long established, well optimized PTA system and not optimized, infant hollow fiber air-stripping technology was difficult. But in other studies, the cost of packed tower air stripping was reported much lower than those reported by Schwarz et al. (1991). Hand et al. (1986) reported costs of $0.013/m^3 water treated for 95% removal of VOCs. Dvorak et al. (1993) showed that the cost of packed tower air stripping alone for 99.75 % TCE removal (with C_{feed} = 2000 ppb TCE) was $ 0.022/m^3 whereas with air stripping including activated carbon off gas treatment was $0.056/m^3. Lipski and Côté (1990) reported that for PTA, the treatment cost for trichloroethylene (TCE) ranges from $0.10/m^3, for air stripping alone, to $0.80/m^3, for treatment trains including stripping with activated carbon off-gas treatment or activated carbon aqueous phase treatment. These studies showed that PTA is still the cheapest VOC treatment process. However, with the development of optimized, lower air pressure drop hollow fiber modules, the cost of membrane air stripping can be expected to decrease significantly.

2.4 SUMMARY

It can be concluded from the review, that the existing conventional processes for VOCs removal/recovery, even with modifications, still suffer from: 1) transfer of contaminants from one phase to another creating yet another removal/ disposal problem; 2) generation of undesirable by-products/intermediates which only compound the problem; and 3) some of the processes are specific to or only economical for certain contaminant

concentration levels. These limitations of existing or modified conventional processes have led to a search for alternative VOC removal methods capable of avoiding/reducing these problems.

The membrane air-stripping process using microporous polypropylene hollow fiber membranes has shown great potential for the removal of VOCs from aqueous streams over conventional treatment processes, particularly in reducing the size of the equipment. It was reported that the overall volume specific mass transfer coefficient obtained for MAS was an order of magnitude higher than that of PTA. Microporous polypropylene hollow fiber membrane modules have been investigated for the system in which contaminated aqueous solution was pumped through the lumen side and the stripping air flowed on the shell side. The studies were focused on the removal of halogenated hydrocarbons such as chloroform, 1,1,2-trichloroethane, trichloroethylene, tetrachloroethylene, carbon tetrachloride, bromoform and bromodichloromethane. The investigations were limited only to contaminated ground/drinking water having ppb concentrations of VOCs. It was stated in these studies that the high air pressure drop on the shell side is one of the main constraints. The effects of pH, free chlorine, ozone, packing densities and membrane geometries have been studied. There was no literature available on the removal of volatile organic compounds, which belonged to alicyclic or aromatic groups using the MAS process. No references were found on the removal of VOCs with concentrations higher than 100 ppm. Such information would be of interest to evaluate this process for potential applications in the treatment of industrial wastewater.

Future studies should investigate the reversal of the setup, i.e., pumping water through the shell side and the air through the lumen side of the hollow fiber module. The later mode of operation may improve the overall mass transfer coefficient as well as reduce the air side pressure drop. Detailed studies are needed with VOCs of alicyclic and aromatic groups as these are widely used as solvents in industries and need to be recovered/removed from the wastewater. Focus should be on the use of these membranes for treatment of wastewater containing higher levels of VOC concentrations. For this purpose, the effect of initial feed concentrations of VOC on overall mass transfer coefficient needs to be investigated.

CHAPTER 3

Literature Review: Theory

This chapter lays the fundamentals of mass transport in membrane air-stripping. The individual mass transfer resistances and their relationship to the overall mass transfer coefficient are critically reviewed. This chapter also discusses the deficiencies in the conventional approach, which led to the development of the goal of this research.

3.1 AIR STRIPPING PRINCIPLES

When a VOC is introduced into an air-water binary system, basic thermodynamics dictate that some of the VOC (solute) will partition into the aqueous phase and some into air phase until equilibrium is reached. If the air in contact with the water is replenished with fresh, solute-free air, the equilibrium will be disturbed. This will result in water containing solute in excess of its equilibrium level and hence, the solute will move from the aqueous phase to the air phase to re-establish equilibrium (Kavanaugh and Trussell, 1980). If VOC containing air is continuously replenished with fresh air, eventually all the solute will be removed from the solution. The departure from equilibrium conditions provides the driving force for mass transfer processes. This is the basic operating principle of the air-stripping process. In treatment processes, equilibrium is seldom reached and the process is then described by mass transfer models incorporating mass transfer resistances.

3.2 HENRY'S LAW CONSTANT

3.2.1 Overview

According to the kinetic theory of gases, molecules of dissolved gases can readily move between the gaseous and liquid phases until equilibrium is established. At high concentrations, this equilibrium condition can be expressed by Raoult's law for an ideal solution:

$$p_p = p_v Y^* \tag{3.1}$$

where:
p_p = partial pressure of the component, atm (the unit is kept in atm for consistency with the development)
p_v = vapor pressure of the component, atm
Y^* = mole fraction of the component in the liquid phase in equilibrium with the gas phase, mole/mole.

The total pressure of an ideal gas mixture is the sum of the partial pressures of all its components according to Dalton's law:

$$p_p = YP_T \tag{3.2}$$

where:
Y = mole fraction of the component in the gas phase, mole/mole
P_T = total pressure, atm.

Unfortunately, most of the solutions encountered in water and wastewater treatments are far from ideal and deviate substantially from the prediction of Raoult's law (Kavanaugh and Trussell, 1980). However, in the case of very dilute nonideal solutions, the equilibrium solute concentration in the vapor phase follows a linear relationship with that in the liquid phase with a slope much smaller than that to be observed according to

Raoult's law (Kavanaugh and Trussell, 1980). This partitioning phenomenon was originally studied by William Henry in early 1800s and is described by Henry's law constant (Kavanuagh and Trussell, 1980; Munz and Roberts, 1982) as:

$$p_p = H_d Y^* \tag{3.3}$$

where:
H_d = dimensional Henry's law constant, atm

Combining eqns. (3.2) and (3.3), the mole fraction of the component in the liquid phase and gas phase can be related at equilibrium conditions as:

$$Y = Y^* \frac{H_d}{P_T} \tag{3.4}$$

Henry's law constant (HLC) serves as a measure of a compound's volatility from water, the larger a compound's Henry's law constant value, the more volatile it is, and the easier it will transfer from the aqueous phase to the gas phase. Despite the importance and the need for HLC values, end-users often experience difficulties in finding appropriate HLC data (Brennan et al., 1998). A reason for such antithesis is that HLC has been referred to, interpreted, and dimensioned in several different forms. In the literature, HLC data may be found reported as hydrophilicity (Hine and Mookerjee, 1975); Ostwald's solubility constant (Abraham et al., 1994); distribution coefficient (Leighton and Calo, 1981); and vapor-liquid equilibrium constant (Turner et al., 1996). In addition, inconsistent dimensioning of HLC among authors arose by quantifying the gas phase and aqueous phase contents in various units. Its dimensionless form (H) is widely used in the environmental field. Since, the total pressure is commonly used as 1 atm, it is left out of

the equation and atm is dropped from the units of Henry's law constant (Cornwell, 1990). In this situation, any set of mass per volume or mole per volume units can be used as long as Y and Y^* are in the same units. Munz and Roberts (1982) and Roberts and Levy (1985) developed dimensionless form of HLC based on mass concentrations:

$$H = X/C^* \tag{3.5}$$

where:
H = dimensionless Henry's law constant
X = mass concentration of the component in the air phase, g/m^3 or ppm
C^* = liquid phase concentration that would be in equilibrium with the air phase concentration, g/m^3 or ppm.

At 1 atm pressure and 0°C, 1 mole of air has a volume of 0.022412 m^3. At other temperatures, the volume of 1 mole of air at 1 atm is 0.000082T m^3. The following approximate conversion between H and H_d can be made (Cornwell, 1990):

$$H = \frac{H_d}{4.56T} \tag{3.6}$$

where:
T = temperature in Kelvin, K

Methods for experimental determination and estimation of HLC have been studied by a number of researchers (Nirmalakhandan et al., 1997; Brennan et al., 1998; Collins, 1998; Altschuh et al., 1999). Two approaches have emerged for the estimation of HLC values. In the first approach, HLC is estimated from a ratio of the vapor pressure to the aqueous solubility of solute (s-vp model) (Mackay and Shiu, 1981; Burkhard et al., 1985; Ashworth et al., 1986). But due to the errors in estimations of vapor pressure and aqueous solubility of the solute, the average factor of error, AFE, defined as the ratio of the predicted HLC to the experimental values, could range from 3 to 4 (Burkhard et al.,

1985). In the second approach, quantitative structure-activity relationship (QSAR) techniques are used to develop models to predict HLC (Hine and Mookerjee, 1975; Nirmalakhandan and Speece, 1988; Meylan and Howard, 1991; Russell et al., 1992; Abraham et al., 1994; Nirmalakhandan et al., 1997). This technique is based on the assumption that the physical/chemical properties and activities of organic molecules are a function of their molecular structures. This type of technique does not normally require experimental inputs as the model parameters are calculated or estimated directly from the molecular structure of the solute (Nirmalakhandan et al., 1997).

Experimentally determined dimensionless HLC values (*H*) for chloroform and toluene found in the literature in the vicinity of 23°C are summarized in Table 3.1.

Table 3.1 Experimental *H* values for chloroform and toluene found in the literature

Chloroform			Toluene		
°C	*H*	Reference	°C	*H*	Reference
22.0	0.1446	Leighton and Calo, 1981	22.7	0.2298	Leighton and Calo, 1981
24.9	0.1508	Leighton and Calo, 1981	23.0	0.2539	Leighton and Calo, 1981
20.0	0.136	Lalezary et al., 1984	25.0	0.271	Mackay et al., 1979
20.0	0.116	Mackay and Shiu, 1981	25.0	0.263	Singley et al., 1980
19.9	0.153	Lamarche and Droste, 1989	19.9	0.189	Lamarche and Droste, 1989
29.8	0.185	Lamarche and Droste, 1989	29.8	0.375	Lamarche and Droste, 1989
25.0	0.129	Mackay and Shiu, 1981	25.0	0.24	Altschuh et al., 1999
20.0	0.224	Munz and Roberts, 1982	25.0	0.263	Robbins et al., 1993
17.5	0.103	Gossett, 1987	25.0	0.2623	Howe et al., 1987
24.8	0.150	Gossett, 1987	25.0	0.273	Turner et al., 1996
25.0	0.182	Turner et al., 1996	25.0	0.269	Sanemasa et al., 1982
20.0	0.220	Roberts et al., 1985			
25.0	0.267	Singley et al., 1980			

From the above table, it become clear that experimental values of H varies widely for the same temperature, such as H for chloroform at 20 °C varies almost by a factor of one from 0.116 to 0.224. The H values for toluene at 25 °C varies from 0.24 to 0.273.

3.2.2 Factors Affecting Henry's Law Constant

Factors affecting HLC values have been studied in detail by a number of researchers (Singley et al., 1980; Kavanuagh and Trussell, 1980; Leighton and Calo, 1981; Mackay and Shiu, 1981; Al-Dhowalia, 1982; Roberts and Levy, 1985; Lamarche and Droste, 1989; Nirmalakhandan et al., 1997). They are briefly described below:

3.2.2.1 Effect of Temperature on Henry's Law Constant

According to the laws of thermodynamics, HLCs should vary with temperature and pressure. For a constant pressure, the relationship of HLC and temperature can be modeled by a vant't Hoff-type relation (Kavanuagh and Trussell, 1980):

$$\log H_d = \frac{-\Delta H^o}{R_c T} + J \qquad (3.7)$$

where:
ΔH^o = enthalpy change due to dissolution of component in water (joules.mol^{-1})
R_c = universal gas constant (8.314 4 joules. deg^{-1}.mol^{-1})
J = empirical constant

The following empirical relationship between HLC and temperature was developed by Leighton and Calo (1981) based on the linear regression of their experimental data on 21 chlorinated hydrocarbons plus benzene and toluene:

$$\ln H_d = A - \frac{B}{T} \qquad (3.8)$$

Where A and B are the empirical compound dependent constants determined by a least-squares analysis for all 23 compounds.

Singley et al. (1980) developed the following relationship between HLC and temperature by correlating their data:

$$\ln H = B_0 + \frac{B_1}{T} \qquad (3.9)$$

Where B_0 and B_1 are empirical constants. Singley et al. (1980) and ESE (1981) estimated the values of B_0 and B_1 through fitting their experimental data to the above equation. Lamarche and Droste (1989) fitted their data to the eqn. (3.9), but have reported different values for the constants from those reported by Singley et al. (1980) and ESE (1981).

3.2.2.2 Effect of Solute Concentration on Henry's Law Constant

The effect of solute concentration on HLC was studied by Munz and Roberts (1982) and Gossett et al. (1985). Munz and Roberts (1982) reported that an increase in solute concentration would have no effect on HLC values based on their investigation on carbon tetrachloride, chloroform and hexachloroethane. Contrary to that, Gossett et al. (1985) found that an increase in solute concentration would result in an increase in HLC. Collins (1998) stated that there were errors in the method used by Gossett et al. (1985) and concluded that there was no significant effect of the concentration of the solute on HLC for halogenated hydrocarbons.

3.2.2.3 Effect of Mixture on Henry's Law Constant

It was concluded by Gossett et al. (1985) based on their study of an aqueous mixture of tetrachloroethylene, dichloromethane, trichloroethylene, 1-1-1 trichloroethane and chloroform that the presence of other VOCs did not impact the HLC values of the individual VOCs within the mixture.

Next we need to examine the other constraints on the performance of MAS systems, i.e., mass transfer resistances.

3.3 MASS TRANSFER IN MEMBRANE AIR-STRIPPING PROCESS

VOCs are transferred from water to air through intimate contact of the two phases both in PTA and in MAS. But in the latter process, the contact is provided at the mouth of the air-filled pores. The driving force for the mass transfer is the concentration difference between two phases. When vacuum is used in conjunction with stripping air, the pressure difference also becomes a part of the driving force.

Mass transfer in membrane air stripping involves three sequential steps (Semmens et al., 1989; Yang and Cussler, 1986). First, a VOC diffuses from the bulk aqueous solution across the liquid boundary layer to the membrane surface. Second, it diffuses through the air filled pores. This diffusion step does not exist in packed tower air stripping. Third, it diffuses through the air boundary layer outside the membrane into the stripping air. Thus, the overall mass transfer resistance is the combined effect of these three separate mass

transfer resistances, as shown schematically in Fig. 3.1. As mass transfer resistances are considered to be proportional to the inverse of the corresponding mass transfer coefficients, the overall liquid-phase based mass transfer resistance ($\frac{1}{K_L}$) can be expressed as follows:

$$\frac{1}{K_L} = \frac{1}{k_L} + \frac{1}{k_m H} + \frac{1}{k_a H} \tag{3.10}$$

Where:
K_L = overall liquid-phase based mass transfer coefficient, m/s
k_L = local liquid-phase mass transfer coefficient, m/s
k_a = local air-phase mass transfer coefficient, m/s
k_m = membrane mass transfer coefficient, m/s
H = dimensionless Henry's law constant, i.e., a ratio of the mass concentrations

3.4 PREDICTION OF INDIVIDUAL MASS TRANSFER COEFFICIENTS

The individual mass transfer coefficients can be predicted for MAS using liquid cross-flow on the shell side and air flow in the lumen side of hollow fiber using dimensionless mass transfer correlations. They are briefly presented below:

3.4.1 Local Liquid-Phase Mass Transfer Coefficient

The local liquid-phase mass transfer coefficient, k_L, can be predicted by the mass transfer correlation analog to the heat transfer correlation developed by Kreith and Black (1980) for cross-flow in closely packed tube bank heat exchangers (eqn. 3.11), and those developed by Yang and Cussler (1986) (eqn. 3.12) and Reed et al. (1995) (eqn. 3.13), for liquid cross-flow on the shell side of hollow fiber membrane modules.

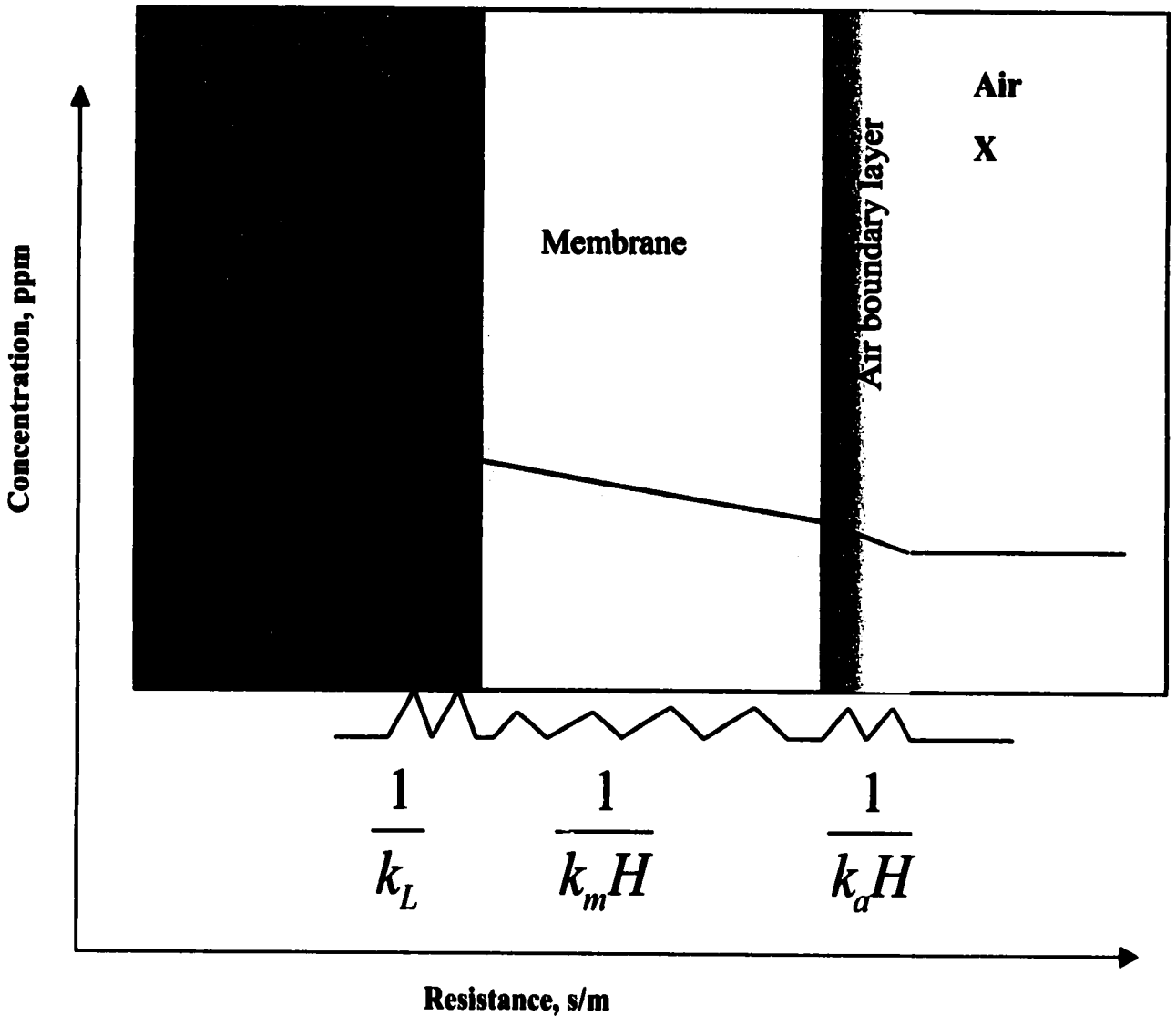

Figure 3.1 Three Mass Transfer Resistances Created in MAS Process

$$Sh = 0.39\, Re^{0.59}\, Sc^{0.33} \tag{3.11}$$

where:
Re = Reynolds number ($d_o u^w / \nu$)
Sh = Sherwood number ($k_L d_o / D_w$)
Sc = Schmidt number (ν / D_w)
d_o = outer diameter of the hollow fiber, m
u^w = aqueous solution velocity on the shell side of the fibers, m/s
ν = kinematic viscosity of water, m^2/s
D_w = diffusion coefficient of compound in water, m^2/s

$$Sh = 1.38\, Re^{0.34}\, Sc^{0.33} \tag{3.12}$$

$$Sh = 1.4\, Re^{0.33}\, Sc^{0.33} \tag{3.13}$$

Yang and Cussler (1986) reported that the Kreith and Black (1980) correlation did not describe their data. So, they developed eqn. (3.12). However, geometrically the two systems were very similar.

3.4.2 Local Air-Phase Mass Transfer Coefficient

The local air-phase mass transfer coefficient, k_a can be estimated by using a correlation for laminar flow in a cylindrical tube (Lévéque, 1928; Sieder and Tate, 1936; Qi and Cussler, 1985a). In this work, the following eqn. (3.14), derived from Lévéque's (1928) correlation, is used by incorporating Henry's law constant, as the boundary layer is gaseous.

$$\frac{1}{k_a H} = \frac{0.617}{H}\left(\frac{L d_i}{v^a D_c^{\,2}}\right)^{0.33} \tag{3.14}$$

where:
v^a = air velocity inside the hollow fiber, m/s
d_i = inner diameter of the hollow fiber, m
L = length of fiber, m

D_c = continuum (ordinary) diffusion coefficient of compound in air phase, m^2/s

It was reported that at low liquid flows in a cylindrical tube, when the Graetz numbers ($d_i^2 v^w / LD_w$) are less than 4, the experimental values deviate from that predicted by Lévêque's (1928) correlation (Gabelman and Hwang, 1999). Such deviations have been observed for hollow fibers by a number of researchers (Wickramasinghe et al., 1992; Prasad and Sirkar, 1990, 1988; Semmens et al., 1989; Zander et al., 1989b). Analogous deviations have also been reported in heat transfer (Norris et al., 1940; Sieder and Tate, 1936). Wickramasinghe et al. (1992) stated that the theory and experiments do not agree at low flows, apparently because of slight polydispersity in hollow fiber diameter and proposed the following relationship based on their data obtained from experiments with liquid flow in the lumen:

$$\overline{k_L} = 1.5x10^{-4} \frac{v^w}{L} \tag{3.15}$$

where:

$\overline{k}_L$ = average local liquid phase mass transfer coefficient, m/s

v^w = liquid velocity inside the hollow fiber, m/s

Eqn. (3.15) does not incorporate any physicochemical properties of the compounds involved and thus it will be same for an identical set of operating conditions irrespective of the types of compounds. But the local film resistance on the lumen of the fiber depends on the film thickness as well as on the diffusion coefficient of the solute and should depend on the physicochemical properties. Wickramasinghe et al. (1992) proposed the

following correlation, which has been developed based on average values and takes into account the physicochemical properties of the compounds:

$$\overline{Sh} = Sh[1-(\frac{18Sh}{Gr}+7)\omega^2+....] \tag{3.16}$$

where:
Sh = Sherwood number = $1.62\ Gr^{0.33}$
$\overline{Sh}$ = average Sherwood number
Gr = Graetz number ($\frac{Pe.d_i}{L}$)
Pe = Peclet number ($d_i\ v^w / D_w$)
ω = coefficient of variation for the fiber radius measurements

The above eqns. (3.15) and eqn. (3.16) were proposed to take into account the polydispersity in hollow fiber diameter. However, the deviations at low flows were reported for heat transfer also, where the tube diameter of the heat exchanger might be free of this polydispersity.

3.4.3 Membrane Mass Transfer Coefficient

The membrane mass transfer coefficient, k_m can be predicted using the following equation (Qi and Cussler, 1985b, Kreulen et al., 1993). As the pores in these membranes are far from cylindrical, incorporation of pore tortuosity is important to account for the abnormality of pore shapes.

$$\frac{1}{k_m H} = \frac{\delta\tau}{D_{eff}\varepsilon H} \tag{3.17}$$

where:
δ = pore length, m
D_{eff} = effective diffusion coefficient of compound in air, m^2/s

τ = pore tortuosity (dimensionless)
ε = fiber porosity (dimensionless)

For membranes having mean pore size less than 0.1 μm, the continuum as well as Knudsen diffusion should be taken into account (Kreulen et al., 1993). The effective diffusion coefficient, D_{eff}, can be estimated approximately using the following relationship (Pollard and Present, 1948):

$$D_{eff} = \left(\frac{1}{D_c} + \frac{1}{D_{Kn}}\right)^{-1} \tag{3.18}$$

where:
D_{Kn} = Knudsen diffusion coefficient of compound in air, m^2/s

For dilute gases, the continuum diffusion coefficient, D_c, can be evaluated by the following empirical eqn. (3.19) developed by Fuller et al. (1966).

$$D_c = 10^{-3} \frac{T^{1.75}\left(\frac{1}{MW_1} + \frac{1}{MW_2}\right)^{0.5}}{P_T\left[\left(\sum_i V_{i1}\right)^{0.33} + \left(\sum_i V_{i2}\right)^{0.33}\right]^2} \tag{3.19}$$

where:
T = temperature, K
MW_1 = molecular weights of the compound, g/mole
MW_2 = molecular weights of air, g/mole
P_T = pressure, atm
$\sum V_{i1}$ = diffusion volumes of the compound, cm^3/mole
V_{i1} = diffusion volumes of the parts of compound, cm^3/mole
$\sum V_{i2}$ = diffusion volumes of air, cm^3/mole

As well, the Knudsen diffusion coefficient, D_{Kn} can be evaluated by the relationship given by Evans et al. (1961), which was simplified by Cussler (1984) as shown in eqn (3.20).

$$D_{Kn} = 4850 d_p \sqrt{\frac{T}{MW_1}} \tag{3.20}$$

where:
d_p = pore diameter, m

Control of continuum or Knudsen diffusion will be dependent on the values of reciprocal terms in eqn. (3.18).

3.5 ESTIMATION OF EXPERIMENTAL OVERALL MASS TRANSFER COEFFICIENT FOR A BATCH MAS SYSTEM

Mass transfer fundamentals for transport of VOCs in a batch MAS system have been reviewed in detail by Mahmud et al. (1998). In this review, the equations developed by Semmens et al. (1989) for calculation of the overall experimental mass transfer coefficient have been modified/corrected where needed. Since the membrane air-stripping system and the operating conditions of this study were similar to those of Semmens et al. (1989), the development of the equations is described below. The equations were established for a system in which the solution was pumped from the reservoir through the lumen of the hollow fibers and back to the reservoir and the air flow was on the shell side counter-currently (Fig. 3.2).

The driving force for mass transfer across the interface is proportional to the concentration difference between the phases. At equilibrium conditions, the concentration of the gas phase, X, is related to the concentration in the liquid phase, C^*, by the dimensionless Henry's law constant H, as:

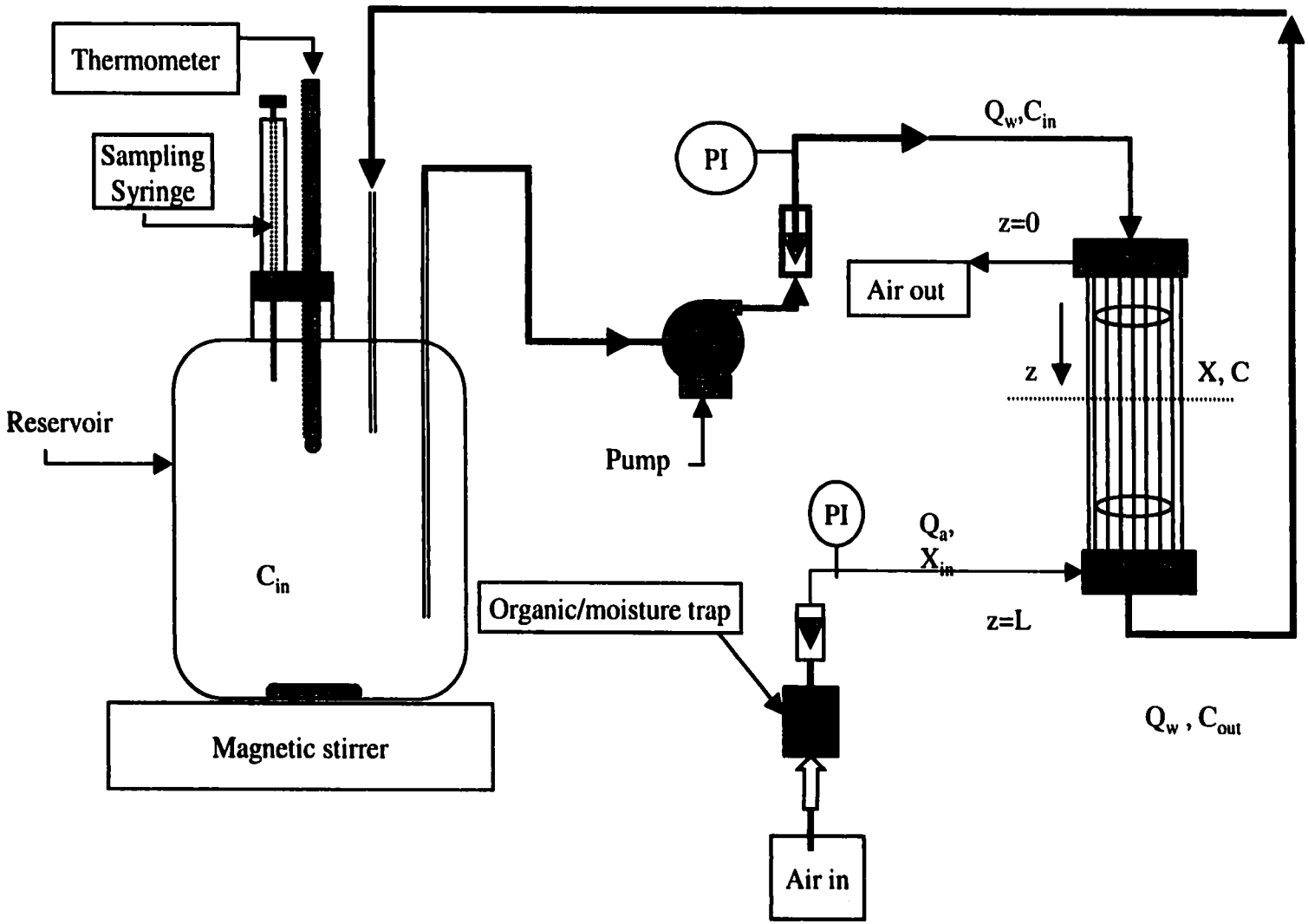

Figure 3.2 Membrane Air -Stripping Experimental Setup Used by Semmens et al. (1989)

$$H = \frac{X}{C^*} \tag{3.21}$$

where:
X = concentration of the component of concern in the air phase at distance z, ppm
C^* = liquid phase concentration that would be in equilibrium with the bulk air phase concentration, ppm.

Mass transfer in the longitudinal direction of a single hollow fiber is given by

$$\frac{dC}{dt} = -\frac{v^w dC}{dz} - K_L a(C - C^*) \tag{3.22}$$

where:
a = surface to volume ratio, m^2/m^3
z = distance from hollow fiber inlet, m
C = concentration of the component of concern in the liquid phase at distance z, ppm
t = time, s

Under steady state conditions, the above relation becomes

$$-\frac{v^w dC}{dz} = K_L a(C - C^*) \tag{3.23}$$

with the boundary conditions $C = C_{in}$ in the aqueous influent (z=0) and $C = C_{out}$ in the aqueous effluent ($z = L$), where L is the length of the hollow fiber.

Solute mass balance between the distance z and the hollow fiber lumen outlet (z=L) yields the following relationship:

$$Q_w C + Q_a X_{in} = Q_w C_{out} + Q_a X \tag{3.24}$$

where:
Q_w = solution flow rate, m^3/s
Q_a = air flow rate, m^3/s
X_{in} = organic concentration in incoming air at $z = L$, ppm

Assuming X_{in} as zero,

$$Q_w C = Q_w C_{out} + Q_a X \tag{3.25}$$

or $$X = \frac{Q_w}{Q_a}(C - C_{out}) \tag{3.26}$$

Substituting eqn. (3.26) in the Henry's Law expression [eqn. (3.21)],

$$C^* = \frac{X}{H} = \frac{\frac{Q_w}{Q_a}(C - C_{out})}{H} = R(C - C_{out}) \tag{3.27}$$

where:
$R = Q_w/Q_a H$

Note that Semmens et al. (1989) and Bhowmick and Semmens (1994) have defined the stripping factor as $R = Q_w/Q_a H$, which is the inverse of the conventional definition used in PTA calculations (i.e., $R = Q_a H/Q_w$). It seems that these authors have used R more as a lumped parameter, apparently without using it as a critical design parameter as in PTA. This is likely due to the single pass nature of PTA compared to the multiple pass nature of hollow-fiber membrane stripping in a batch system. In PTA systems, if R is less than 1, the level of removal will be limited to a certain value that is proportional to R (Treybal, 1980). In batch hollow fiber systems, due to the multiple passes, the level of removal is not limited even when R is less than 1. In this thesis, the nomenclature of the stripping factor $R = Q_w/Q_a H$ will be used.

Substituting C^* into eqn. (3.23) and integrating over the length of the stripper, the following equation can be derived:

$$\int_{C_{in}}^{C_{out}} \frac{dC}{(1-R)C + RC_{out}} = \frac{-K_L a}{v^w} \int_0^L dz \tag{3.28}$$

Solving eqn. (3.28) for the boundary conditions,

$$\frac{1}{1-R} \ln \left| (1-R)C + RC_{out} \right|_{C_{in}}^{C_{out}} = \frac{-K_L aL}{v^w} \tag{3.29}$$

Further solving eqn. (3.29) will provide

$$\frac{1}{1-R} \ln \frac{(1-R)C_{out} + RC_{out}}{(1-R)C_{in} + RC_{out}} = \frac{-K_L aL}{v^w} \tag{3.30}$$

Solving eqn. (3.30) for the ratio of influent and effluent concentration for a single pass through the module, the expression becomes

$$\frac{C_{in}}{C_{out}} = \frac{\exp[(\frac{K_L aL}{v^w})(1-R)] - R}{1-R} = M \tag{3.31}$$

The above relationship shows that the organic removal should be enhanced by increasing the mass transfer coefficient, the length of the module, or the ratio of the surface area to the volume within the module. The lower liquid velocity should improve the removal efficiency. The surface to volume ratio, *a*, for a hollow-fiber module is constant and depends on the inner diameter, d_i, of the fiber and given as:

$$a = \frac{4\pi n d_i L}{\pi n d_i^2 L} = \frac{4}{d_i} \tag{3.32}$$

where:
n = number of fibers
d_i = inner diameter of the hollow fiber, m

The change in organic concentration in the completely mixed reservoir of a batch membrane stripping system can be given by:

$$\frac{V_w dC_t}{dt} = Q_w(C_{out} - C_{in}) = Q_w(\frac{1}{M} - 1)C_{in} \qquad (3.33)$$

where:
V_w = volume of the solution in the reservoir, m^3
C_t = concentration in the reservoir after time t, ppm

The following assumptions were made to derive the above equation: 1) the concentration in the reservoir and at the module inlet are the same; 2) the time scale required to reach a steady state within the hollow fibers is much smaller than that of concentration change in the reservoir; and 3) the change in the volume of the water in the reservoir with time was ignored.

Rearranging and integrating eqn. (3.33) with the boundary conditions $C_{in} = C_0$ at time 0 and $C_{in} = C_t$ at time t, Semmens et al. (1989) derived the following equation:

$$\ln(\frac{C_0}{C_t}) = \frac{Q_w}{V_w}(1 - \frac{1}{M})t = kt \qquad (3.34)$$

Thus, if the concentration of the organics in the water reservoir is monitored over time, a plot of $ln(C_0/C_t)$ versus time should yield a linear relationship with a slope of k. Substituting the value of M from eqn. (3.31) in eqn. (3.34) and solving for K_L, and insertion of definition of a, results in the following equation:

$$K_L = \frac{v^w d_i}{4L}(1-R)^{-1} \ln\{[\frac{Q_w}{(Q_w - V_w k)}](1-R) + R\} \qquad (3.35)$$

The values for parameters in eqn. (3.35) are available numerically from the experiments. The only exception is R, as it depends on H. The method of evaluating H was described in section 3.2.

Eqn. (3.35) is valid when the solution flows on the lumen side. According to Qi and Cussler (1985a), the same equation can be used when solution flow is on the shell side by interchanging the surface to volume ratio, a, and its equivalent internal fiber diameter term, $4/d_i$. Thus, the above equation can be rewritten for liquid flow in the shell side as follows (Mahmud et al., 1998):

$$K_L = \frac{u^w}{aL}(1-R)^{-1} \ln\{[\frac{Q_w}{(Q_w - V_w k)}](1-R) + R\} \qquad (3.36)$$

where:
u^w = aqueous solution velocity outside the hollow fiber, m/s

3.6 MASS TRANSFER STUDIES

The mass transfer equations describing the relationship and the dependency of mass transfer and other parameters for stripping processes using polypropylene membranes have been studied by a number of researchers (Kiani et al., 1984; Qi and Cussler, 1985a, 1985b, 1985c; Yang and Cussler, 1986; Semmens et al., 1989; Zander et al., 1989a; Kreulen et al., 1993; and Bhowmick and Semmens, 1994).

The overall liquid phase based mass transfer coefficient (K_L) for MAS is usually lower than that for conventional air-stripping process due to the mass transfer resistance ($\frac{1}{k_m H}$) created by the membrane itself (Kiani et al., 1984; and Yang and Cussler, 1986). Direct measurement of the mass transfer resistance due to the membrane have been conducted for air and liquid filled pores by a number of researchers (Kiani et al., 1984; Qi and

Cussler, 1985c; Yang and Cussler, 1986). It has been stated that mass transfer resistance created by the membrane could be negligible for gas filled pores (Yang and Cussler, 1986) but could become significant for liquid filled pores (Kiani et al., 1984; Yang and Cussler, 1986). However, there is controversy over the importance of membrane mass transfer resistance for air filled pores (Qi and Cussler, 1985c; Yang and Cussler, 1986, Semmens et al. 1989; Kreulen et al., 1993). It has also been stated that membrane resistance may dominate overall mass transfer resistance when both liquid and gas velocities become large (Yang and Cussler, 1986). In their studies on the absorption of pure carbon dioxide in water using polypropylene hollow fibers (Celgard X-20), Karoor and Sirkar (1993) reported that the CO_2 gas phase mass transfer resistance ($\frac{1}{k_a H}$) was eliminated as the pores were filled with pure CO_2. They also concluded that at higher liquid velocities, the mass transfer resistance due to the membrane became the controlling resistance. Membrane resistance for polypropylene membranes was directly measured as a function of membrane thickness by Qi and Cussler (1985c) and Kreulen et al. (1993) for systems with chemical reaction. They controlled the membrane thickness by clamping pieces of polypropylene flat sheet membranes together. The membrane pores were reported as being gas filled. The reported values for membrane mass transfer resistance by Qi and Cussler (1985c) and Kreulen et al. (1993) differed by three orders of magnitude. Kreulen et al. (1993) stated that the high membrane resistance value observed by Qi and Cussler (1985c) was possibly due to wetting of the pores, but no justification for this assumption was given. Malek et al. (1997) stated that all the pores might not be totally dry and predicted that a number of pores at the inlet of the hollow fiber might

become wetted across the full membrane thickness due to an operating pressure that was higher than the breakthrough pressure.

Semmens et al. (1989) reported stripping of VOCs from aqueous solutions by MAS involving no chemical reaction, using the same Celgard X-20 polypropylene hollow fiber membranes as Karoor and Sirkar (1993). A VOC laden aqueous solution was pumped through the lumen side and stripping air was passed counter currently through the shell side of the hollow fiber system. They predicted individual local liquid phase, local gas phase and membrane mass transfer resistances using the following equations:

$$\frac{1}{k_L} = 0.617\left(\frac{Ld_i}{v^w D_w^{\,2}}\right)^{0.33} \tag{3.37}$$

where:
k_L = local liquid phase mass transfer coefficient, m/s
d_i = inner diameter of the hollow fiber, m
L = length of fiber, m
v^w = aqueous solution velocity inside the hollow fiber, m/s
D_w = diffusion coefficient of compound in water, m^2/s

$$\frac{1}{k_a H} = 45.5\frac{d_o^{0.4} v^{0.27}}{u^{a\,0.6} D_c^{\,0.67} H} \tag{3.38}$$

where:
k_a = local air phase mass transfer coefficient, m/s
H = dimensionless Henry's law constant
v = kinematic viscosity of air, m^2/s
u^a = air velocity outside the hollow fiber, m/s
d_o = outer diameter of the hollow fiber, m
D_c = continuum diffusion coefficient of compound in air phase, m^2/s

and
$$\frac{1}{k_m H} = \frac{\delta}{D_c H} \tag{3.39}$$

where:
k_m = membrane mass transfer coefficient, m/s
δ = pore length, m

Eqn. (3.37) was derived from the correlations of Lévéque (1928) developed for flow in cylindrical pipes. Eqns. (3.38) and (3.39) were developed by Knudson and Katz (1958) and Sherwood et al. (1975), respectively.

Using eqns. (3.37)-(3.39), individual mass transfer resistances for chloroform were calculated for the conditions given by Semmens et al. (1989). Based on these values, the overall liquid phase based mass transfer coefficient for chloroform was calculated and compared in Fig. 3.3 with those observed by Semmens et al. (1989). The predicted overall liquid phase based mass transfer coefficient was much greater than that observed. This indicates that one or more of the individual mass transfer coefficient(s) predicted by eqns. (3.37)-(3.39) was (were) higher than that observed and warrants further careful study.

It was observed from the drawing of the batch experimental setup given by Semmens et al. (1989) that their reservoir had some headspace. Some of the VOCs might have concentrated in this headspace. It was not clear if this aspect was considered in their analysis.

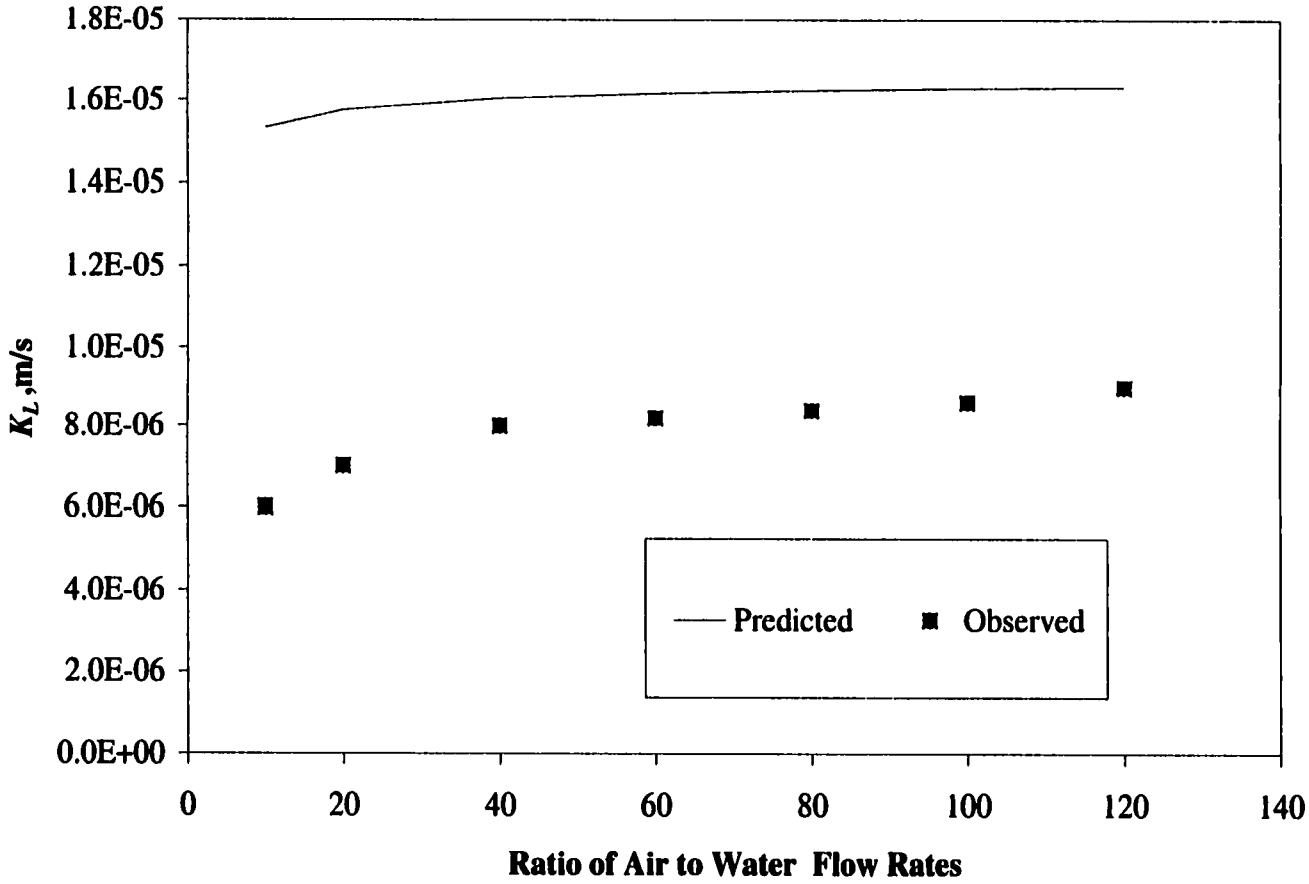

Figure 3.3 Predicted Vs Observed K_L Values by Semmens et al. (1989) [Liquid flow rate=75 ml/min]

3.7 SUMMARY

The methods for estimation of Henry's law constants have some inconsistencies and experimental confirmation is needed. The empirical correlations between HLC and temperature have some limitations and were developed based on specific sets of data.

Experimental values of Henry's law constant were found to vary widely. *H* values for the temperature at which the mass transfer tests will be conducted, need to be experimentally determined for individual as well as for mixtures of the VOCs to identify if there are interactions between them.

Direct investigations with chemical reactions were performed to determine the contribution of the membrane mass transfer resistance, but the results differed from each other by three orders of magnitude (Qi and Cussler, 1985c and Kreulen et al., 1993). Further investigations are required to determine the contribution of the individual mass transfer resistances in more detail for this process, especially when no chemical reaction are involved. This is necessary to verify the mass transport mechanism and to improve the process efficiency. An investigation using very low liquid velocities is also needed to verify the statement that the lower liquid velocity should improve the VOC removal efficiency (section 3.5).

Much of the analysis on the importance of individual mass transfer resistances is based on assumptions that the local mass transfer coefficients are accurately predicted by literature correlations. Significant deviations have been observed between predicted and

experimental data. The Kreith and Black (1980) correlation, used widely to predict the heat transfer coefficient for cross-flow on the shell side in a closely packed tube bank heat exchanger, did not describe Yang and Cussler (1986)'s data, although, geometrically the two systems were very similar. Further investigation is required to find out if the Kreith and Black (1980) correlation accurately predicts the local mass transfer coefficient for the cross-flow in a closely-packed hollow fiber module. Lévéque's (1928) correlation also over-estimated the local liquid phase mass transfer coefficient in the lumen of a cylindrical tube/hollow fiber when the velocity was low. Alternative correlations were developed to replace/improve Lévéque's correlation for liquid film resistance only. An investigation is needed to verify if the alternative correlations are satisfactory for the prediction of the local mass transfer coefficient for low air velocities.

CHAPTER 4

Materials and Experimental Methods

This chapter explains in detail the experimental methods used in this study. The experimental methods are described in the following sections: a) materials; b) hollow fiber membrane and membrane module; c) membrane air-stripping experimental setup; d) choice of organics for investigation; e) analytical methods and equipment; and f) description of the experiments conducted.

4.1 MATERIALS

Materials for this study were of analytical grade and were used without further modification, unless otherwise stated.

Chloroform with purity of 99.8% [BDH Inc., Toronto, ON, Canada] was used to prepare the feed solution and the standards for the gas chromatographs. Toluene with purity of 99.8% [BDH Inc., Toronto, ON, Canada] was used to prepare the feed solution and the standards for the gas chromatograph. Potassium hydrogen phthalate greater than 99.9 % purity [Kanto Chemical Co. Inc, Japan] was used for total carbon (TC)/ total organic carbon (TOC) standard preparation. Sodium hydrogen carbonate of purity more than 99.8% [Kanto Chemical Co. Inc, Japan] and anhydrous sodium carbonate of purity more than 99.7 % [Kanto Chemical Co. Inc, Japan] were used for inorganic carbon (IC)

standard preparation. Orthophosphoric acid [Anachemia Science, Lachine, PQ, Canada] was used in the TC analysis. Water used throughout the study was reverse osmosis grade obtained from a Reverse Osmosis System [Model WMQ600, Zenon Environmental Inc., Burlington, ON, Canada] with less than 50 ppb inorganic carbon.

4.2 HOLLOW FIBER MEMBRANES AND MEMBRANE MODULE

A Liqui-Cel® Extra- Flow 2.5" X 8" laboratory scale membrane contactor [Separation Products Division, Hoechst Celanese Corporation, Charlotte, NC, USA] was used. The module was made of polypropylene microporous hollow fibers [Celgard, Hoechst Celanese Corporation, Charlotte, NC, USA]. These fibers were hydrophobic, and hence should not be wetted by water. The detailed specifications of the fiber and the module are given in Tables 4.1 and 4.2, respectively.

Table 4.1 Hollow fiber membrane specifications

Characteristics	
Fiber outer diameter[1]	300 μm
Fiber inner diameter[1]	240 μm
Fiber wall thickness[1]	30 μm
Effective fiber length[2]	15 cm
Pore diameter[1]	0.03 μm
Pore tortuosity[3]	2.5
Porosity[1]	40%
Max. transmembrane differential pressure[1]	414 kPa
Max. operating temperature range[1]	1 to 60 °C

[1] Supplied by manufacturer.
[2] Refer to foot note # 2 after Table 4.2.
[3] The pores in these membranes are known to be far from cylindrical. To consider the abnormality of pore shapes, a tortuosity factor of 2.5 as reported by Prasad and Sirkar (1988) for these membranes has been used.

Table 4.2 Hollow fiber membrane module specifications

Characteristics	
Cartridge Dimension[1]	8 cm x 28 cm (2.5" x 8")
Shell inside diameter[1]	5.55 cm
Center tube outer diameter[1]	2.22 cm
Shell side volume[1]	~ 330 ml
Lumen side volume[1]	~ 90 ml
Number of fibers[2]	9,950
Void fraction[3]	0.654
Effective membrane surface[1]	1.4 m^2
Effective surface to volume ratio[1], *a*	2930 m^2/m^3
Fiber potting material[1]	Polyethylene
Housing material[1]	Polypropylene
Housing max. pressure[1]	414 kPa

[1] Supplied by the manufacturer.
[2] Manufacturer supplied information regarding effective fiber length and number of fibers as 0.16 m and 10,000 respectively. Schöner et al. (1998) measured the effective fiber length and number of fibers as 0.15 m and 9,950, respectively. Effective surface area provided by the manufacturer matches the calculated values using the numbers provided by Schöner et al. (1998). As it was not possible to open the module for measurement, the figures from Schöner et al. (1998) were utilized.
[3] Calculated.

4.3 MEMBRANE AIR-STRIPPING EXPERIMENTAL SETUP

A membrane air stripping experimental setup (Figure 4.1) was designed, fabricated, assembled and tested at the Institute of Chemical Process and Environmental Technology (ICPET) of National Research Council of Canada (NRC) in Ottawa. It satisfied the objective of providing liquid flow through the shell side and counter current stripping air flow through the lumen side of the hollow fiber module. The system included a reservoir (volume = 6.675 x 10^{-3} m^3), a hollow fiber membrane module, an aqueous solution/pure water feed circulation line and an air stripping line. All connecting tubing was teflon tubes and were thermally insulated. The feed from a glass reservoir was circulated through the membrane module with a centrifugal micro pump [Model 101000, Micropump, Inc., Vancouver, WA, USA] driven by a variable-speed (90 - 9000 rpm)

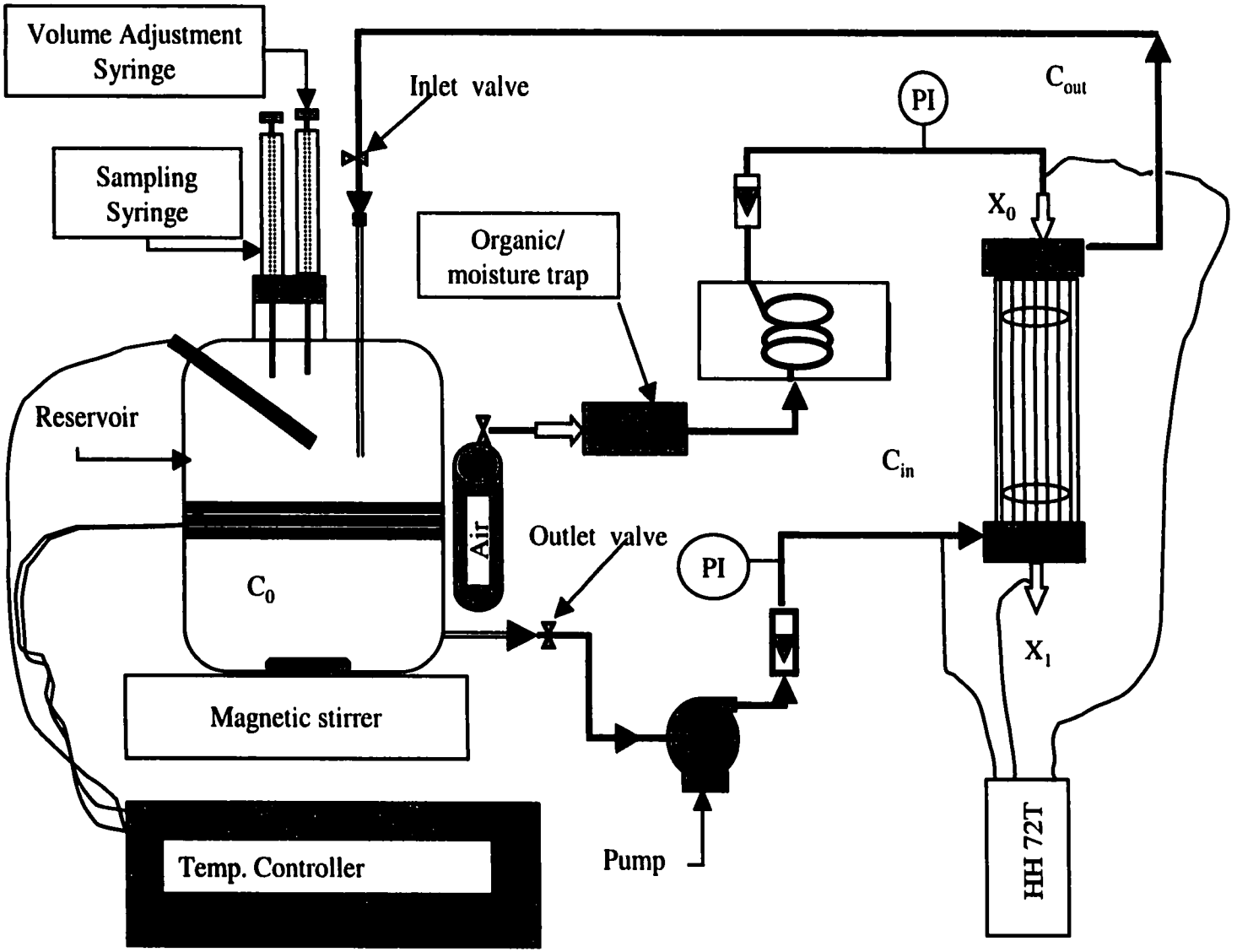

Figure 4.1 Membrane Air-Stripping Experimental Setup

pump drive [Model 75225 -12, Barnant Company, Barrington, IL, USA] capable of providing liquid flow from 0 to 4.42 x 10^{-4} m^3/s. The liquid flow and the pressure drop were measured using a rotameter [F-50375N, Blue White Flow-meter, Westminster, CA, USA] and a precision digital pressure gauge [PG 5000, PSI-Tronix, Tulare, CA, USA], respectively. The temperature of the feed was maintained using a temperature control system including a flexible electric heating tape [Barnstead/Thermolyne, Dubuque, IA, USA], a thermocouple [YSI 400, Yellow Springs Instrument Co., Inc, Yellow Springs, OH, USA] and a thermistemp temperature controller [Model 71A, Yellow Springs Instrument Co., Inc, Yellow Springs, OH, USA]. The inline feed temperature was monitored before the membrane module inlet with a microcomputer thermometer [Model HH-72T, Omega Engineering, Mississuaga, ON, Canada].

To avoid a headspace in the reservoir, the change in the liquid volume in the system due to sampling or mass transfer was compensated using a 10 ml hypodermic syringe [Becton Dickinson and Company, Franklin Lakes, NJ, USA] connected to the reservoir. About 1 ml of the solution was kept in the volume equalization syringe at all times to avoid the possibility of air entering the reservoir. This approach easily and inexpensively solved the potential headspace problem, eliminating the need for an expensive floating cover in a laboratory-scale setup.

Compressed air from an air cylinder [Praxair Products Inc., Mississauga, ON, Canada] was passed through a hydrocarbon/moisture trap [Model HMT200-4, Chromatographic Specialties Inc., Brockville, ON, Canada] and a constant temperature water bath before

entering the membrane module. An air rotameter with a precision valve [E-32112-8, Gilmont Accucal Flow-meter, Cole-Parmer Instrument Co, IL, USA.] was used for flows up to 7.5 x 10^{-5} m^3/s and a separate rotameter [F-504E, Blue White Flow-meter, Westminster, CA, USA] was used for flows greater than 7.5 x 10^{-5} m^3/s. The rotameters were calibrated with a wet test meter [Precision Scientific, IL, USA]. A precision digital pressure gauge [PG 5000, PSI-Tronix, Tulare, CA, USA] was used to monitor the pressure drop. Inline air temperatures were monitored before and after the module with a microcomputer thermometer [Model HH-72T, Omega Engineering, Mississuaga, ON, Canada]. The stripped air was released to a fume hood or passed through a cryo focus (cold trap) to trap the water vapor/chloroform by condensation for analysis.

During the experiments, the feed solution in the reservoir was kept homogenous using a magnetic stirrer and, unless otherwise stated, by feed recirculation. A required volume of reverse osmosis grade water was injected through the sampling port into the reservoir thirty seconds prior to each sample collection to compensate for the sample withdrawn for analysis as well as the reduction of liquid due to transport of water/VOC to the stripping air. Gas tight syringes [Hamilton Co., Reno, NV, USA] were used for sample collection. After each test with an aqueous solution of VOCs, the solution was drained from the system. Then, the system was filled with RO water and drained and refilled at least 4 times before the system was refilled with RO water. Water was then circulated for 3 to 4 hours with stripping air flow on the lumen side. Water was then drained and the system kept empty until the next test.

4.4 CHOICE OF ORGANICS FOR INVESTIGATION

Chloroform: Chloroform was chosen as it represents aliphatic halogenated hydrocarbon. It has been investigated by other researchers at its low concentrations (ppb) using MAS systems with air in the shell and the solution in the lumen side and thus, some experimental data are available for comparison.

Toluene: Toluene was chosen as a representative aromatic hydrocarbon and it is also included in the list of priority pollutants normally found in some contaminated groundwaters and many industrial wastewaters. No significant research has been reported for its removal from aqueous solution using polypropylene hollow fiber membrane air-stripping systems.

Selection of the range of concentrations of these VOCs in the aqueous solutions was based on the concentrations normally encountered in industrial wastewater. Some physicochemical properties of these compounds are given in Table 4.3.

4.5 ANALYTICAL METHODS AND EQUIPMENT

The analytical methods and equipment used for analysis of the samples differed from experiment to experiment. The choice of methods and equipment was very difficult due to the wide range of concentrations studied. More than one method was used to analyze the same sample to minimize errors. A TOC analyzer was used only to quantify the VOC concentration in the samples collected from MAS tests involving aqueous solutions of a single VOC. Conversions from TOC/TC values to VOC concentrations were carried out

using the ratio of molecular weight of VOC to its carbon content in a molecule. For example, molecular weight (MW) of chloroform is 119.39 g/mole and its carbon content (c) is 12.01 g/mole of chloroform, thus the MW/c ratio is 9.9483. As TOC analyzer gives a lumped value and cannot distinguish individual compounds, gas chromatography was used from time to time to establish the contribution of carbon from sources other than VOC to the measured TC/TOC. The samples from the mixture of VOCs were analyzed by gas chromatography only. Analytical methods and equipment are briefly presented below.

Table 4.3 Physicochemical properties of compounds used in this study

Compound	Temp. °K	Raoult's law constant	X^{w}_{sat}, ppm	D_c x10^5 m^2/s	D_{Kn} x10^4 m^2/s	D_w x10^9 m^2/s
Water	294	0.0245[1]	15246[2]	2.50[3]	5.88[4]	
Chloroform	296			0.923[3]	2.29[4]	0.893[5]
Toluene	296			0.816[3]	2.61[4]	0.855[6]

[1] Raoult's law constant for water calculated assuming 100% pure water.

[2] X^{w}_{sat} = Saturated water concentration in air, calculated from saturated vapor pressure of water in air.

[3] D_c= Continuum diffusion coefficient of the component in air phase, calculated using the correlation given by Fuller et al. (1966).

[4] D_{Kn} = Knudsen diffusion coefficient, calculated using the correlation given by Cussler (1984).

[5] Diffusion coefficient of chloroform in water, calculated using the correlation given by Wilke and Chang (1955), multiplied with a factor of 0.9 to match the observed deviation by Smith et al. (1980), Roberts and Dändliker (1983) and Cussler (1984).

[6] Diffusion coefficient of toluene in water, calculated using the correlation given by Wilke and Chang (1955).

4.5.1 Total Carbon Analyzer

The TC and the TOC of the feed in the reservoir were determined by a TOC analyzer [Model TOC-5050, Shimadzu Corporation, Kyoto, Japan]. The concentration range of the TOC analyzer was 50 ppb to 4,000 ppm for TC and 50 ppb to 5,000 ppm for IC. The furnace of the total carbon analyzer was maintained at 680°C. The carrier gas was

ultrapure grade compressed air [Praxair Canada Inc., Mississauga, ON, Canada] at a flow rate of 150 ml/min. Twenty five percent orthophosphoric acid was used in the IC chamber of the TOC analyzer. The sample size was 26 µl for TC/TOC. An auto-sampler [Model ASI-5000, Shimadzu Corporation, Kyoto, Japan] was used for sample injection. The principles of operation and standards preparation were according to the manufacturer's manual and Standard Methods (Greenberg et al., 1992). Calibration was repeated frequently and a standard was analyzed prior to the analysis of each batch of samples that normally consisted of 8 to10 samples.

4.5.2 Gas Chromatograph (Purge & Trap)

The gas chromatograph (purge and trap), referred to as GC (P&T) hereafter, included a gas chromatograph [Varian - Vista Series 6000, Varian Instrument Group, Walnut Creek Division, Walnut Creek, CA] to which a liquid purge and trap sample concentrator [Tekmar- LSC -2, Tekmar Company, Cincinnati, OH] was attached. The GC system also included a flame ionization detector (FID), a packed column [Carbopack B 60/80 Mesh, 1% SP-1000, 8 feet by 1/8 inch SS, Supelco Canada Ltd., Oakville, ON] and an integrator [Waters 820 Chromatography Data Station, Water Chromatography Division, Millipore Corporation, Milford, MA]. As water can deteriorate the chromatographic column as well as extinguish out the flame, purge and trap unit was used to avoid injection of aqueous samples directly into the gas chromatograph. Another reason for the use of a purge and trap unit was that the injection of a large sample (5 ml) provided a better detection limit (down to 60 ppb for chloroform).

When necessary, reverse osmosis grade water was added to the samples for dilution purpose. The dilution factors were varied depending on the concentration of the samples. A detailed description of this GC (P&T) setup was presented by Lamarche (1986). As GC (P&T) was used mainly to analyze the low concentration of chloroform in the samples collected at the end of MAS tests, the calibration was conducted in the range of 0 to 11 ppm. Calibration detail is given in Appendix - A. Calibration was checked via three injections from a freshly prepared standard solution. No internal standard was used. The retention time for chloroform was around 12.6 minutes. The flow conditions, purge and trap settings, GC and Waters 820 data stations settings are given in Tables 4.4, 4.5 and 4.6, respectively.

Table 4.4 Flow conditions of gases for GC (P&T)

Purpose	Gas	Pressure, kPa	Flow rate, ml/min
Carrier gas	UHP* Nitrogen	531	30
Purge gas	UHP Nitrogen	138	40
Detector gas	Carbon free air	414	250-300
Detector gas	UHP Hydrogen	276	30

*Ultra high pure

Table 4.5 Purge & Trap settings

Time operations	Time, min	Temperature operation	Temperature, °C
Purge	11	Purge ready	40
Desorb	4	GC oven	50
Bake	7	Desorb preheat	115
		Desorb	180
		Bake	210

Table 4.6 GC (P & T) and Waters 820 Data Station settings

Analysis settings		Temperature settings		Water 820 Data Station	
Items	Value	Item	Values	Items	Value
Auto zero	OFF	Initial temp.	45 °C	Data acquisition	2 points/sec
Attenuation	128	Initial time	3 min	Coarse sensitivity	500
Sensitivity range	10^{-12}	Program	8 °C/min	Fine sensitivity	500
Zero	No	Final temp.	220 °C	Baseline points	10
		Final time	12 min		
		Detector temp.	220 °C		

4.5.3 HP6890 Gas Chromatograph

The gas chromatograph [HP 6890 series GC System, Hewlett Packard, Wilmington, DE], referred to as GC6890 hereafter, had a FID, a capillary column [SPB-5, 30m x 0.53mm, 1.5 μm film, Supelco Canada Ltd., Oakville, ON] and was connected to an integrator [HPGC Chem Station, Hewlett Packard, Wilmington, DE]. The flow conditions, GC and chem stations settings are given in Table 4.7 and 4.8, respectively. The enhanced integration method was used.

Table 4.7 Flow conditions of gases for GC6890

Purpose	Gas	Pressure, kPa	Flow rate, ml/min
Carrier gas	UHP Helium	56.74	5.0
Detector make up gas	UHP Helium	56.74	15.0
Detector gas	Carbon free air		250.0
Detector gas	UHP Hydrogen		22.0

Two methods were developed for sample analysis. Their characteristics are given in Table 4.9. In the first method the sample was injected directly into the column, its temperature was kept at 110°C to avoid condensation of water in the column. This

method was used from time to time when the aqueous solution involved only single VOC, i.e., either chloroform or toluene, as solute. The data obtained by this method were used to determine the presence of organic compounds other than the solute (chloroform or toluene) and their contribution to the TOC values.

Table 4.8 GC6890 and Chem Station settings

Analysis settings		Chem Station			
Items	Value	Items	Value	Items	Value
Zero	OFF	Data acquisition	200 Hz	Initial pick width	0.0202
Attenuation	0	Slope sensitivity	236.88	Initial area reject	0.585
Sensitivity range	0	Min. Pick width	0.001	Initial height reject	0.242

Table 4.9 GC6890 methods of analysis

Direct injection of water sample		Injection of extracted sample in n-pentane	
Item	Values	Items	Value
Initial temp.	110 °C	Initial temp.	60 °C
Initial time	2 min	Initial time	2 min
Program	30 °C/min	Program	35 °C/min
Final temp.	200 °C	Final temp.	280 °C
Final time	0 min	Final time	1.71 min
Detector temp.	280 °C	Detector temp.	280 °C

In the second method, the VOC(s) was (were) extracted in n-pentane before sample injection. 950 µl of aqueous sample and 950 µl of n-pentane were mixed in a 2 ml GC vial. About 100 µl of headspace was left to avoid overflow of sample/n-pentane during addition. The vial was shaken manually. The aqueous solution and VOC laden n-pentane separated spontaneously into two phases. 2 µl of VOC laden n-pentane was injected

directly into GC column. The remaining water after partitioning of VOC into n-pentane was frequently tested for the presence of VOCs. Retention times for chloroform and toluene were approximately 2.53 and 3.82 minutes, respectively, for this method. Calibration details are presented in Appendix - B. This second method was used when the aqueous solution included toluene individually or when both chloroform and toluene were present in the aqueous solution.

4.6 DESCRIPTION OF THE EXPERIMENTS CONDUCTED

The experiments were carried out at ambient temperature. Since the removal efficiency becomes higher at lower solution velocity (see section 3.5), the solution flow rates were kept as low as possible. Care should be taken, however, to maintain the pressure on the shell side (solution side) higher than that on the lumen side (air side), otherwise air will enter into the shell side. The economical and technical aspects of stripped-air treatment were the other reasons for selection of low air flow rates.

4.6.1 Experiments for Water Transport

These experiments were conducted to determine the rate of water transport across the membrane. Two types of experiments, referred to as dry and wet tests, were performed. In dry tests, the shell side of the membrane module was dried by an air stream for over 72 hours prior to the experiments. Then, the shell side of the module was filled with water, which was circulated for 30 minutes to remove any trapped air. The stripping air flow on the lumen side was started 10 minutes prior to the collection of the first sample to stabilize the system. In wet tests, the shell side of the membrane module was filled with

water, which was circulated for 48 hours prior to starting the stripping air flow. The reason for selecting 48 hour contact period with water is given under results and discussion (Section 6.3). The stripping air flow was allowed for 30 minutes to attain steady-state and to remove any condensed water in the lumen side of the hollow fibers prior to air sampling.

The total amount of water transported from the water phase (shell side) to the air phase (lumen side) was measured by trapping water vapor in the stripping air as it exited the module using a cryo focus trap immersed in liquid nitrogen. The transport rate was determined by weighing the amount of water condensed during a predetermined period. Stripping air flow rates were varied from 1.75×10^{-5} to 5.00×10^{-5} m^3/s and the liquid flow rate was maintained at 6.33×10^{-5} m^3/s. Pressure drops for air and water were about 0.5 to 2.0 and 20.0 kPa, respectively. Water and air temperatures were maintained at $21.0 \pm 0.2^{\circ}C$. The run times were between 10 and 61 minutes. A number of replicates were conducted at each air flow rate.

4.6.2 Experiments for the Removal of Chloroform from Aqueous Solutions

In these experiments, both dry and wet tests were conducted. For both tests, concentrated chloroform solutions were prepared in a separate flask and the required volume was transferred to the MAS system reservoir.

The dry tests were conducted as follows:

a) The shell side of the membrane module was dried by an air stream for over 72 h prior to the experiments.

b) The reservoir was filled to a desired level with RO grade water.

c) The remainder of the reservoir was filled with the concentrated chloroform solution.

d) The pump was started to fill the rest of the system (feed circulation line and the shell side of the module) while additional water was added. Trapped air, if any, was purged from the system. The feed solution was mixed by vigorous stirring in addition to circulation through the system for 60 minutes prior to starting the stripping air flow.

e) The first solution sample was collected from the reservoir 10 minutes after starting the stripping air flow to insure the system had stabilized.

The wet tests were conducted as follows:

a) The reservoir was filled with RO grade water, which was circulated for 48 h.

b) Before adding the concentrated chloroform solution, stripping air was passed in the lumen side for 30 minutes to remove any accumulated condensed water on the lumen side of the fibers and to stabilize the system.

c) When the concentrated chloroform solution was added to the reservoir, an equal quantity of water was drained while water circulation was continued through the module.

f) Trapped air, if any, was purged from the system. The feed solution was mixed by vigorous stirring in addition to circulation through the system for 60 minutes prior to starting the stripping air flow.

g) As in the dry tests, the first solution sample was collected from the reservoir 10 minutes after starting the stripping air flow to permit the system to stabilize.

The samples were collected from the reservoir for analysis every 10 minutes in the beginning but the interval was increased at later stages. Stripping air flow rates were varied from 3.33×10^{-5} to 8.33×10^{-5} m^3/s, while the liquid flow rate was kept constant at 3.33×10^{-5} m^3/s. Initial chloroform concentrations in the feed solutions were 680 ± 30 ppm. The temperature of the solution as well as the air was kept at 23.0±0.2°C. The pressure drops for the air side and solution side were 1.2 to 3.0 and 10.0 kPa, respectively. The total run times for dry and wet tests were 140 and 160 minutes, respectively.

The following analyses were conducted when the feed aqueous solution involved only chloroform. The feed concentration in the reservoir was analyzed for TC regularly while TOC was periodically analyzed to determine the presence of any IC. In addition, some samples collected towards the end of experiments were analyzed using GC (P&T) to determine the chloroform concentration. It has been stated in Section 4.5, these analyses were conducted to establish the contribution of carbon from sources other than chloroform to the measured TC/TOC. Additionally, all the samples from a number of tests with chloroform were analyzed using either both TOC analyzer and GC (P&T) or both TOC analyzer and GC6890 to identify other compounds in the samples. Samples were collected using gas tight syringes [Hamilton Co., Reno, NV].

4.6.3 Effect of Feed Chloroform Concentration on the Overall Mass Transfer Coefficient

The impact of the feed chloroform concentration was ascertained via wet tests, conducted in the same method as described in Section 4.6.2 except stripping air flow rate was kept constant at 5.83×10^{-5} m^3/s. The initial feed chloroform concentrations were in the range of 50 to 1000 ppm. These tests were carried out as a preliminary investigation on the possibility of using MAS process for removal/recovery of VOCs from industrial wastewater having a wide range of VOC concentrations. The analysis of the samples were the same as described in Section 4.6.2.

4.6.4 Experiments for the Removal of Toluene from Aqueous Solutions

Only wet tests were conducted as described in Section 4.6.2. Stripping air flow rates were varied from 3.33×10^{-5} to 7.50×10^{-5} m^3/s, while keeping the liquid flow rate constant at 3.33×10^{-5} m^3/s. Initial toluene concentrations in the feed solutions were within 170 ± 30 ppm. The temperature of the solution as well as the air was kept at 23.0 ± 0.2 °C. The pressure drops on the air side and solution side were 1.2 to 2.5 and 10.0 kPa, respectively. The total run times were 160 minutes

Analyses of the samples were usually conducted using the TOC analyzer. All the samples from a number of tests were analyzed using both TOC analyzer and GC6890 to identify any compounds other than toluene in the solution to ascertain their contribution to the TC values.

4.6.5 Experiments for the Removal of Mixture of Chloroform and Toluene from Aqueous Solutions

In these experiments, only wet tests were conducted in the same way as described in Section 4.6.2. Stripping air flow rates were varied from 3.33 $x10^{-5}$ to 6.66 x 10^{-5} m^3/s, while the liquid flow rate was kept constant at 3.33$x10^{-5}$ m^3/s. The temperature of the solution as well as the air was kept at 23.0±0.2 °C. The pressure drops on the air side and solution side were 1.2 to 2.3 and 10.0 kPa, respectively. The total run times were 160 minutes. Analyses of the samples were conducted using GC6890.

4.6.6 Determination of Henry's Law Constants

Although Henry's law constants can be determined by many experimental methods (Leighton and Calo, 1981; Munz and Roberts, 1982; Nirmalakhandan et al., 1997; Brennan et al., 1998; Altschuh et al., 1999), the method proposed by Munz and Roberts (1982) was used in this study. According to this method, H is determined directly by the measurement of the liquid phase concentration of a VOC that is in equilibrium with the air phase in a closed system. Gas tight syringes [Hamilton Co., Reno, NV] adapted with "Luer Lock" plugs were used for this experiment. The plugs were prepared by bending "Luer needles". 10 ml of stock solution was transferred into a syringe. The solution was left in the syringe for 1 h before determining its concentration, which was recorded as measured initial concentration, C_l. Then, the solution volume in the syringe was reduced to 5 ml. Subsequently, 5 ml of air was introduced into the syringe. A 24 h period was allowed to reach the equilibrium. During this period, the syringes were shaken 4 times,

for 2 minutes at each time. The liquid phase VOC concentration was measured after the 24 h equilibration period and was recorded as equilibrium concentration, C^*.

Although, the syringes were gas tight, the possibility of losses of VOCs during this 24 hour period should not be ignored (Lamarche, 1988; Lamarche and Droste, 1989). To take into account any loss of VOCs from the syringe during this 24 hours period, loss tests were conducted in the following way. As in H determination, 10 ml of stock solution was transferred into a syringe. The solution was left in the syringe for 1 h before determining its concentration, which was recorded as initial concentration of loss test, C_i. Then, the solution volume in the syringe was reduced to 5 ml. Unlike H determination, no air was introduced into the syringe after that. The 5 ml solution was left in the syringe for another 24 hours. During this 24 h period, the syringes were shaken 4 times for 2 minutes at each time as was done for H determination. After this 24 h period, the VOC(s) concentration in the solution was determined and recorded as final concentration of loss test, C_f. The ratio of C_f/C_i was calculated for each syringe for each VOC. C_l was multiplied by this ratio to obtain the estimated initial concentration, C_o. The ratio accounts for the loss of VOCs in the syringe

The mass balance of the VOC for the syringe was as follows:

$$C_o V_L = C^* V_L + X V_a \qquad (4.1)$$

where:
C_o = estimated initial concentration of the VOC in the liquid phase, ppm.
V_L = volume of the liquid, m^3
C^* = equilibrium concentration in the liquid phase after 24 h, ppm
X = equilibrium concentration in the air phase, ppm

V_a = volume of the air, m^3

Solving the above equation for X and substituting in eqn. (3.5) yields:

$$H = \frac{(C_0 - C^*)V_L}{C^* V_a} \tag{4.2}$$

As $V_L = V_a$, the above equation can be rewritten as:

$$H = \frac{C_0}{C^*} - 1 \tag{4.3}$$

Thus, only initial and equilibrium liquid phase concentrations were needed for calculating H. The chloroform samples were analyzed by TOC analyzer. The toluene samples were analyzed by GC6890.

Experiments for binary chloroform/toluene solutions were conducted by the same methods. The samples were analyzed by GC6890.

4.6.7 Adsorption Tests

Adsorption tests were conducted to determine the amount of VOC adsorbed on the polymer surfaces, with which the feed solution was in contact. The experimental steps are described below:

a) The total volume of the liquid in the system, which includes the reservoir, the pump, the rotameter, the shell side volume of module, connecting tubes and valves, was first determined. It was found to be 7.03×10^{-3} m^3.

b) Module air inlet and outlet were sealed tight with glass plugs to avoid any air circulation.

c) The system was filled with water, which was circulated in the system for some time.

d) The circulation of water was stopped. Feed circulation line's inlet and outlet valves were closed (Fig. 4.1), thus the pump, the rotameter, the module and the connecting tubes were isolated from the reservoir. Then, the water from the reservoir was partly drained.

e) A VOC solution was prepared in a separate flask and was transferred to the reservoir (volume of the reservoir was 6.675×10^{-3} m^3). The solution was stirred with a magnetic stirrer. A sample was collected from the reservoir for analysis.

f) The reservoir was connected to the system by opening the valves. The solution was circulated in the system for 60 minutes. The final sample was collected from the reservoir for analysis.

Samples were analyzed by a TOC analyzer when the adsorption tests were conducted for chloroform, while the GC6890 gas chromatograph was used when tests were conducted for toluene. Experiments were conducted at four different concentrations for each VOC at 23 ±0.2°C.

4.6.8 Effect of Headspace

Experiments were carried out to determine the magnitude of the transfer of VOCs from water to the headspace (i.e., the space filled with air above the liquid level) in the reservoir using chloroform as a model compound. The volume of the solution in the reservoir depended on the solution level, which is indicated as A, B, C and D (Fig.4.2). The total solution volume in the reservoir when completely filled was 6.675×10^{-3} m^3.

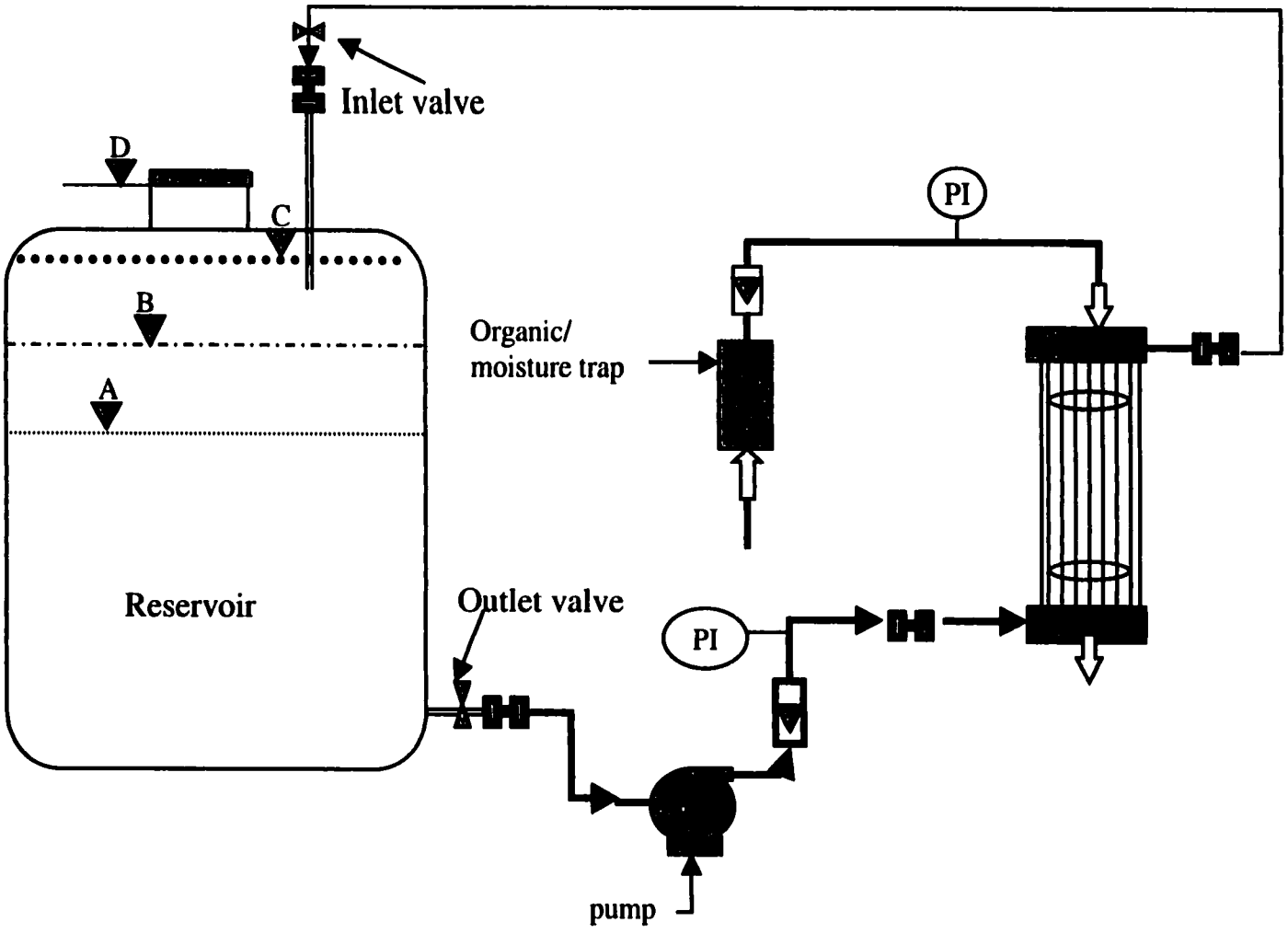

Figure 4.2 Liquid Levels during Headspace Tests

The feed solutions were prepared in the reservoir in the following way. The reservoir was rinsed thoroughly several times with RO water. The inlet and outlet valves were closed (Fig. 4.2). The reservoir was then filled with a known volume of water and closed with a septum. A required quantity of chloroform, known by weighing the syringe before and after injection of chloroform into the reservoir, was added to the water through the septum with a syringe. The chloroform was dissolved in water by the aid of a magnetic stirrer. After dissolution of chloroform was completed, the solution was mixed for another 120 minutes. The mixing was stopped before the sample was collected for TC analysis. The experiments were duplicated at 23 $\pm$0.2°C for each level.

The detailed results of the tests have been presented in Appendix – C. It was observed that the volume of headspace had a significant effect on amount of chloroform transferred from the liquid phase to the air phase. The transfer of chloroform increased with the increase of the volume of headspace. The total reduction in chloroform concentrations of the solution varied from 2.82% at solution level C to 10.76% at solution level A. This was expected due to the tendency of VOC to partition into the two phases according to basic thermodynamic principles. This partitioning is enhanced by the physical mixing (agitation) provided during the MAS process.

Given the significant changes in concentration caused by the presence of headspace, they should be accounted for or it would lead to an erroneous result in the mass transport calculations. Accordingly, all other experiments in this study were conducted without headspace (i.e., solution level at height D in Fig. 4.2) to avoid this problem.

4.6.9 Reverse Stripping Tests

Reverse stripping tests were carried out using RO grade water as the feed liquid. These tests were conducted to quantify reverse stripping of any carbon from the stripping air flowing on the lumen side into the liquid phase flowing on the shell side. The tests were conducted twice to ensure reproducibility. The system was operated such that no air entered into the liquid part of the system. Stripping air and the liquid flow rate were maintained at 6.67 x 10^{-5} m^3/s and 3.33x10^{-5} m^3/s, respectively. The temperature was kept at 23 ±0.2°C. The total run times were 140 minutes. The samples were analyzed for TC.

The results showed no noticeable evidence of reverse stripping of organic compounds from air into water. Detailed results have been presented in Appendix - D.

4.6.10 Determination of Pressure Drops on Lumen and Shell Side of the Hollow Fiber

The pressure drops on the lumen side were determined by varying air flow rates from 0.5 x 10^{-3} m^3/min to 5.0 x 10^{-3} m^3/min. The pressure drops on the shell side were determined by varying water flow rates from 0.4 x 10^{-3} m^3/min to 4.0 x 10^{-3} m^3/min. The pressure drops were recorded with precision digital pressure gauges [PG 5000, PSI-Tronix, Tulare, CA, USA].

CHAPTER 5

Modeling

This chapter presents the development of the models to predict the water transport in the hollow fibers and to estimate the shell side water velocity. This chapter also specifies the correlations and equations found in the literature as well as the methodologies used for prediction of the mass transport in membrane air-stripping of VOC(s).

5.1 PREDICTION OF WATER TRANSPORT

The direct measurement of the membrane resistance by changing the membrane thickness is not possible for a hollow fiber. Reduction in the number of individual resistances was attempted for measuring the transport rate of water from the water phase on the shell side to stripping air flowing through the lumen of the hollow fiber. In such a system, since no liquid phase resistance exists for the transport of water, the following equation can be derived:

$$\frac{1}{K_L} = \frac{1}{K_G^w S} = \frac{1}{k_m^w S} + \frac{1}{k_a^w S} \tag{5.1}$$

where:

K_G^w = overall gas-phase based mass transfer coefficient for water, m/s

k_m^w = mass transfer coefficient due to membrane for water, m/s

S = dimensionless Raoult's law constant for water

k_a^w = local air-phase mass transfer coefficient for water, m/s

Note that Raoult's law constant is used instead of Henry's law constant because water is almost pure, thus its concentration is high. The change in water vapor concentration in the air stream in the longitudinal direction in the lumen side of a single hollow fiber is given under steady state conditions by (Fig. 5.1):

$$\frac{v^a dX^w}{dz} = K_G^w a(X_{sat}^w - X^w) \tag{5.2}$$

where:

$\frac{dX^w}{dz}$ = water vapor concentration gradient along length of fiber lumen, ppm/m

X^w = water vapor concentration in the air phase at distance z, ppm

X_{sat}^w = saturated water vapor concentration, ppm

Rearranging eqn. (5.2),

$$\frac{dX^w}{X_{sat}^w - X^w} = K_G^w \frac{a}{v^a} dz \tag{5.3}$$

Upon integration eqn. (5.3) yields

$$\ln(X_{sat}^w - X^w) = -\frac{K_G^w a}{v^a} z + Y \tag{5.4}$$

Where, Y is a constant. When $z = 0$, $X^w = 0$,

$$\ln X_{sat}^w = Y \tag{5.5}$$

Hence,

$$\ln\left(\frac{X_{sat}^w - X^w}{X_{sat}^w}\right) = -\frac{K_G^w a}{v^a} z \tag{5.6}$$

At the end of the module, when $z = L$ (length of the fiber), $X^w = X_L^w$, therefore,

$$\ln\left(\frac{X_{sat}^w - X_L^w}{X_{sat}^w}\right) = -\frac{K_G^w a}{v^a} L \tag{5.7}$$

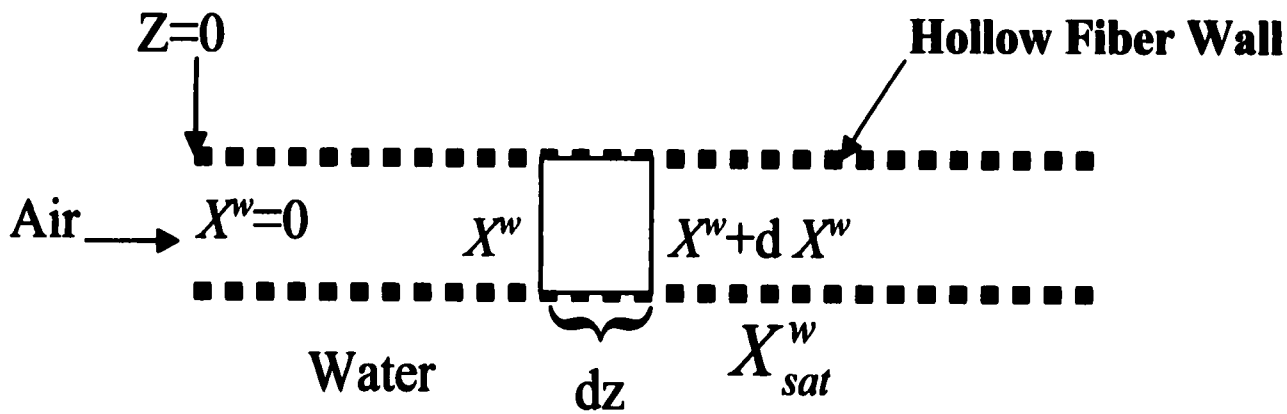

Figure 5.1 Change of Water Vapor Concentration in the Air Phase in Hollow Fiber

Rearranging eqn. (5.7),

$$X_L^w = X_{sat}^w (1 - e^{\frac{-K_G^w a L}{v^a}}) \tag{5.8}$$

K_G^w can be calculated using eqn. (5.1), knowing $\frac{1}{k_a^w S}$ and $\frac{1}{k_m^w S}$. The air phase mass transfer coefficient, $k_a^w S$ can be estimated by eqn. (5.9) developed from Lévéque's (1928) correlation, incorporating Raoult's law constant since the compound is pure water and the boundary layer is gaseous.

$$\frac{1}{k_a^w S} = \frac{0.617}{S} \left(\frac{L d_i}{v^a D_c^{w\,2}}\right)^{0.33} \tag{5.9}$$

where:

D_c^w = continuum diffusion coefficient of water in air phase, m^2/s

$\frac{1}{k_m^w S}$ can also be predicted using the following eqn. (5.10), which is similar to eqn. (3.17).

$$\frac{1}{k_m^w S} = \frac{\delta \tau}{D_{eff}^w \varepsilon S} \tag{5.10}$$

where:

D_{eff}^w = effective diffusion coefficient of water in air, m^2/s

The values of X_L^w predicted by eqn. (5.8) and X_L^w obtained experimentally will be referred to as predicted and experimental X_L^w, respectively. If the experimental and predicted X_L^w agree with each other, then the membrane transport is simply diffusion through air-filled pores. If they do not, some other mechanisms, such as surface diffusion and capillary condensation, should be considered.

5.2 ESTIMATION OF WATER VELOCITY OUTSIDE THE HOLLOW FIBERS

The water velocity outside the hollow fiber, u^w for the present study was estimated using the following approach. As shown in Fig. 5.2, the module used in this study contains a central baffle that deflects the liquid flow on the shell side in the module but not the air flow in the lumen side of the fibers. The baffle blocks the center tube so that the incoming liquid exits the center tube in the upstream half of the tube, perpendicular to the fibers creating cross flow. The liquid flows from the first compartment through the gap in between the middle baffle and the module housing to the second compartment. The liquid then flows across the fibers, enters the center tube and exits the module.

The water velocity in each compartment was first calculated assuming no hollow fibers in the module and then it was corrected using the void fraction. The length of each compartment, h, was half of the module length, L, as the module was blocked in the center. It was assumed that the center tube was perforated such that water would flow through the entire cross section of the center tube. Since the velocity of the liquid would decrease as it approached the module housing wall, a volume averaged velocity would be utilized in an empty module. Then

$$u' = \frac{\int \frac{Q_w}{2\pi r_c h} dr_c}{\int dr_c} \tag{5.11}$$

where:
r_c = module radial position ($r_{in} < r_c < r_{out}$, Fig. 5.2), m
r_{in} = outer radius of the center tube, m
r_{out} = inner radius of the membrane module, m

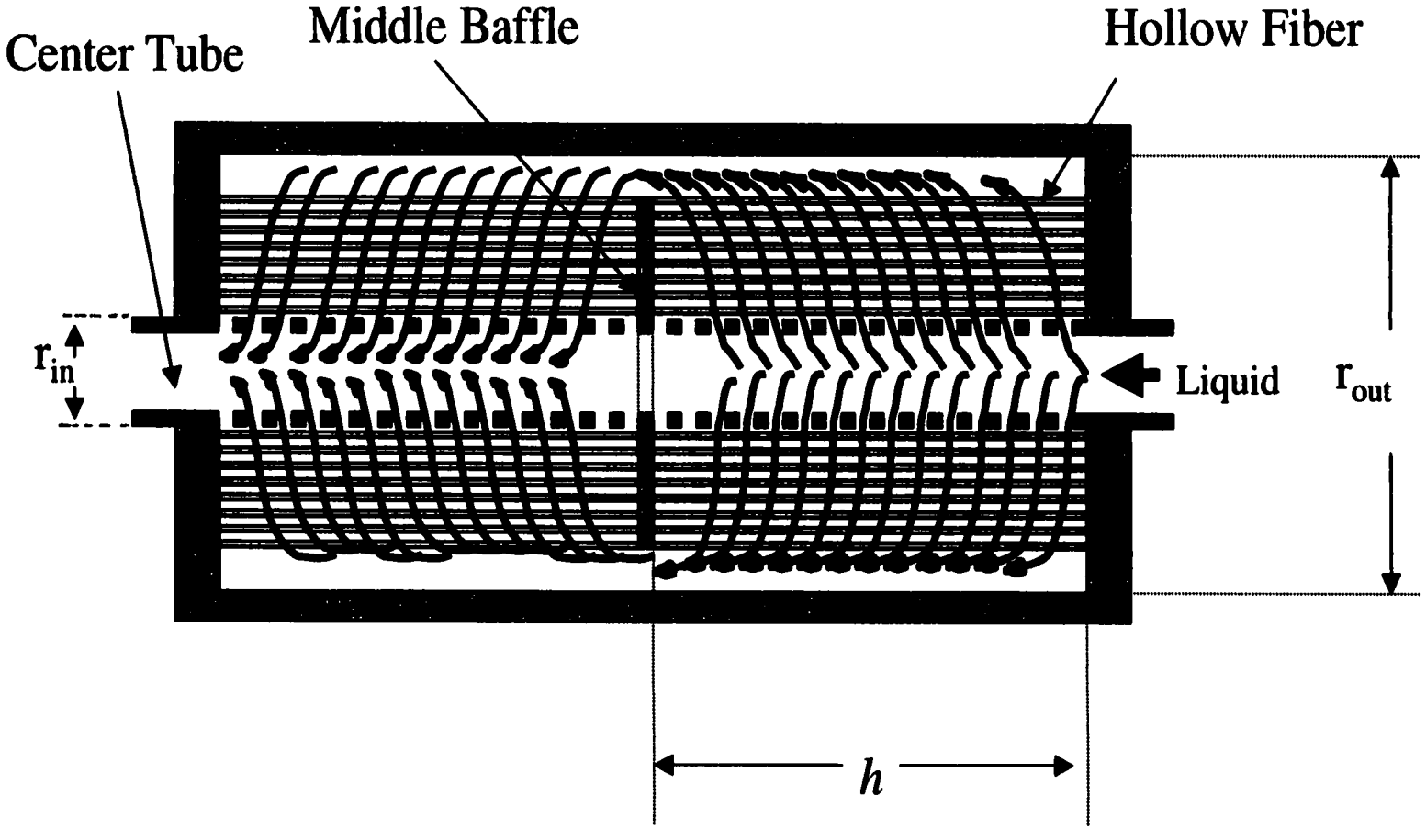

Figure 5.2 The Schematic View of Hollow Fiber Membrane Module with Liquid Cross-Flow on the Shell Side

$$u' = \frac{\frac{Q_w}{2\pi h} \ln r_c \Big|_{r_{in}}^{r_{out}}}{r_c \Big|_{r_{in}}^{r_{out}}} \tag{5.12}$$

$$u' = \frac{Q_w}{2\pi h} \frac{1}{r_{out} - r_{in}} \ln\left(\frac{r_{out}}{r_{in}}\right) \tag{5.13}$$

The final water velocity in between the hollow fibers in the module can be calculated by:

$$u^w = \frac{u'}{void\,fraction} \tag{5.14}$$

5.3 MODELING MEMBRANE AIR-STRIPPING OF INDIVIDUAL VOCs.

The local liquid phase mass transfer coefficients were predicted using eqns (3.11), (3.12) and (3.13). The air phase mass transfer coefficients were predicted using eqn. (3.14) and the membrane mass transfer coefficients were predicted using eqn. (3.17). The overall mass transfer coefficients were predicted combining the individual mass transfer coefficients as per eqn. (3.10). The observed overall mass transfer coefficients were obtained using eqns. (3.34) and (3.36). The predicted and the observed overall mass transfer coefficients were compared and further modeling was performed as discussed under results and discussion.

5.4 PREDICTION OF MAS FOR MIXTURE OF TWO VOCs.

Predictions were made for each compound assuming they were air-stripped separately, without interaction. Predicted values were compared with the results of MAS experiments of mixtures of two VOCs. Henry's law constants were measured for the

binary system experimentally to verify any interaction between the compound while partitioning between the water and the air phases. These results were used to verify the hypothesis of no interaction during air-stripping.

5.5 STATISTICAL ANALYSES

The following statistical analyses were performed on the data where possible.

$$\text{Sample mean (average), } \bar{y} = \frac{\sum_{i=1}^{n_s} y_i}{n_s} \tag{5.15}$$

where:
y_i = measured values of the samples, units
n_s = number of samples

$$\text{Sample standard deviation, STDEV} = \left[\frac{1}{n_s - 1}\sum_{i=1}^{n_s}(y_i - \bar{y})^2\right]^{0.5} \tag{5.16}$$

$$\text{Coefficient of variation, } cv = \frac{\text{STDEV}}{\bar{y}} \tag{5.17}$$

CHAPTER 6

Results and discussion

In this chapter, the results obtained in this study are presented and discussed in the following sequence. Results from adsorption tests are presented first as they have impact on the MAS of VOC(s). Henry's law constant is placed next as the measured values are used in the following sections. Results from water transport experiments are then presented. Chloroform transport is discussed after water transport as some important conclusions from the water transport experiments are further confirmed in this section. Some model equations are developed and their predictability of the current experimental results as well as those reported in the literature are discussed. Comparative performance of MAS for removal of chloroform is also presented, followed by the effect of chloroform concentration on its removal from aqueous solution. Removal of toluene from aqueous solution is discussed, which is followed by removal of mixture of chloroform and toluene from aqueous solution. Finally, the results from the pressure drop tests are discussed.

6.1 ADSORPTION TESTS

The results from the adsorption tests, conducted to determine the extent of VOCs adsorption on the polymer surface, are briefly presented below. The mass of the VOCs adsorbed was calculated using eqn. (6.1).

Mass of VOC adsorbed = $C_{ba}V_w - C_{aa}V_T$ (6.1)

where:
C_{ba} = concentration of the VOC in the reservoir before adsorption, ppm
C_{aa} = concentration of the VOC in the system after adsorption, ppm
V_w = volume of the reservoir, m^3
V_T = total volume of solution in the system, m^3

6.1.1 Chloroform Adsorption

The results from the chloroform adsorption tests are given in Table 6.1. It was found that the mass of chloroform adsorbed varied from 76 to 227 mg depending on the initial concentration of the solution. It should be noted that the system tested consists of polypropylene hollow fibers with an effective surface area of 1.4 m^2, a module housing made of polypropylene and connecting tubes made of Teflon®. The amount of chloroform adsorbed was linearly related to the initial solution concentration. This indicates that the chloroform adsorbed at the start of a MAS test, when the concentration was higher, and might be desorbed at later stages as the concentration decreases.

Table 6.1 Adsorption of chloroform

Initial (Before adsorption)			Steady state (After adsorption)			Adsorbed
Conc.	Solution volume	Mass of $CHCl_3$	Conc.	Solution volume	Mass of $CHCl_3$	Mass of $CHCl_3$
Ppm	10^3 x m^3	mg	ppm	10^3 x m^3	mg	mg
740	6.675	4941	671	7.025	4714	227
578	6.675	3860	526	7.025	3692	168
415	6.675	2772	378	7.025	2656	116
242	6.675	1612	219	7.025	1537	76

6.1.2 Toluene Adsorption

The results from the toluene adsorption tests are given in Table 6.2. It was found that the adsorption varied from 306 to 722 mg depending on the initial concentration of the solution. The masses of toluene adsorbed were much higher than those of chloroform at equivalent initial concentrations. This indicates that toluene has greater affinity for polypropylene/teflon.

Table 6.2 Adsorption of toluene

Initial (Before adsorption)			Steady state (After adsorption)			Adsorbed
Conc.	Solution volume	Mass of C_7H_8	Conc.	Solution volume	Mass of C_7H_8	Mass of C_7H_8
ppm	10^3 x m^3	mg	ppm	10^3 x m^3	mg	mg
410	6.675	2736	287	7.025	2014	722
337	6.675	2250	244	7.025	1712	539
333	6.675	2221	237	7.025	1666	555
202	6.675	1346	148	7.025	1039	306

6.2 HENRY'S LAW CONSTANT

As stated in section 4.6.6, the losses of VOCs from the syringes were determined and are presented in Table 6.3. The after loss factor C_f/C_i obtained for each syringe was taken into account when Henry's law constant was calculated.

H was determined for chloroform in three series of experiments. Each series consisted of eight syringes. In each series, H was obtained for eight different chloroform concentrations. The average value of H was calculated for all the 24 samples from these three series. The results from HLC determination of chloroform are presented in Table 6.4.

Table 6. 3 Loss of the VOCs in the syringes for test periods of 24 hours

Chloroform				Toluene			
Syringe	C_i, ppm[1]	C_f, ppm[2]	C_f/C_i	Syringe	C_i, ppm	C_f, ppm	C_f/C_i
1	688	665	0.966	1	477	457	0.956
2	407	387	0.962	2	443	420	0.948
3	237	225	0.951	3	415	385	0.927
4	133	126	0.948	4	353	326	0.922
5	74	72	0.970	5	264	256	0.968
6	43	42	0.974	6	183	176	0.962
7	15	14	0.935	7	156	141	0.907
8	5	5	1.000	8	109	101	0.921

[1] C_i = initial concentration of loss test
[2] C_f = final concentration of loss test after 24 h

The final value of H for chloroform obtained from averaging all 24 samples at 23°C is 0.1512. All experimental data are presented in Fig. 6.1 as dimensionless Henry's law constant, H, versus initial chloroform concentration. The figure shows no evidence of any effect of initial chloroform concentration on Henry's law constant in the concentration range studied.

The results from H determination of toluene are presented in Tables 6.5 to 6.7. Unlike chloroform, one single toluene solution was used to fill all the eight syringes of a series when H for toluene was determined. Thus, the results are presented in three separate tables as the variation in C_l is thought to give some idea on the errors arising from sample handling and GC6890 analysis.

Table 6.4 Henry's law constant determination for chloroform

Series	Syringe #	C_l, ppm[1]	C_o, ppm[2]	C^*, ppm[3]	H
1st	1	855.55	826.73	712.90	0.1597
	2	529.75	504.24	443.59	0.1367
	3	327.40	311.43	267.91	0.1624
	4	191.50	181.49	163.35	0.1111
	5	119.48	115.94	101.77	0.1392
	6	67.45	65.73	56.80	0.1571
	7	41.58	38.87	32.93	0.1803
	8	24.77	24.77	21.29	0.1636
2nd	1	880.62	850.96	736.97	0.1547
	2	529.70	494.67	433.94	0.1399
	3	321.13	305.47	266.71	0.1453
	4	194.29	184.13	165.24	0.1143
	5	122.66	119.03	100.58	0.1835
	6	75.61	73.68	65.66	0.1221
	7	51.03	47.70	43.18	0.1048
	8	36.51	36.51	29.84	0.2233
3rd	1	869.28	840.00	732.99	0.1460
	2	546.76	520.43	450.16	0.1561
	3	318.94	303.38	268.60	0.1295
	4	190.21	180.27	160.37	0.1241
	5	111.12	107.83	92.62	0.1643
	6	62.18	60.59	52.23	0.1601
	7	38.30	35.80	30.14	0.1876
	8	21.99	21.99	18.90	0.1632
$\bar{y}$					0.1512
STDEV					0.02715
cv					0.17954

[1] C_l = measured initial concentration
[2] $C_o = C_l \times C_f/C_i$ = estimated initial concentration after loss of chloroform during 24 h,
[3] C^* = equilibrium concentration after 24 h, ppm

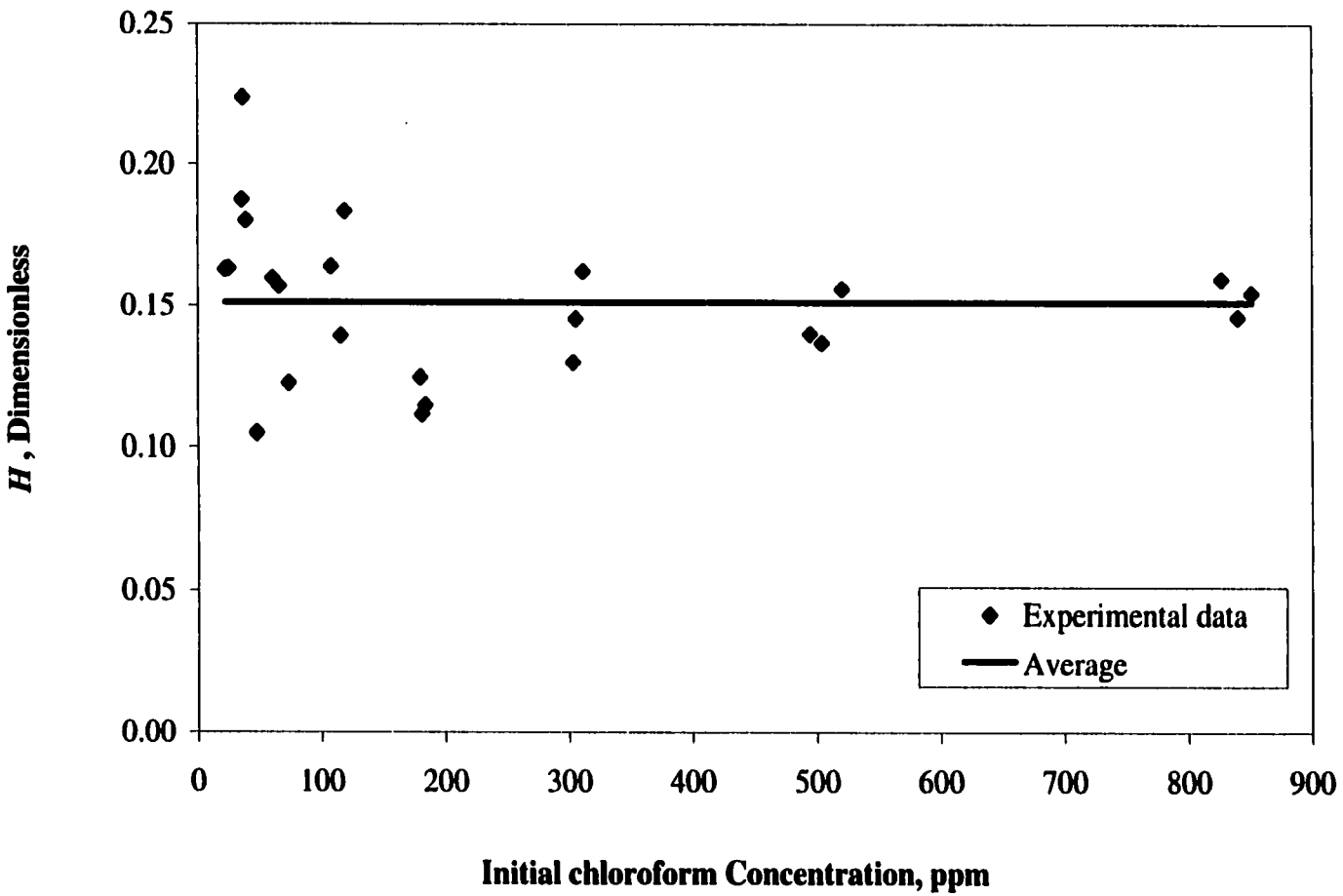

Figure 6.1 Effect of Initial Chloroform Concentration on Its Henry's Law Constant

Table 6.5 Henry's law constant determination for toluene (1st series)

Syringe #	C_l, ppm	C_o, ppm	C^*, ppm	H
1	220.06	210.34	166.64	0.2623
2	218.71	207.34	164.93	0.2572
3	214.67	199.01	164.36	0.2108
4	213.33	196.76	159.54	0.2333
5	229.74	212.74	162.28	0.3109
6	218.84	210.51	168.30	0.2508
7	215.96	195.79	166.54	0.1756
8	215.84	198.81	169.84	0.1706
$\bar{y}$	217.14			0.2339
STDEV	2.5166			0.0471
cv	0.0116			0.2012

Table 6.6 Henry's law constant determination for toluene (2nd series)

Syringe #	C_l, ppm	C_o, ppm	C^*, ppm	H
1	195.73	187.09	184.41	0.0145[1]
2	222.77	211.19	205.64	0.0270[1]
3	208.18	193.00	156.25	0.2352
4	212.06	195.59	159.54	0.2260
5	216.57	209.67	170.39	0.2305
6	221.27	212.85	168.30	0.2647
7	216.16	195.96	158.60	0.2356
8	223.14	205.53	169.84	0.2102
$\bar{y}$	214.49			0.2337[2]
STDEV	9.2104			0.0178[2]
cv	0.0429			0.0763[2]

[1] Apparent outliers as they differ by an order of magnitude from the rest.
[2] Result excluding outliers.

From the results presented in Tables 6.5 to 6.7, the average H value obtained from averaging all 22 samples at 23°C for toluene is 0.2305 with a standard deviation of 0.043973 and coefficient of variation, *cv* of 0.190749.

Table 6.7 Henry's law constant determination for toluene (3rd series)

Syringe #	C_l, ppm	C_o, ppm	C^*, ppm	H
1	215.22	205.71	166.64	0.2345
2	221.50	209.98	164.93	0.2732
3	214.35	198.71	164.36	0.2090
4	219.71	202.64	159.54	0.2702
5	215.27	208.42	162.28	0.2843
6	215.93	207.70	168.30	0.2341
7	214.33	194.31	174.82	0.1115
8	217.84	200.65	169.84	0.1814
$\bar{y}$	216.77			0.2248
STDEV	2.6534			0.0574
cv	0.0122			0.2555

The literature values of H obtained for chloroform and toluene at temperatures close to 23°C are presented in Table 3.1. Comparison was made in Table 6.8 between H values obtained in this study and those estimated by using Henry's law constant versus temperature correlations. The agreement of data seems reasonable with the literature values summarized in Table 3.1 and the estimated values given in Table 6.8.

Table 6.8 Comparison among the observed and estimated values of H at 23°C

Source	Chloroform	Toluene	Remark
Present Study	0.1512 ± 0.027	0.2305 ± 0.044	
Singley et al., 1980	0.2369	0.2372	Using eqn. (3.9)
Lamarche and Droste, 1989	0.1593	0.1973	Using eqn. (3.9)
Leighton and Calo, 1981	0.1486	0.2417	Using eqn. (3.8)
Kavanuagh and Trussell, 1980	0.1475		Using eqn. (3.7)

The results from the experiments conducted to determine HLC for the mixture of chloroform and toluene are presented in Tables 6.9 and 6.10, respectively. The eight syringes were filled with the same solution.

Table 6.9 Henry's law constant determination for chloroform in the mixture

Syringe #	C_l, ppm	C_o, ppm	C^*, ppm	H
1	824.29	813.65	710.82	0.1447
2	831.85	791.93	712.55	0.1114
3	839.30	798.17	712.52	0.1202
4	860.39	815.65	685.48	0.1899
5	841.56	816.31	706.32	0.1557
6	830.13	808.54	696.02	0.1617
7	801.83	749.71	673.74	0.1128
8	828.54	828.54	685.12	0.2093
$\bar{y}$	834.48			0.1507
STDEV	16.616			0.0360
cv	0.0199			0.2388

Table 6.10 Henry's law constant determination for toluene in the mixture

Syringe #	C_l, ppm	C_o, ppm	C^*, ppm	H
1	257.46	246.09	199.99	0.2305
2	255.68	242.39	199.74	0.2135
3	256.11	237.43	198.85	0.1940
4	255.93	236.04	191.64	0.2317
5	255.69	247.55	190.82	0.2973
6	264.80	254.72	219.44	0.1608
7	245.66	222.71	175.13	0.2716
8	256.19	235.97	183.52	0.2858
$\bar{y}$	255.95			0.2356
STDEV	5.1644			0.0470
cv	0.0202			0.1996

These results indicate that there was practically no effect of one compound on the other in respect of partitioning. The H for chloroform alone was 0.1512 ± 0.027 compared to 0.1507 ± 0.036 when measured from a binary aqueous solution of chloroform/toluene. The H for toluene was 0.2305 ± 0.044 alone versus 0.2356 ± 0.047 when measured from a binary aqueous solution of chloroform/toluene. Thus, the H of one VOC was not impacted by the presence of the other VOC.

6.3 WATER TRANSPORT

Preliminary experiments conducted to determine the water transport showed very scattered values for X_L^w, the water concentration in the stripping air at the exit of the membrane module, even at constant air flow rate and temperature (Fig. 6.2). The accuracy in the measurement of the parameters, such as temperature, air flow were double checked and were found not responsible for this inconsistence of X_L^w. Later, it was found that the contact time of the membrane with water during the test period had not been controlled in the preliminary experiments. Fig. 6.3 shows the change of X_L^w with a change of membrane's contact time with water in an experiment with continuous air and water flows (Appendix - E). It was noticed that X_L^w was almost equal to X_{sat}^w in the beginning, decreased gradually with an increase in contact time and then leveled off within 24 to 30 h. An experiment was also conducted without having a continuous air flow on the lumen side. Air flow was resumed from time to time during this experiment and each time water vapor was trapped in the condenser 30 minutes after the air flow was resumed. The results of this experiment, also shown in Fig. 6.3, are almost the same as those of continuous air flow experiment. From these observations, it was hypothesized that some form of wetting/blocking of the membrane pores might have occurred as a result of extended contact with water and that this phenomenon stabilized within 30 h. Another experiment, in which air flow was started after 48 hours of membrane/water contact, showed a similar result (see Fig. 6.3). On the basis of these results, a 48 h pre-wetting period was chosen to ensure that the MAS tests were conducted under steady-state conditions with respect to the wetting. Fig. 6.4 shows X_L^w observed for wet and dry

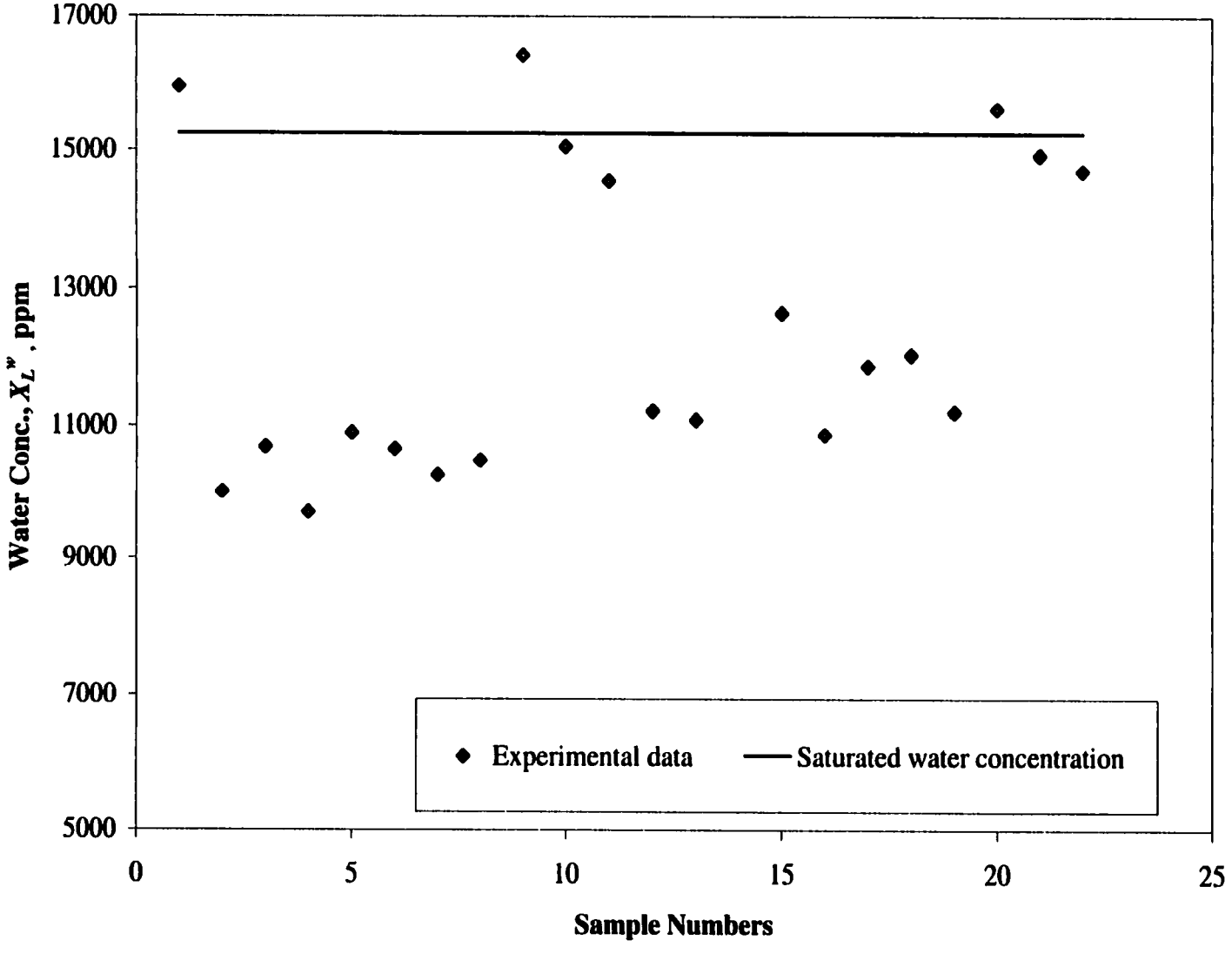

Figure 6.2 Water Concentration in the Exit Air Observed in Preliminary Experiments

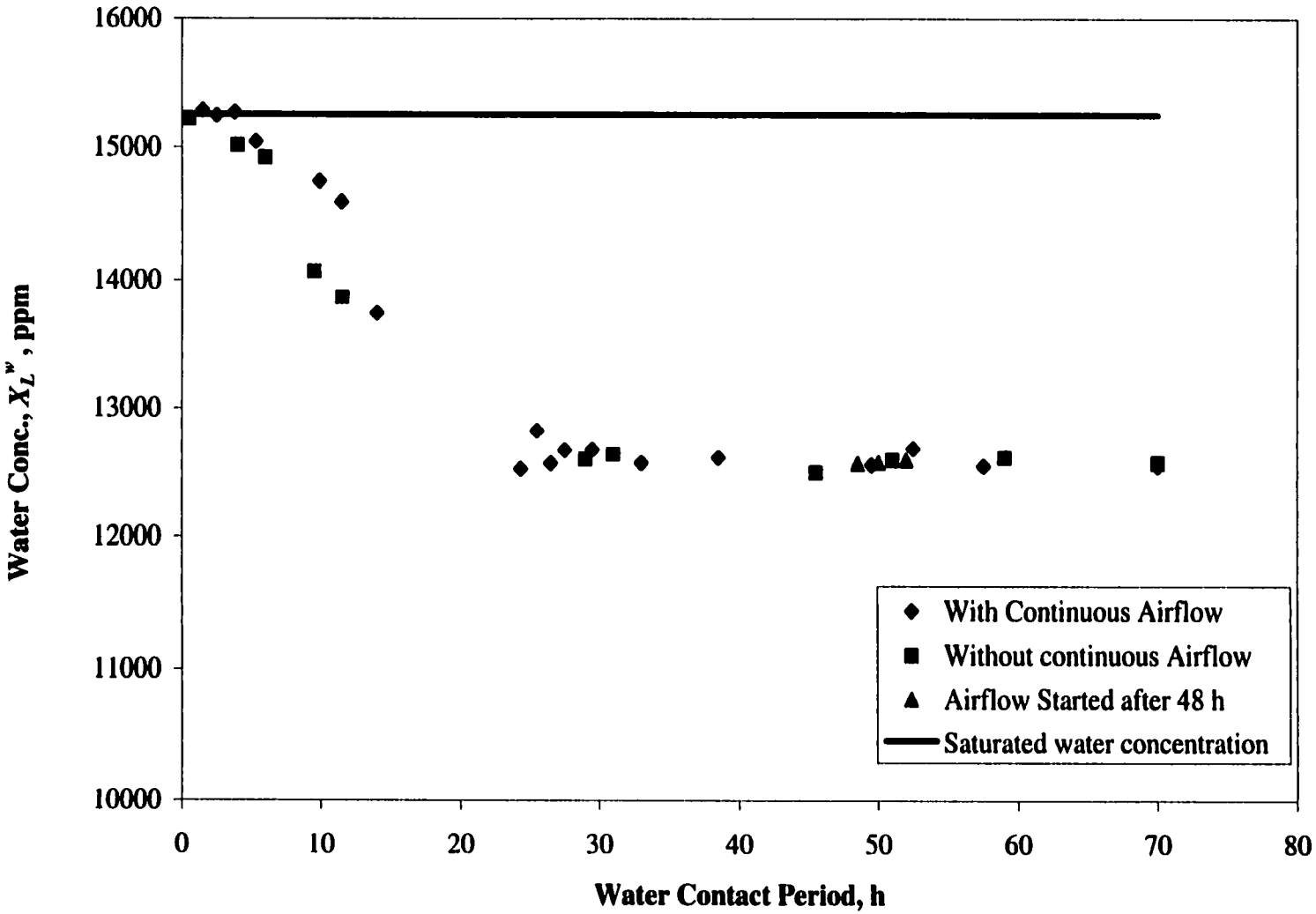

Figure 6.3 Effect of Water Contact Period on Water Concentration in Stripping Air, X_L^w

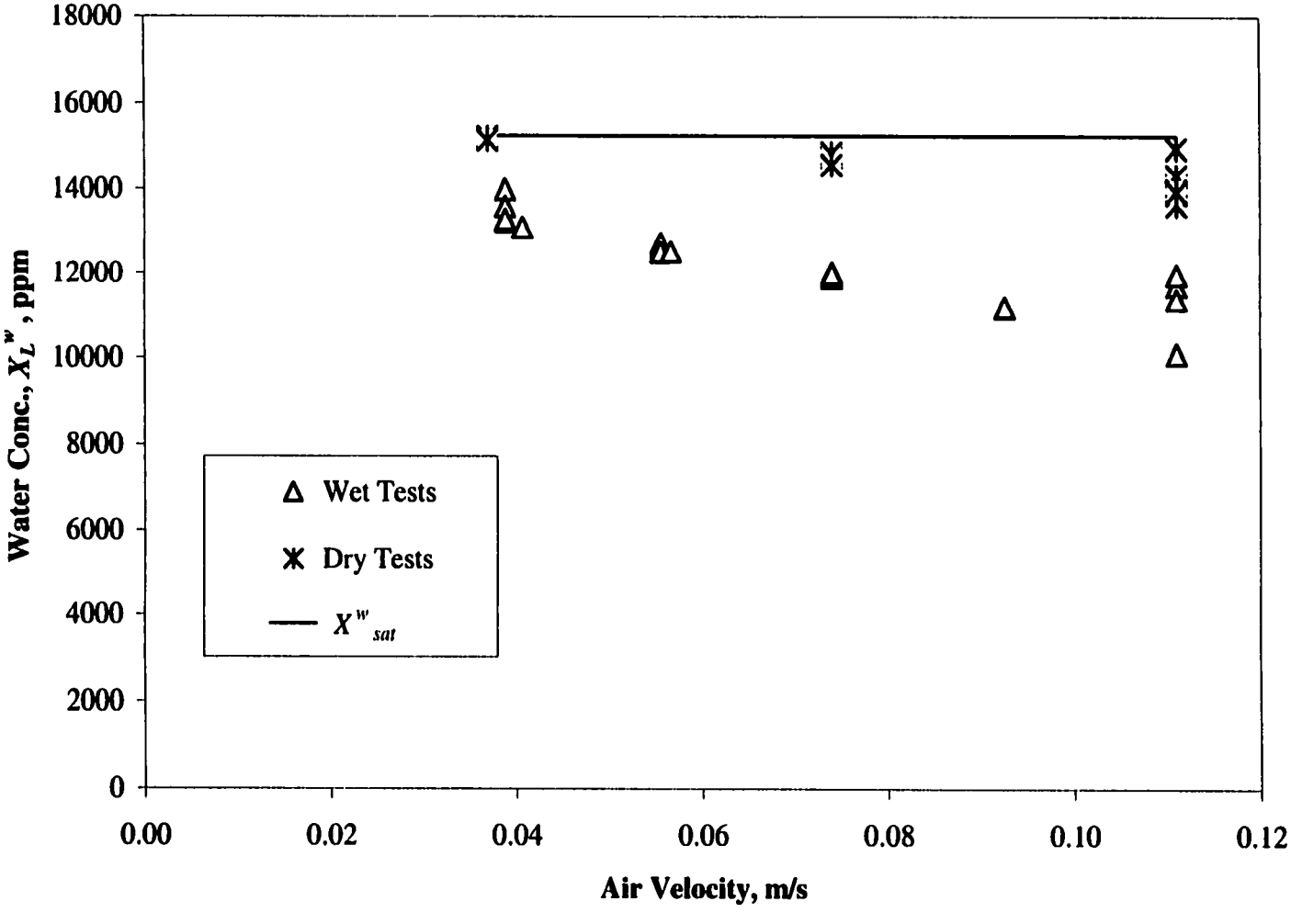

Figure 6.4 X_L^w, Water Concentration in Stripping Air at the Exit

tests at different air flow rates (Appendices – F and G). The figure shows that X_L^w for wet tests were lower than those for dry tests when the remaining operating conditions were the same. It was also observed that the values of X_L^w for dry tests were very close to the saturated water vapor concentration in the air phase, X_{sat}^w. X_L^w for dry tests were calculated by eqn. (5.8) assuming the pores were filled with air throughout their entire length. It was found that the predicted X_L^w was almost the same as the saturated water vapor concentration in the air phase, X_{sat}^w. Hence, the predicted and experimental values for dry tests agree reasonably well as shown in Fig. 6.5. Thus, it can be concluded that the transport mechanism is dominated by molecular diffusion through air-filled pores and the gas phase boundary outside the pores.

Since, the experimental values of X_L^w for the wet tests were lower than those for the dry tests (Fig. 6.4), this indicates that the overall mass transfer resistances for wet tests were higher than the dry tests. This led to the examination of what might have contributed to this additional mass transfer resistance. One possible reason for the presence of additional mass transfer resistance was that some pores were filled with water as claimed by Malek et al. (1997). In this study, this was extremely unlikely as the pressure difference between the shell side and the lumen side was less than 20 kPa, while the required pressure difference for water to penetrate the pores as predicted by eqn. (2.2) for these membranes should be 4246 kPa. Moreover, the transmembrane pressure differences were the same for the wet and the dry tests.

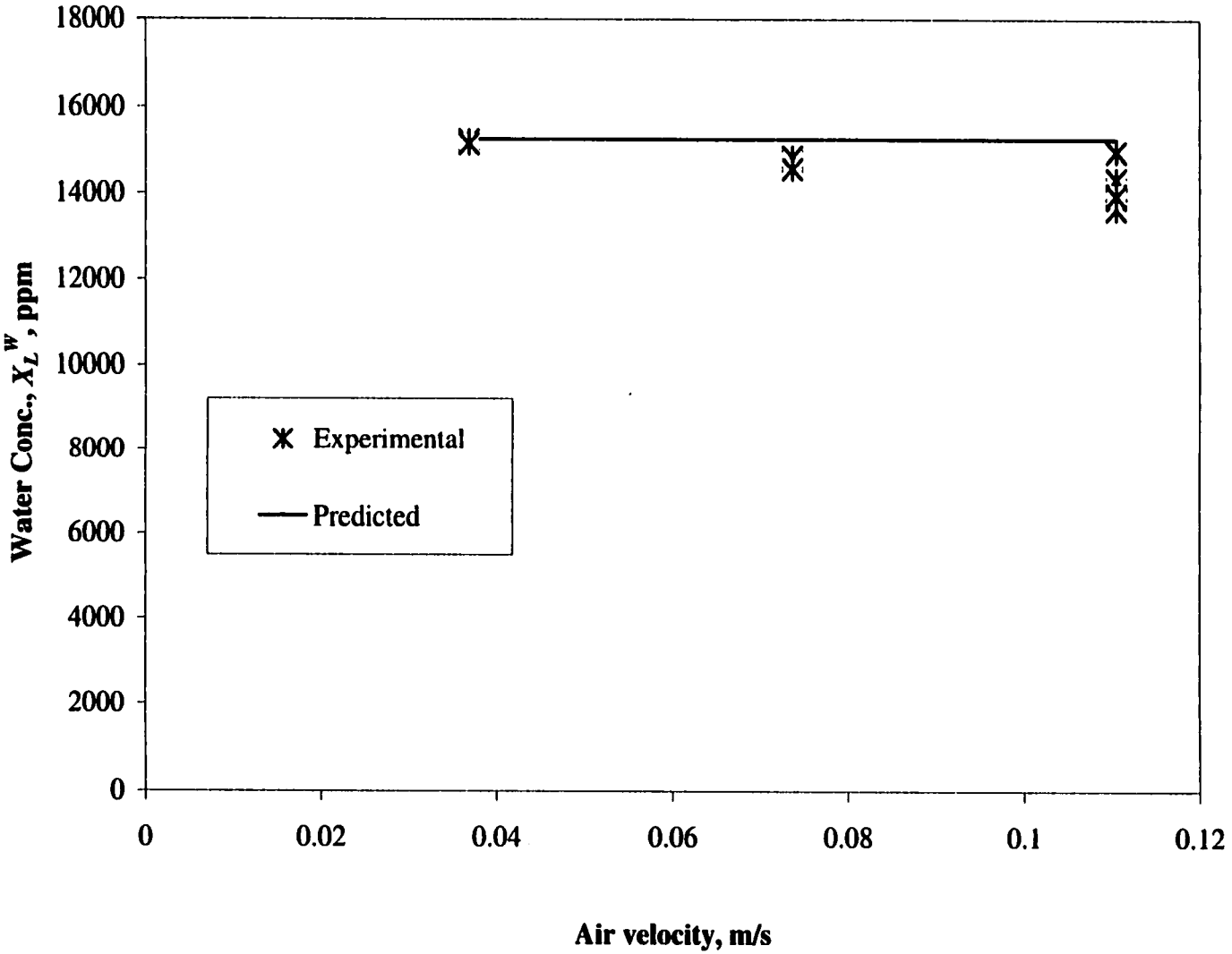

Figure 6.5 Predicted and Experimental Water Concentration in the Stripping Air at the Exit for Dry Tests

Capillary condensation of water vapor in the pores or in the lumen side of the fiber was another possibility. But, water vapor condensation in the lumen side of the fiber as observed by Côté et al. (1989) was very unlikely since water transported to the lumen side was immediately swept away by the stripping air stream and should not have contribute to increased mass transfer resistance. It is mentioned in Section 4.6.1 that air was passed through the lumen side for 30 minutes before collection of the first sample to remove any accumulated condensed water on the lumen side of the fibers. The observed air-side pressure drops on the lumen of the fiber were the same for the wet and the dry tests for same air flow rates. Thus, the possibility of water condensation in fiber lumen is precluded. However, the possibility of water vapor condensation in the membrane pores required further investigation. This was done in the MAS study of chloroform from aqueous solution and discussed in the next section.

6.4 REMOVAL OF CHLOROFORM FROM AQUEOUS SOLUTION

Before presenting the results for chloroform transport mechanism, the analytical methods used and the interpretation of the values are discussed briefly.

6.4.1 Interpretation of the Analytical Values

Data from a typical air stripping experiment of chloroform are given in Table 6.11. In this table, the third column represents the TC concentrations in the reservoir measured by the TOC analyzer. It has been mentioned in the analytical methods that some samples collected towards the end of the experiments were also analyzed by gas chromatography (P & T). Since GC analysis indicated that the TC values of these end samples were

contributed from sources other than chloroform. The average of the last three TC values (1.19 ppm) after deduction of the values of chloroform concentration detected by GC(P&T) was subtracted from the values in column 3 to construct column 4. Thus, the values in column 4 are considered to be the TC values, which can be attributed to chloroform alone. Column 4 was multiplied by factor of 9.9483, which allows the conversion of TC (ppm) to chloroform (ppm), to construct column 5. Furthermore, all the samples for this particular run were analyzed by GC(P&T) and the results are given in column 7. The differences between columns 5 and 7 are given in column 8. It can be seen from column 8 that the difference between these two methods is not significant even when the dilution factor for the most concentrated sample was 200 fold. The TOC analyzer can produce an error up to 2% while gas chromatographs can give errors over 10% (Greenberg et al., 1992).

Table 6. 11 Data from a test to remove chloroform from aqueous solution*

Sample name	Time, min	TC data, ppm TC	Corrected data,	ppm $CHCl_3$ based on TC	$ln(C_o/C_t)$	ppm $CHCl_3$ based on GC (P&T)	% Difference
1	2	3	4	5	6	7	8
Co	0	106.30	105.11	1045.65	0.0000	1010.04	3.4
C1	10	45.80	44.61	443.77	0.8571	434.14	2.2
C2	20	17.04	15.85	157.66	1.8919	161.70	-2.6
C3	30	7.14	5.95	59.17	2.8719	62.46	-5.6
C4	40	3.19	2.00	19.88	3.9628	18.39	7.5
C5	50	2.15	0.96	9.53	4.6979	8.64	9.3
C6	60	1.62	0.43	4.26	5.5036	4.15	2.5
C7	80	1.22			7.6945[1]	0.48	
C8	100	1.25			8.1671[1]	0.30	
C9	120	1.20			8.9185[1]	0.14	

* Air and solution flow rates were 7.5 x 10^{-5} m^3/s and 3.33 x 10^{-5} m^3/s, respectively.
[1] Based on the chloroform concentration obtained by GC (P & T)

For some MAS experiments with chloroform as solute, all the samples collected from the beginning to the end of the MAS experiment were subjected to GC6890 analysis through direct injection. An overlapping view of the chromatographs of 8 samples from a single run is presented in Fig. 6.6. The chloroform concentration of sample C8, collected at the end of the test was less than the detection limit of GC6890 and was not visible in the chromatography. Numerical representation of the samples in terms of GC area counts are also shown in Fig. 6.6. It is clear from the figure that the areas of the peaks corresponding to chloroform decreased with time. Eventually, the peak disappeared. The area of peaks that appeared earlier than chloroform did not change with time. Considering TC value is contributed from both chloroform and some organic compounds other than chloroform, subtraction of the average of the last three data in column 3 is totally justifiable.

Column 5 of Table 6.11 versus time is presented graphically in Fig. 6.7. It is clear from this figure that up to 99.99% of chloroform was removed within 80 minutes from an initial solution of 1046 ppm chloroform. The removal rate of chloroform was very high.

To calculate the rate constant (k) according to eqn (3.34), $ln(C_0/C_t)$ versus time was plotted as shown in Fig. 6.8. Linear regression, when applied to the entire range of the experimental data, yielded a rate constant with 95% C.I. of 0.0842 ± 0.0069 with $R^2 = 0.9618$. It is obvious in Fig. 6.8 that the last few points deviate from the linear relationship. It has been stated in Section 6.3 that some chloroform adsorbed in the beginning of an MAS run when the solution was exposed to polymeric walls of hydrophobic nature in the system. This chloroform possibly desorbed in later stages of

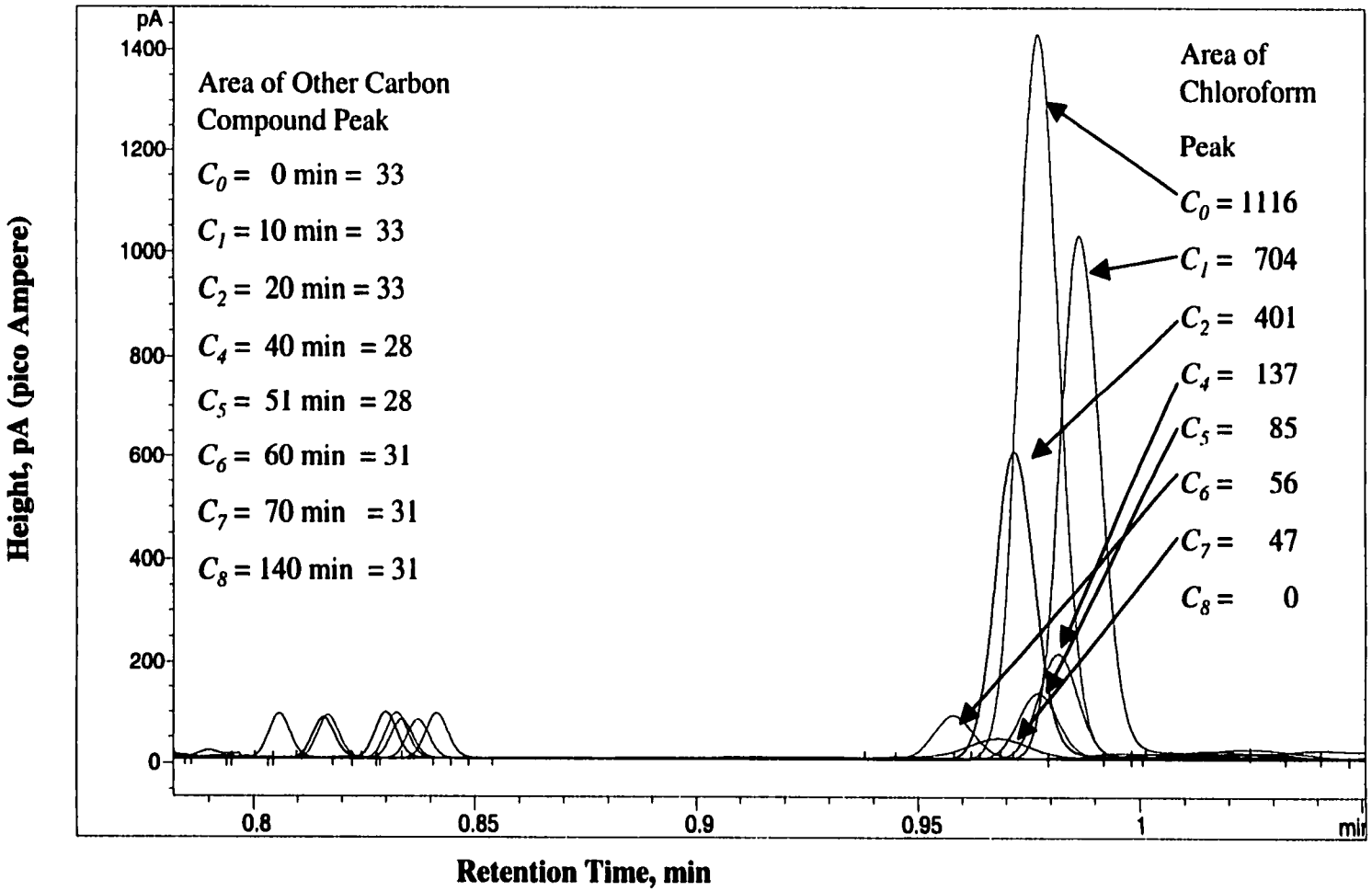

Figure 6.6 Overlapping View of Chromatographs of 8 Chloroform Samples Obtained from a Single MAS

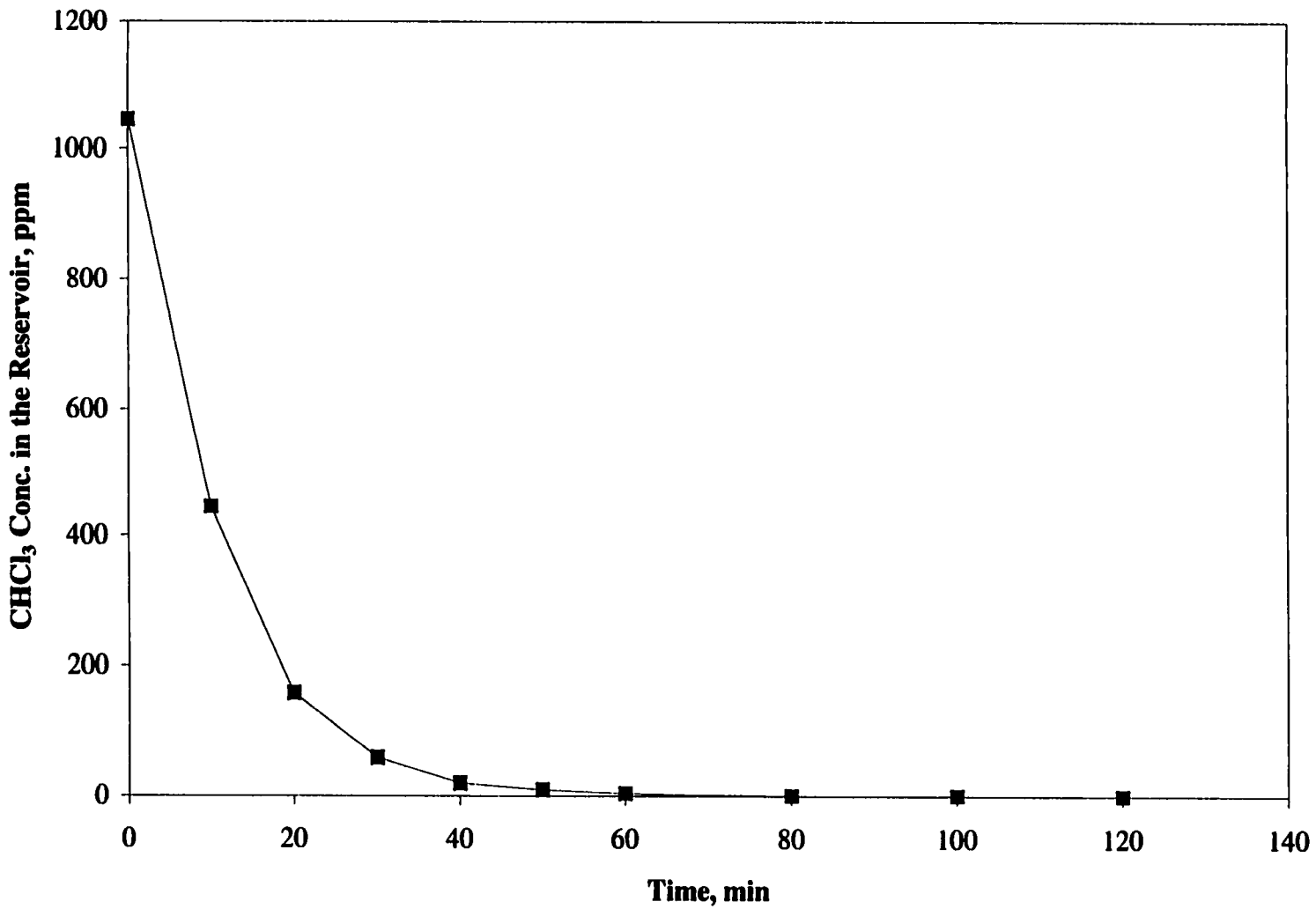

Figure 6.7 Removal of Chloroform from Aqueous Solution

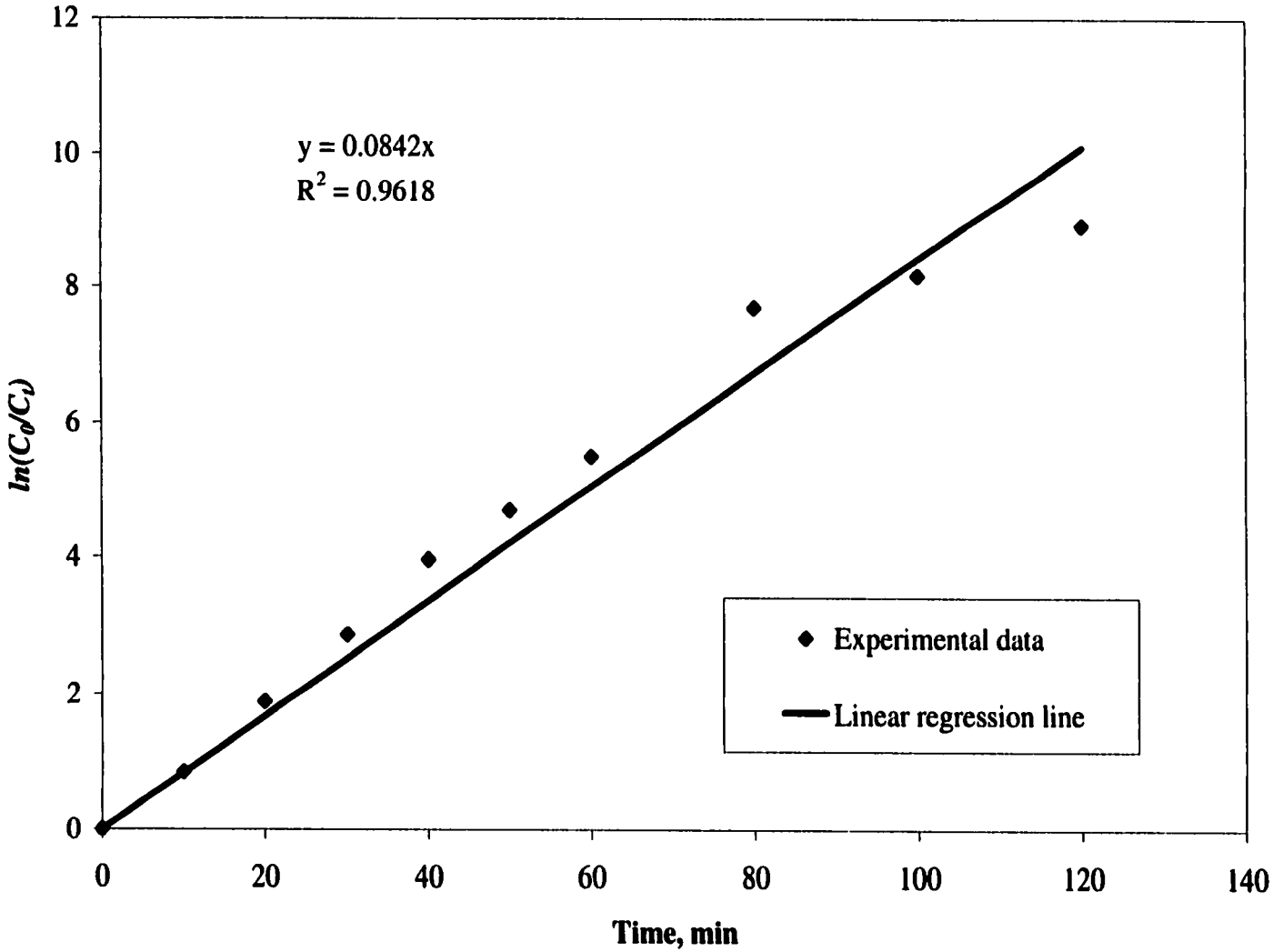

Figure 6.8 $ln(C_0/C_t)$ **Vs Time (Covering Entire Range of Experimental Period)**

the experiment, resulting in increased chloroform concentrations in the last few samples from the reservoir. This will further bring down the values for $ln(C_0/C_t)$. Therefore, the last three samples were excluded in the linear regression analysis as shown in Fig. 6.9. A rate constant with 95% C.I. of 0.094 ± 0.0028 with $R^2 = 0.9971$ was obtained.

6.4.2 Chloroform Transport

Experiments conducted for MAS of chloroform from aqueous solutions under both dry and wet conditions, confirmed the presence of an additional mass transfer resistance for wet tests compared to the dry tests. A typical example is presented in Fig. 6.10, which shows a higher rate constant (faster removal of chloroform) for the dry tests than for the wet tests when other operating conditions were otherwise identical. The observed overall mass transfer coefficients, K_L, were calculated from the rate constants using eqn. (3.36) for both dry and wet tests and compared in Fig. 6.11 (Appendices – H and I). From this figure, it was clear that K_L for wet tests were lower than those for dry tests when the other operating conditions were the same.

Considering capillary condensation of water vapor in the pores, an assumption was made that water penetrated into and filled a portion of the pore and chloroform molecules were transported through this water layer by diffusion (Mahmud et al., 2000). Then, the mass transfer resistance due to the membrane was predicted using the following modified equation:

$$\frac{1}{k_m H} = x\frac{\delta\tau}{D_{eff}\varepsilon H} + (1-x)\frac{\delta\tau}{D_w\varepsilon} \qquad (6.2)$$

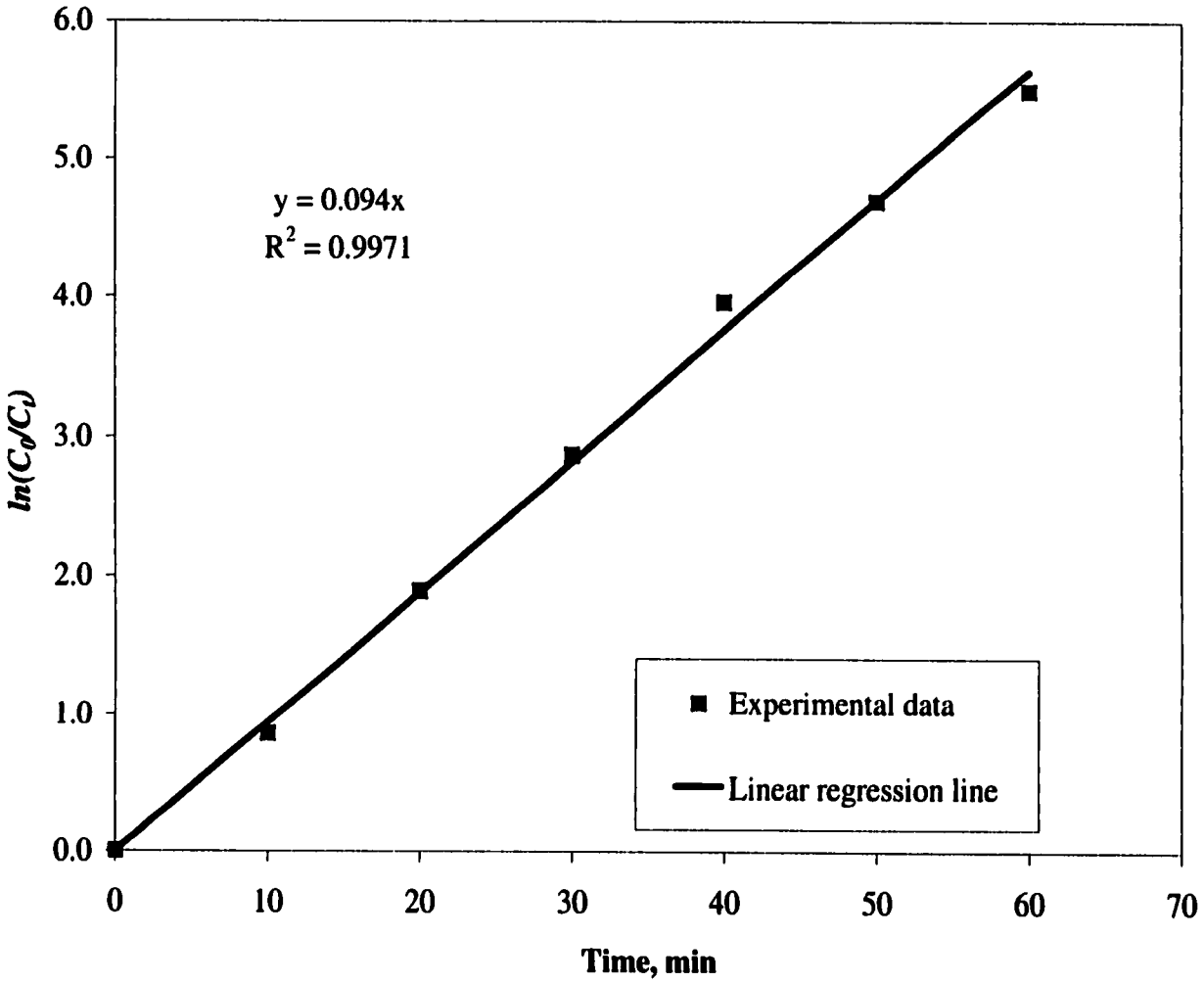

Figure 6.9 $ln(C_0/C_t)$ **Vs Time (Excluding the Last Three Points of Fig. 6.8)**

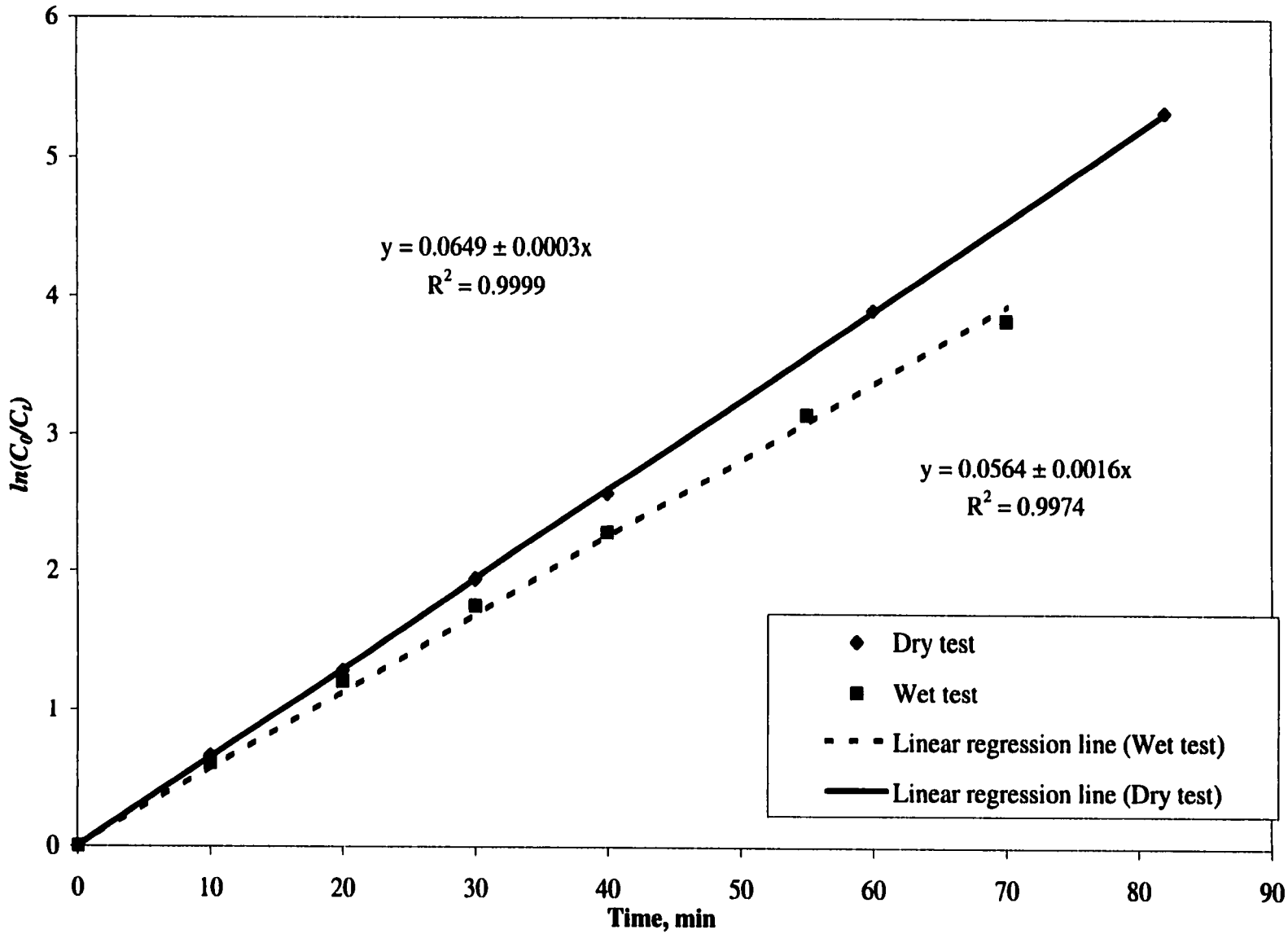

Figure 6.10 Comparison Between Rate Constants for Dry and Wet Test for MAS of Chloroform (Air Velocity = 0.111 m/s & Solution Velocity = 5.95 x 10^{-3} m/s)

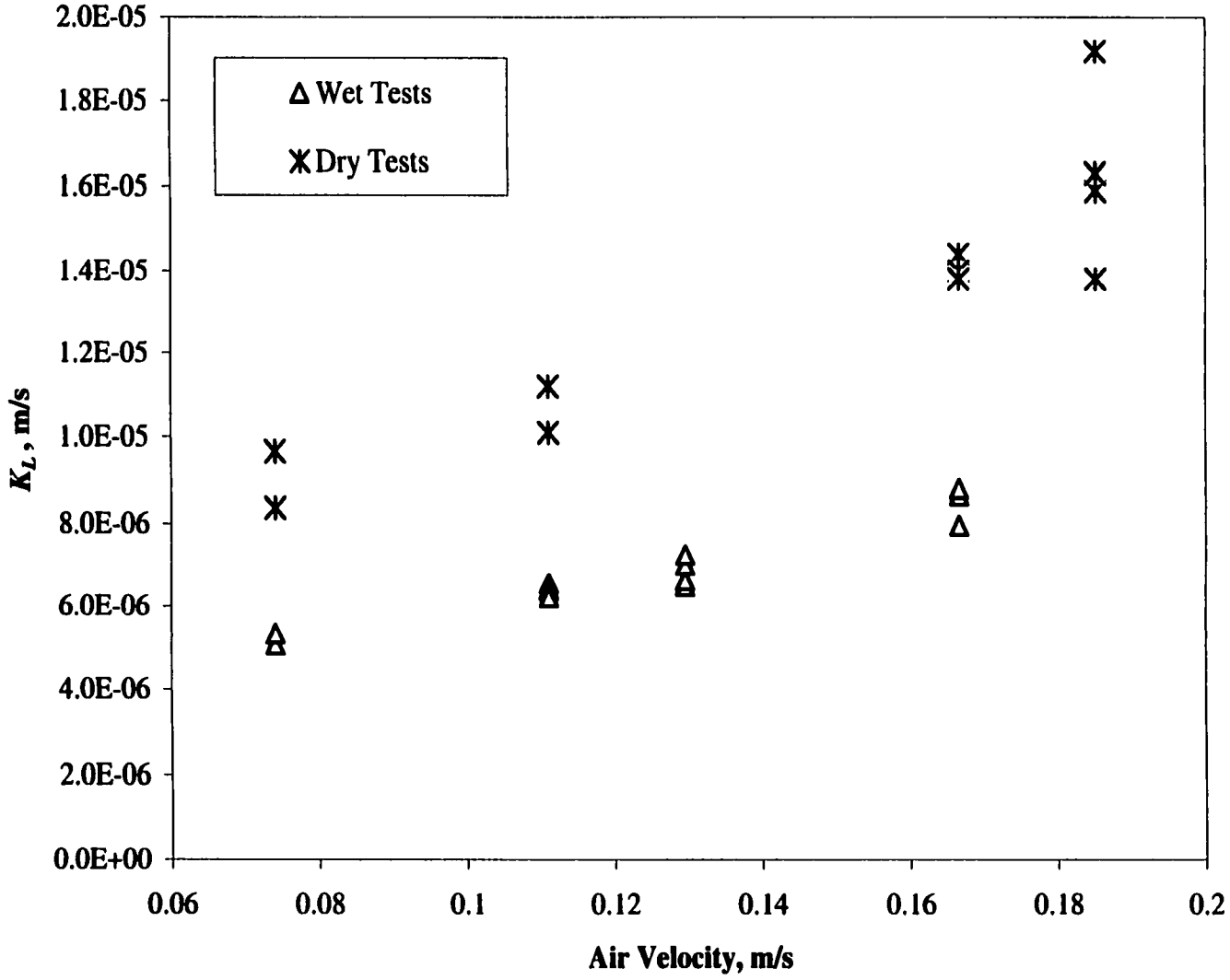

Figure 6.11 Comparison of Observed K_L for Dry and Wet Tests for Chloroform (Solution Velocity = 5.95 x 10^{-3} m/s)

where:
x = fraction of the pore filled with air
$1-x$ = fraction of the pore filled with water

An attempt was made to calculate the K_L values theoretically. Fig. 6.12 presents the experimental K_L values for dry tests and those predicted by theoretical equations. Note x =1.0 was used since pores were filled with air when membranes were dry. Three model predictions were used combining eqns. (3.10), (3.14), (6.2) while different equations were used for the local liquid-phase mass transfer coefficient. These were eqns. (3.11), (3.12) and (3.13) developed by Kreith and Black (1980), Yang and Cussler (1986) and Reed et al. (1995), respectively. The Kreith and Black (1980) correlation yielded better predictions than the correlations of Yang and Cussler (1986) and Reed et al. (1995). From this figure it becomes clear that the chloroform transport is dominated by molecular diffusion through the liquid phase boundary layer, air filled pores and the gas phase boundary outside the pores over other transport mechanisms such as surface diffusion.

A similar analysis was conducted for wet tests using $x = 0.75$, considering the partial filling of the pores with condensed water. The value of x was determined through trail and error to fit the data. As Fig. 6.13 indicates, the Kreith and Black (1980) correlation was again found to be superior. It should be noted that Yang and Cussler (1986) expected that the Kreith and Black (1980) correlation, developed for cross-flow in a closely packed tube bank, would represent their data but actually it did not. One of the reasons might be, as reported by Yang and Cussler (1986), that their module was prepared in the laboratory and the fibers were sufficiently separated to behave as single fibers rather than a closely packed bundle of fibers. The fibers used in the present study were closely packed in the

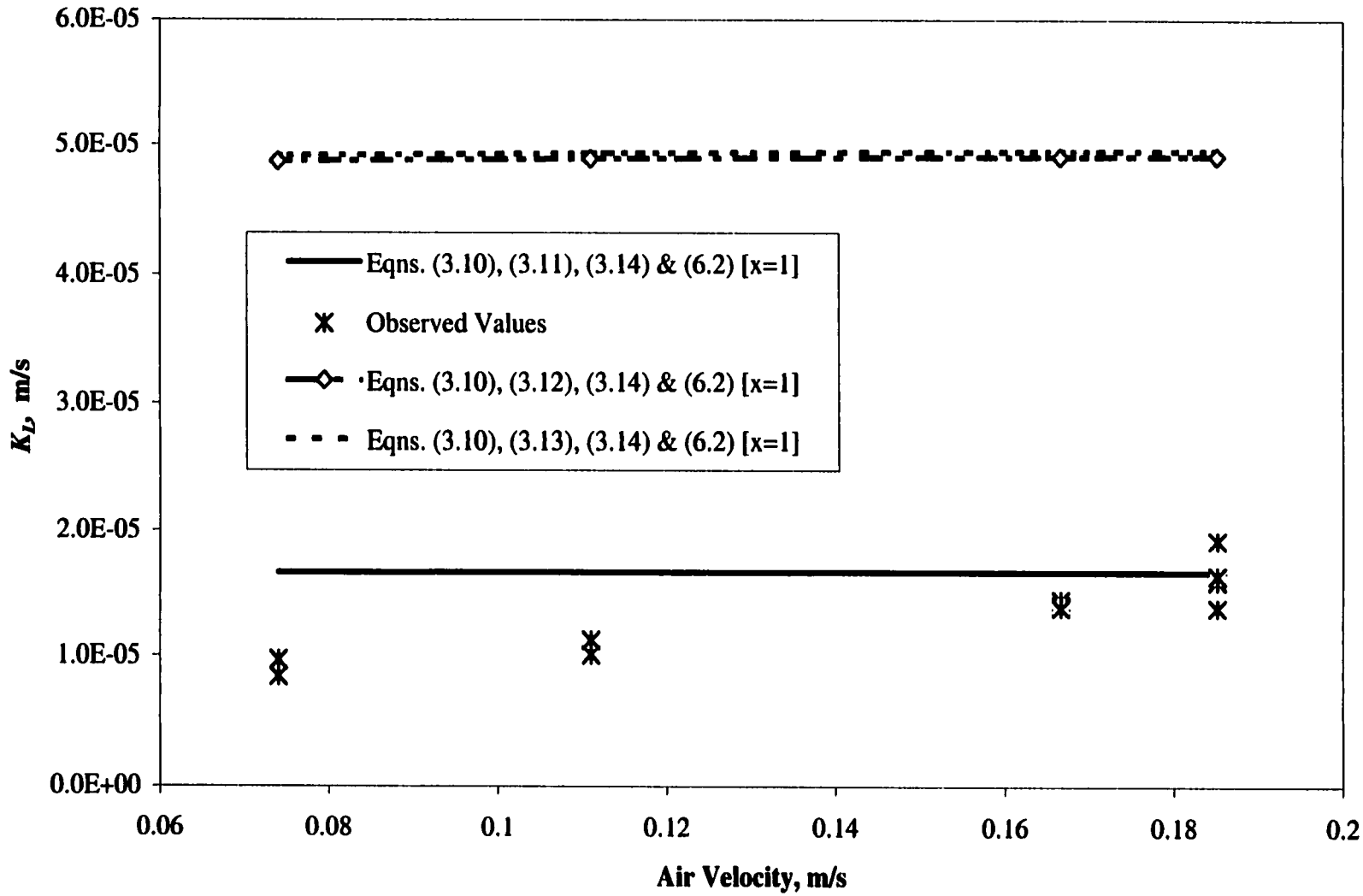

Figure 6.12 Comparison Between Predicted and Observed K_L for MAS of Chloroform (Dry Test)

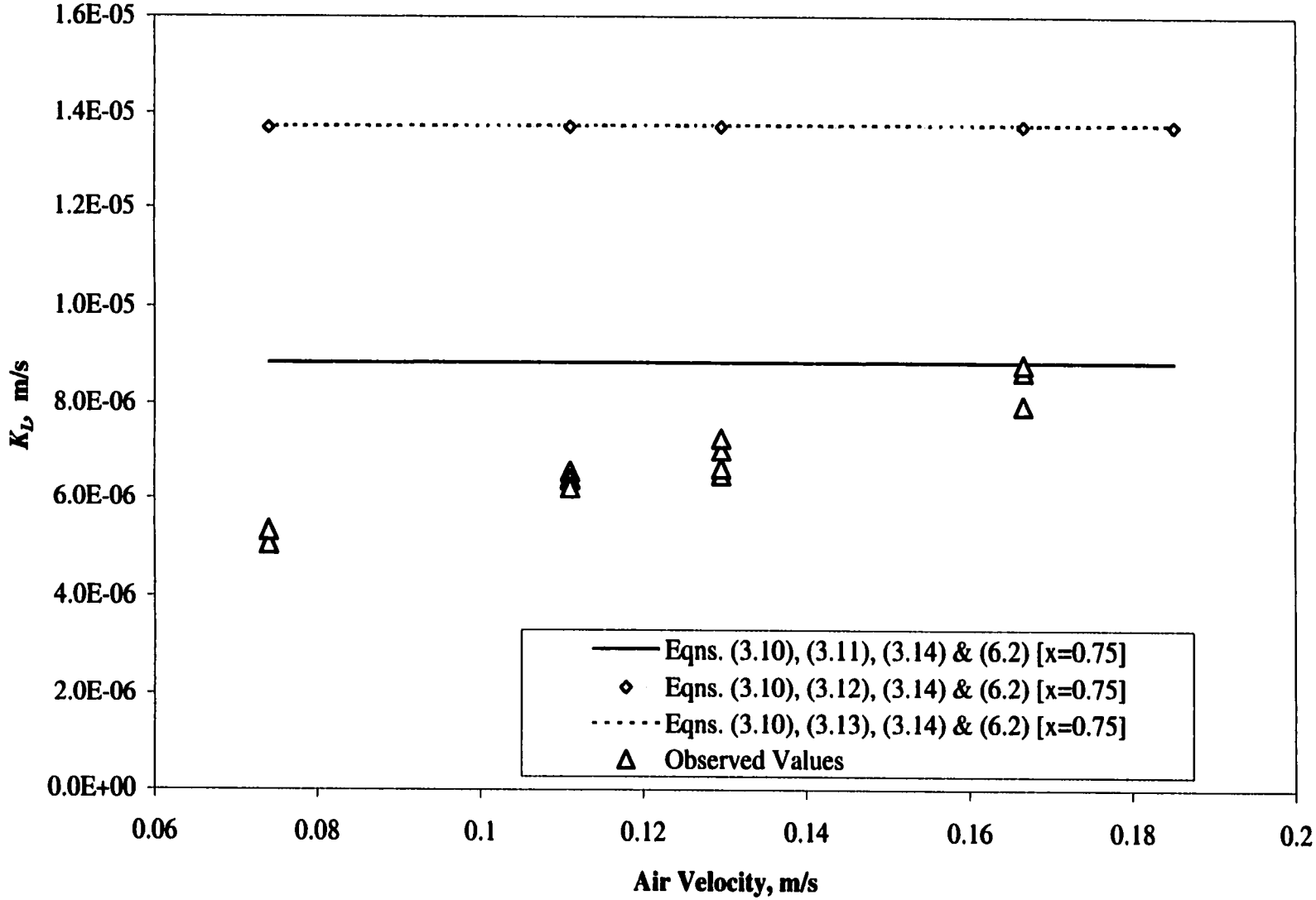

Figure 6.13 Comparison Between Predicted and Observed K_L for MAS of Chloroform (Wet Test)

module and had liquid cross-flow. Therefore, the system used by Kreith and Black (1980) is a better analogy to our system. Thus, it is reasonable that the Kreith and Black (1980) equation has a better prediction capacity.

The values of $\frac{1}{k_L}$, $\frac{1}{k_a H}$ and $\frac{1}{k_m H}$ were calculated by eqns. (3.11), (3.14) and (6.2) using x =1.0 for dry tests and x = 0.75 for wet tests, respectively for air and liquid flow rates of 3.33×10^{-5} m^3/s. The overall mass transfer resistance $\frac{1}{K_L}$ was obtained by adding individual resistances as per eqn. (3.10). They are shown in Fig. 6.14. The $\frac{1}{k_m H}$ value calculated for wet tests in this study was two orders of magnitude higher than that for dry tests and was almost equal to the liquid phase resistance. Thus, its contribution to the overall mass transfer resistance became significant. In commercial applications, the operating period of MAS is usually long, hence it is more natural to consider that the pores are partially wetted. This aspect has to be taken into account in the design of MAS units. The value of $\frac{1}{k_m H}$ for dry tests was calculated by eqn. (6.2) to be 139.75 s/m by setting x = 1.0, thus $\frac{1}{k_m}$ was 21.13 s/m after taking Henry's Law constant into account. This value is comparable to 33.33 s/m reported by Kreulen et al. (1993) as $\frac{1}{k_m}$. On the other hand, $\frac{1}{k_m H}$ for wet tests was calculated by eqn. (6.2) to be 5.26×10^4 s/m by setting x = 0.75. This value is also comparable to the value of 10^5 s/m, measured by Qi

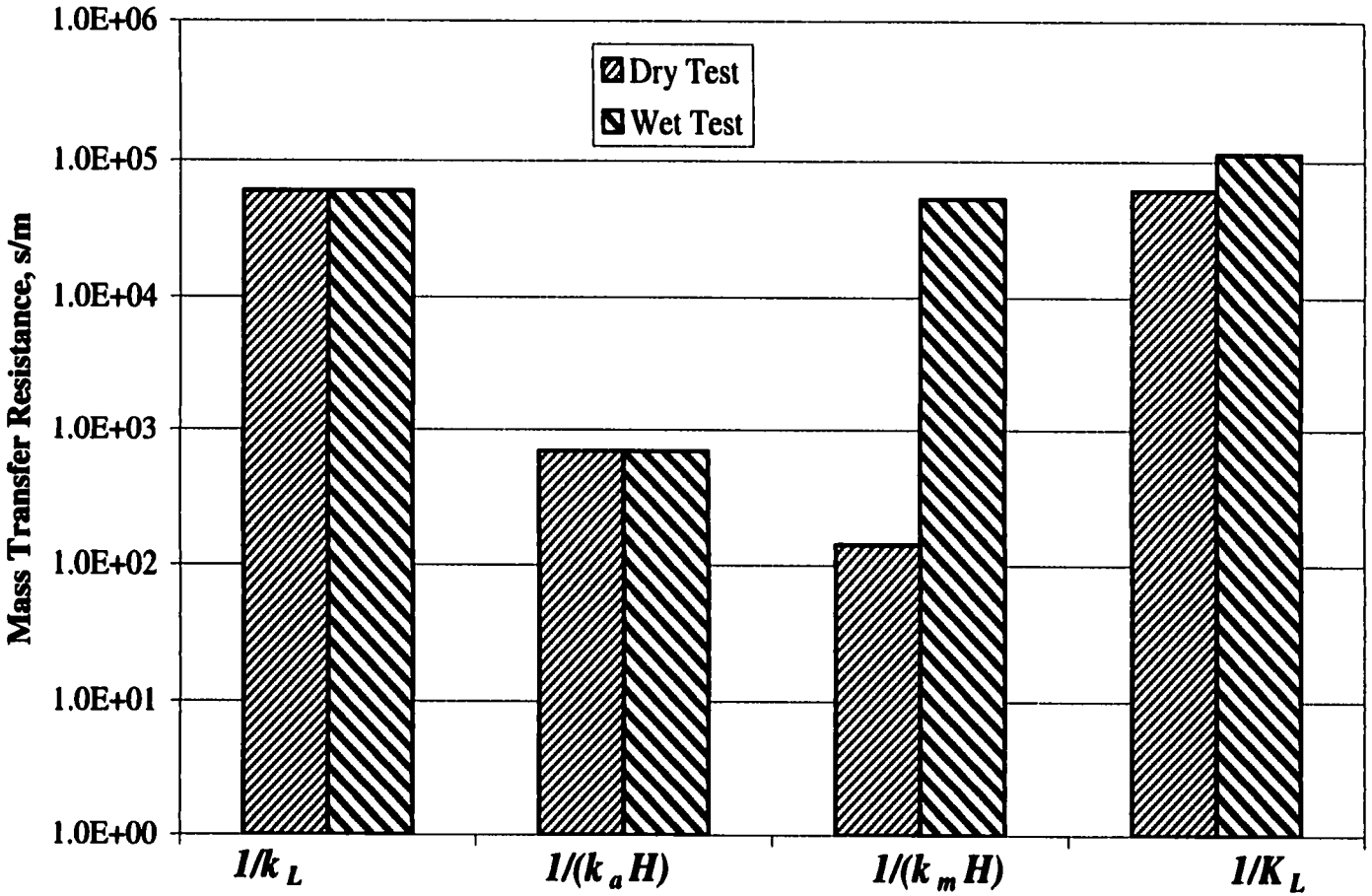

Figure 6.14 Comparison of Calculated Mass Transfer Resistances for MAS of Chloroform for Air and Liquid Flow Rates of 3.33 x 10^{-5} m^3/s

and Cussler (1985c), who presumed it was for air-filled pores. The comparison of partially wet and dry pores in this work explains Kreulen et al.'s (1993) conjecture that the pores in Qi and Cussler's work (1985c) were partially wetted. Despite the differences in the systems studied by Kreulen et al. (1993), Qi and Cussler (1985c) and the present study, the resulting membrane mass transfer resistances are comparable, because the basic transport mechanisms were likely the same.

Applying eqns. (3.10), (3.37), (3.38) and (6.2) with $x = 0.65$, the overall mass transfer coefficients of chloroform were predicted and the results were compared with the data of Semmens et al. (1989). Note that eqns. (3.37) and (3.38) were developed for liquid flow on the lumen side and parallel air flow on the shell side, respectively, which was used in the study by Semmens et al. (1989), unlike in present study. Only continuum diffusion was considered in our calculations to remain consistent with the original paper. The agreement between predicted and reported observed values is very good as shown in Fig. 6.15. The slight differences in values of x between Semmens et al. (1989) and the present study (0.65 and 0.75, respectively) are likely dependent on the experimental conditions. The lack of consideration for the wet/dry state of the pores may also explain different overall mass transfer resistances obtained by other researchers.

At this stage, there is no conclusive evidence on the form and location of condensed water and its impact on restricting the transport. Thus, the mechanism of water transport through the partially wetted pore is unknown. One possibility is that a layer of adsorbed water covered the pore wall that led to the reduction of the effective pore radius, thus

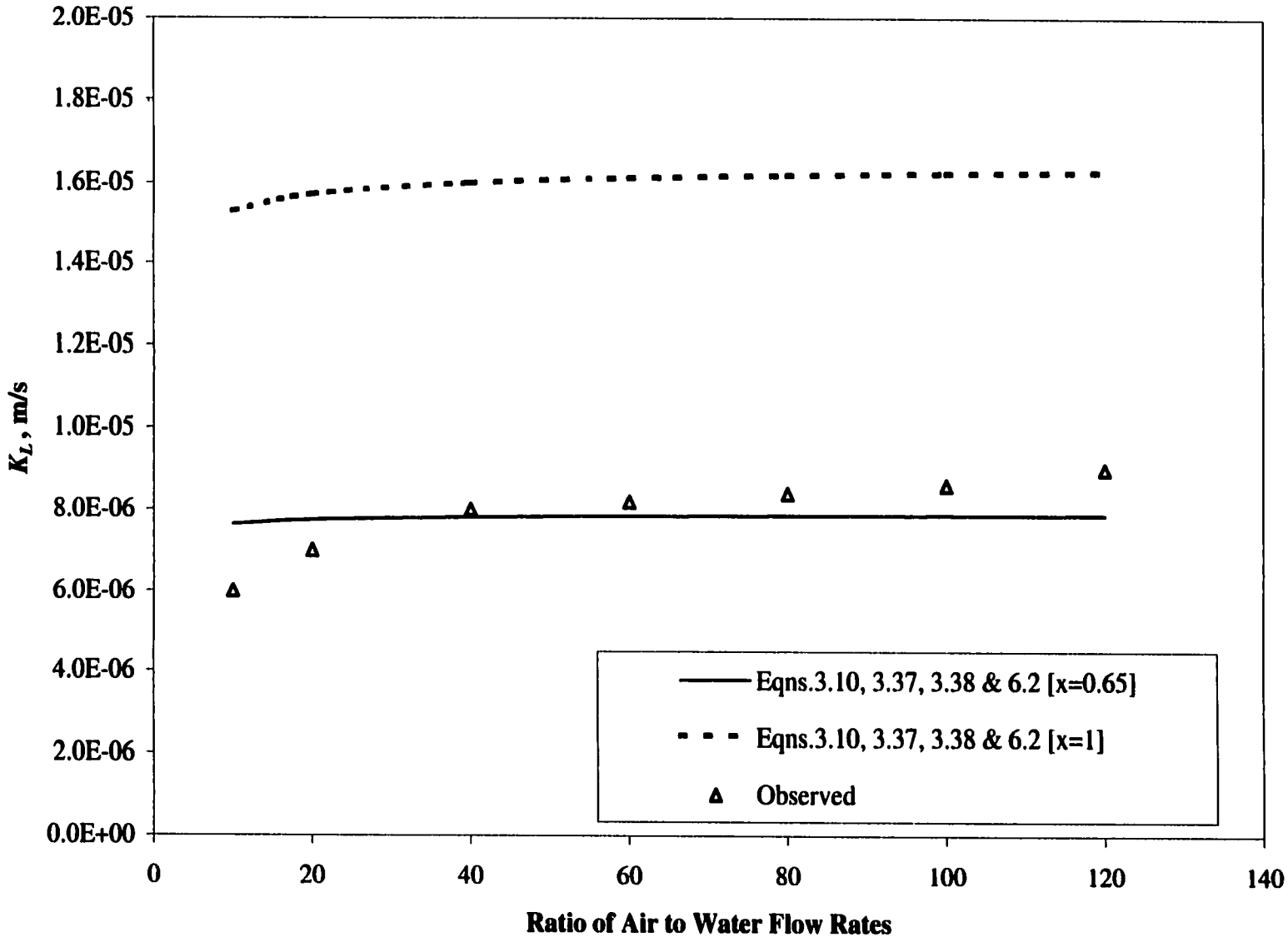

Figure 6.15 Comparison Between Predicted K_L With or Without Liquid in the Pores and Observed K_L by Semmens et al. (1989) [Liquid flow rate=75 ml/min]

narrowing the air channel for water diffusion as shown in Fig. 6.16a. Another could be that droplets covered the pore partially as shown in Fig. 6.16b. The pores in these membranes are known to be far from cylindrical. Capillary condensation could occur in the narrow radius portion of the irregularly shaped pores (Fig.6.16c) and hence reduce the effective pore radius. Another possibility is that water blocked a portion of the pore as shown in Fig. 6.16d. The deposition of water as shown in Fig. 6.16a is very unlikely due to the high surface tension of water. If water blocked the pore as shown in Fig. 6.16d, the length of diffusion path of water vapor through air is reduced. This should reduce the membrane resistance and increase the water transport. But, the experimental results did not support this. Water might or might not diffuse through the condensed water in the pore. Water vapor might also condense and evaporate repeatedly within the pores. But, whatever the form of the water in the pores, the chloroform had to diffuse through this water to reach the other side of the pores.

6.4.3 Effect of Air Velocity on Chloroform Removal

In these experiments, the results of which are shown in Fig. 6.11, liquid velocity was constant while the air velocity was changed. Thus, the liquid film resistance should be constant. The mass transfer resistance due to the membrane should not change with the change of air velocity. The rate constant k, increased with the increase of air velocity as shown in Fig. 6.17 for wet tests. The rate constants obtained from dry tests showed the same trend. As a result, the overall mass transfer coefficients of chloroform increased with an increase in air velocity for both wet and dry tests (Fig. 6.11), as expected by the reduction of the gas film resistance. However, the sensitivity to the variation in air

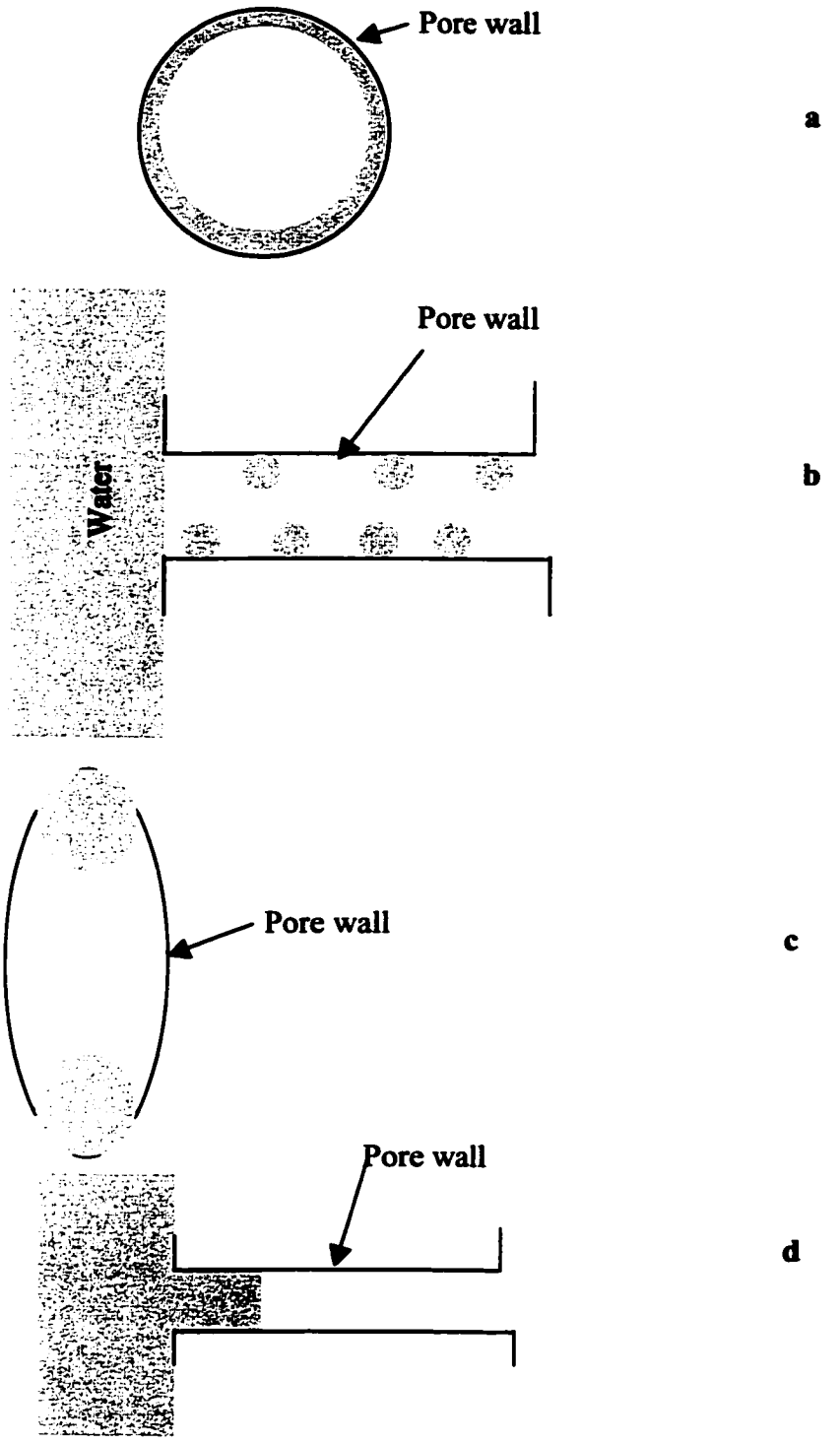

Figure 6.16 Water Condensation in Pores

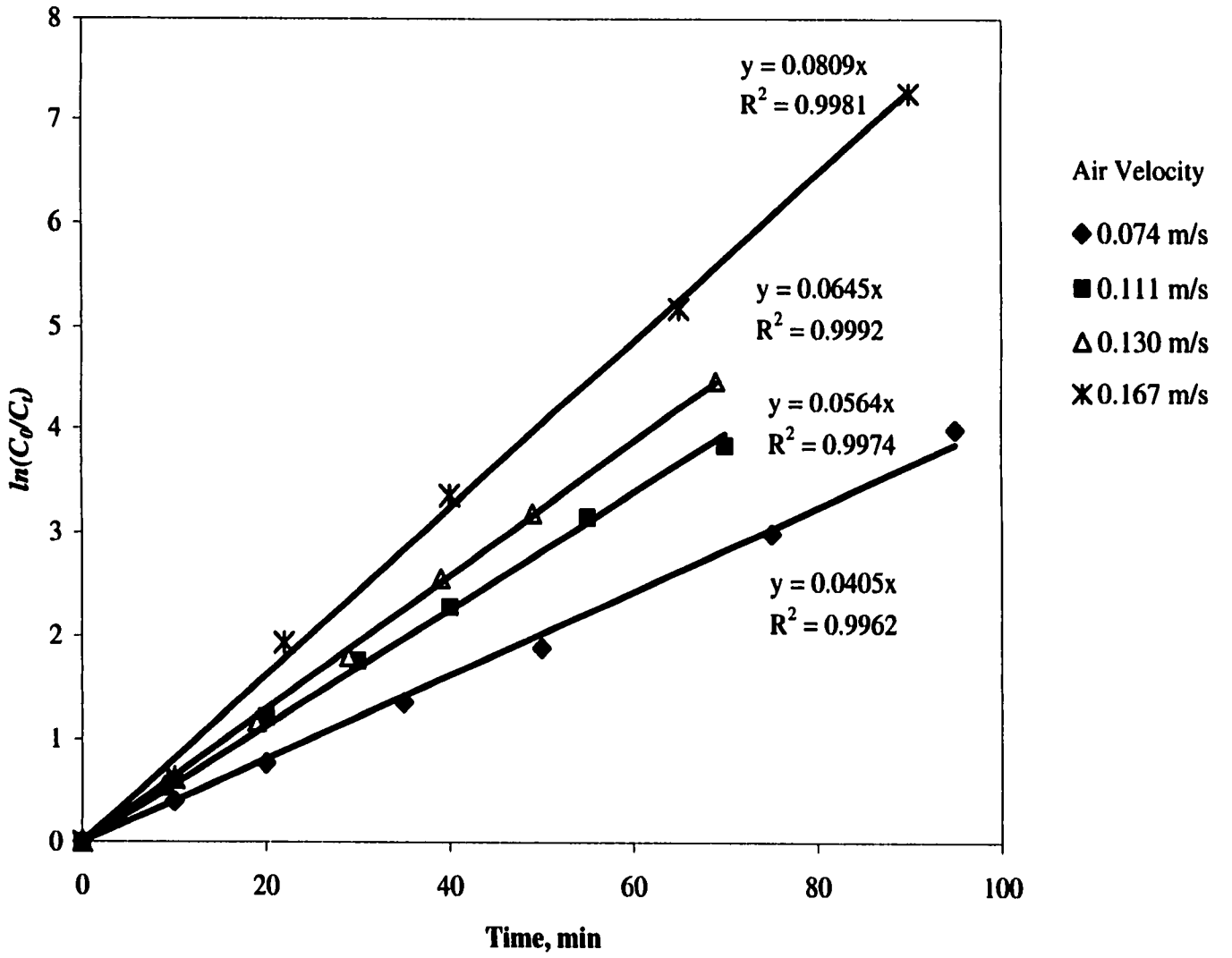

Figure 6.17 Comparison of the Rate Constants Observed at Different Air Velocities for Wet Tests of MAS of Chloroform (Solution Velocity = 5.95 x 10^{-3} m/s)

velocity was much stronger than predicted by eqn. (3.14) based on Lévéque's (1928) correlation (see Figs. 6.12 and 6.13). For the experiments in this study eqn. (3.14) overestimated the local air-phase mass transfer coefficient in the range of air velocities studied. The Graetz numbers for this study ranged from 3.08×10^{-3} to 6.93×10^{-3}, which are much lower than 4, the lower limit for the applicability of the Lévéque's (1928) model (Wickramasinghe et al., 1992). Thus, the deviations of the experimental values from those predicted by Lévéque's (1928) correlation are not surprising. Wickramasinghe et al. (1992) proposed eqn. (3.15) for the average local mass transfer coefficient on the lumen side. Although eqn. (3.15) was given for the local liquid-phase mass transfer coefficient, $\overline{k_L}$, the equation can be used for the local air-phase mass transfer coefficient, $\overline{k_a}$, when air flows on the lumen side. Thus, $\overline{k_a}$ and $\frac{1}{\overline{k_a}H}$ were calculated based on eqn. (3.15) for different air velocities. $\frac{1}{k_L}$ was calculated by Kreith and Black (1980) correlation [eqn. (3.11)] and $\frac{1}{k_m H}$ was obtained by eqn. (6.2) with x = 0.75 corresponding to wet tests. The overall mass transfer resistance $\frac{1}{K_L}$ was then obtained by adding individual values of $\frac{1}{k_L}, \frac{1}{\overline{k_a}H}$ and $\frac{1}{k_m H}$. The predicted overall mass transfer coefficients and the experimental data from this study are compared in Fig. 6.18. The agreement is good at low air velocities but the model under-estimates the overall mass transfer coefficient, K_L at relatively higher velocities. This is probably caused by underestimation of $\overline{k_a}$ by eqn. (3.15).

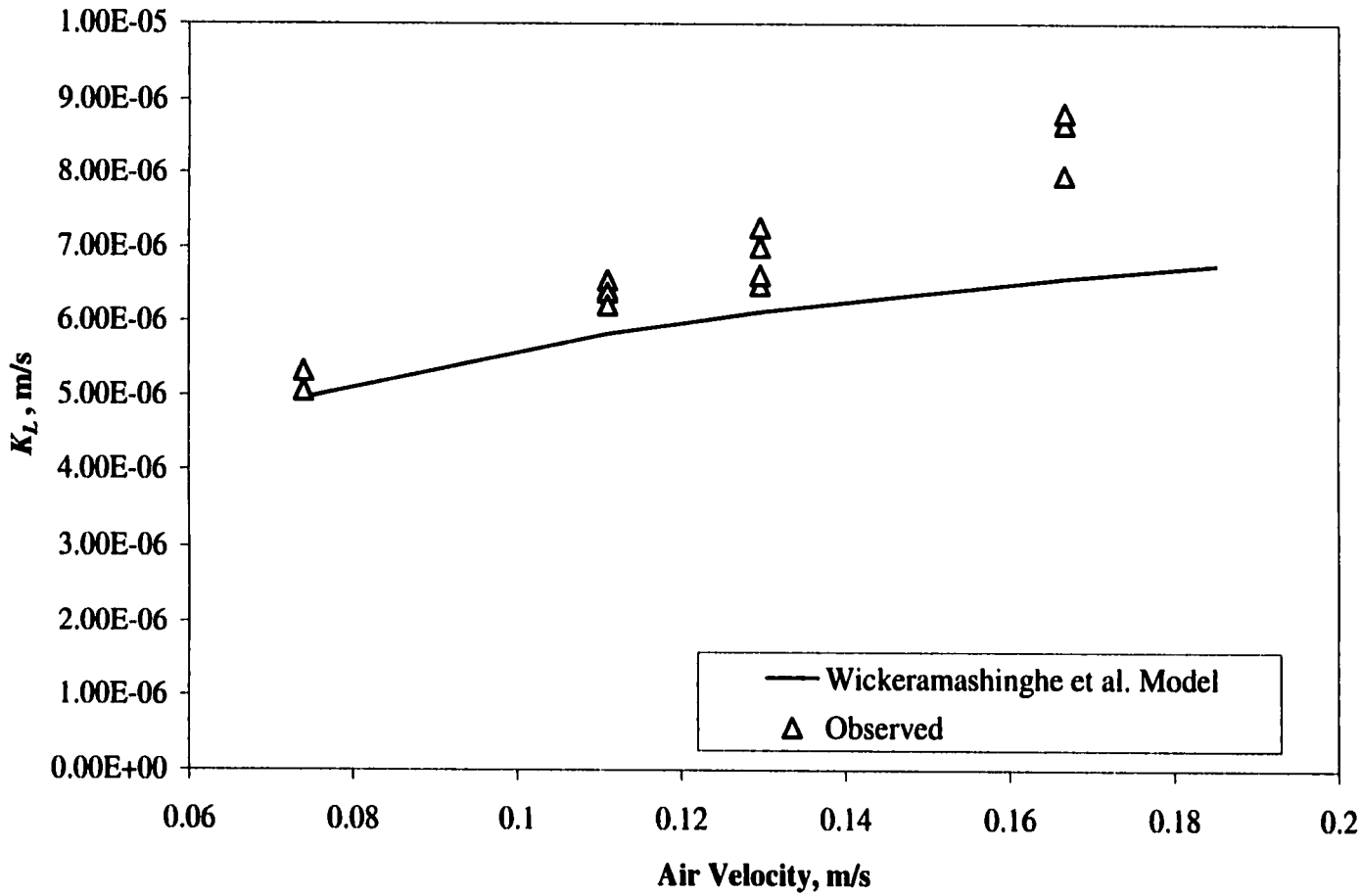

Figure 6.18 Modeling of Experimental Data (Wet Tests) Using Wickeramashinghe et al. (1992) Correlation

In an attempt to describe the data in a better way, eqn. (3.16) was also evaluated. The reason for this evaluation was that the eqn. (3.15) did not include any physicochemical parameters, which does not seem reasonable. Although, Wickramasinghe et al. (1992) showed that the average Sherwood number calculated by eqn. (3.16) fit their data well, it did not fit the data of this study. The reason was apparently that their calculation was for liquid flow in the lumen, whereas in this study, air-flow was in the lumen. The diffusion coefficients for a compound for gas phase are almost 10^4 higher than that for liquid phase. The values of the Graetz numbers for this study were very small and the $\overline{Sh}$ became negative and thus the correlation was found to be inapplicable for prediction of air film resistance at low flows on the lumen of hollow fibers.

Another attempt was made to modify Lévéque's correlation (eqn. (3.14)) for a better fit. Rearranging eqn. (3.14) to

$$\frac{1}{k_a H} = [\frac{0.617}{H}(\frac{Ld_i}{D_c^2})^{0.33}](\frac{1}{v^a})^{0.33} \qquad (6.3)$$

it became clear that quantities in the square bracket do not change when air velocity v^a is changed. In the following equation, the exponent applicable to $\frac{1}{v^a}$ was changed from 0.33 to q

$$\frac{1}{k_a H} = [\frac{0.617}{H}(\frac{Ld_i}{D_c^2})^{0.33}](\frac{1}{v^a})^{q} \qquad (6.4)$$

where:
q = exponent

The best value of q was found as follows: First, $\frac{1}{k_a H}$ values were calculated for each air velocity by subtracting the theoretical values of $\frac{1}{k_L}$ and $\frac{1}{k_m H}$ from the experimental $\frac{1}{K_L}$ values. The $\frac{1}{k_a H}$ values so obtained were then used in eqn. (6.4) to calculate the best fit q values by nonlinear regression analysis. The model provided the best value of q with a 95% confidence interval as 2.1928 ± 0.0157 with a standard error of 0.02605, a model sum of square of 2.47 x 10^{10} and a minimum sum of the square roots of the residuals of 1.24 x 10^{9} for the wet system. Therefore, eqn. (6.4) becomes

$$\frac{1}{k_a H} = [\frac{0.617}{H}(\frac{Ld_i}{D_c^2})^{0.33}](\frac{1}{v^a})^{2.19} \qquad (6.5)$$

which is applicable for the wet system.

For the dry system, the best q value with a 95% confidence interval was 2.0058 ± 0.0262 with a standard error of 0.038906, a model sum of square of 7.74 x 10^{10} and with a minimum sum of the square roots of the residuals as 7.58 x 10^{8}. Therefore, eqn. (6.6) is applicable for the dry system.

$$\frac{1}{k_a H} = [\frac{0.617}{H}(\frac{Ld_i}{D_c^2})^{0.33}](\frac{1}{v^a})^{2.01} \qquad (6.6)$$

The overall mass transfer coefficients, K_L for wet tests were calculated using eqns. (3.10), (3.11), (3.14) and (6.2) with x = 0.75. They were also calculated by eqns. (3.10), (3.11), (6.5) and (6.2) with x = 0.75. Note that the Lévéque's correlation eqn. (3.14) was modified to eqn. (6.5) in the latter approach. Both approaches were compared with experimental K_L values in Fig. 6.19. The figure shows that the modified eqn. (6.5) fits the

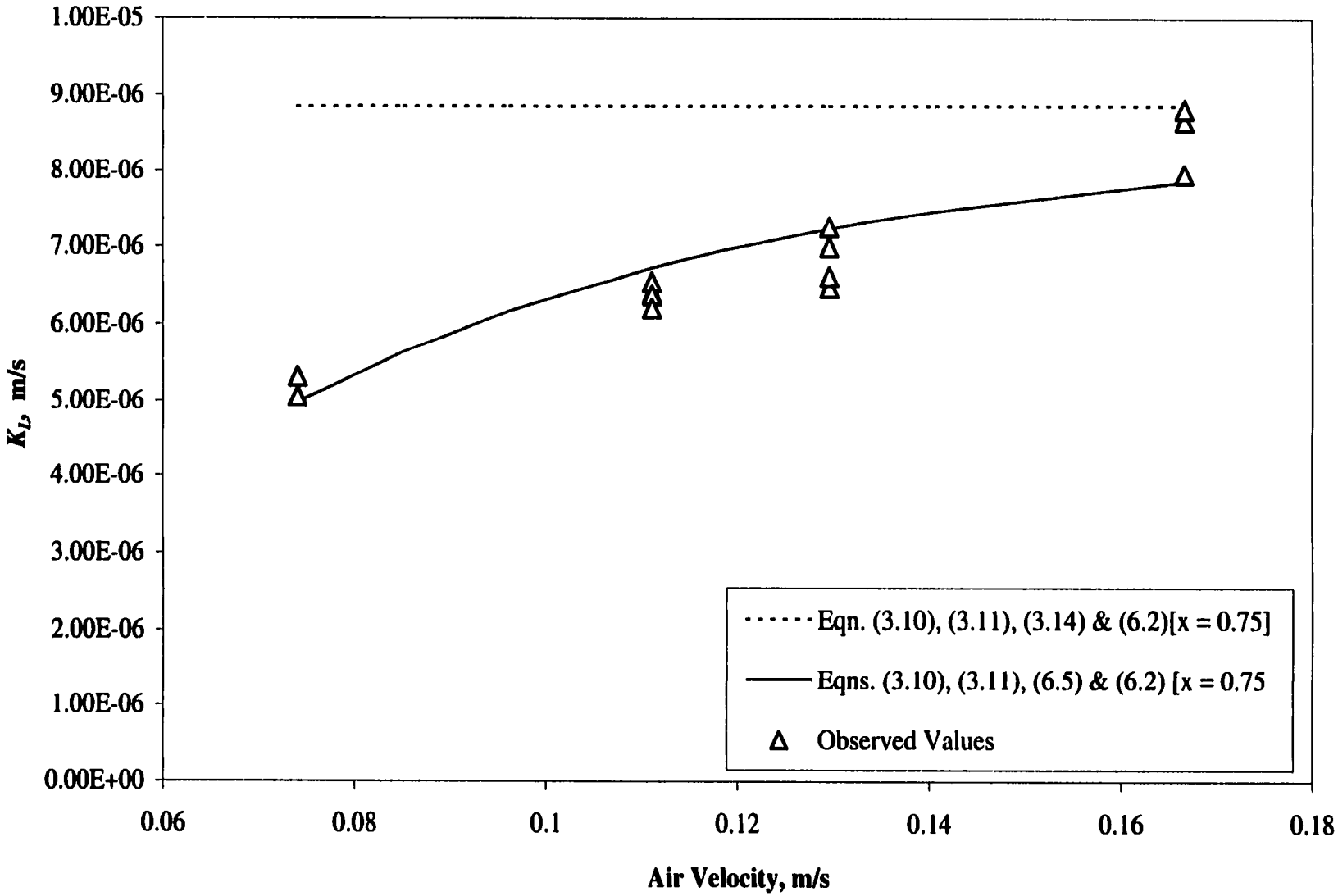

Figure 6.19 Comparison of Lévéque Equation and Modified Lévéque Equation with Experimental Data (Wet Tests)

experimental data far better. Similarly, the overall mass transfer coefficients for dry tests were predicted combining eqns. (3.10), (3.11), (3.14) and (6.2) with x = 1.0 and also using eqns. (3.10), (3.11), (6.6) and (6.2) with x = 1.0. The comparison of such obtained K_L values with experimental K_L values were made in Fig. 6.20. Again, the modified equation [eqn. (6.6)] reproduced the experimental data in a far better way.

It can be concluded from above that modification of the Graetz number is needed to describe the effect of low gas velocities for better prediction of experimental values.

From the above results and the modeling, it becomes clear that the higher air velocities beyond a certain optimum velocity on the lumen will not increase substantially the removal of VOCs by MAS process as the mass transfer resistance become almost negligible. The optimum air velocity was found to be about 0.2 to 0.25 m/s. This low air flow also reduced the total volume of stripped air to be treated.

6.4.4 Comparative Performance of MAS for Removal of Chloroform

The values of the overall mass transfer coefficients, K_L obtained in this work for the removal of chloroform from aqueous solution were twice as large as those reported by Semmens et al. (1989), whose batch system had similar air velocities on the shell side and at least an order of magnitude higher water velocities on the lumen side. The K_L values from the present study were also twice as large as those reported by Zander et al. (1989a) who used a continuous single pass system. Their system also had air velocities (on the shell side) at least three times higher and water velocities (on the lumen side) an

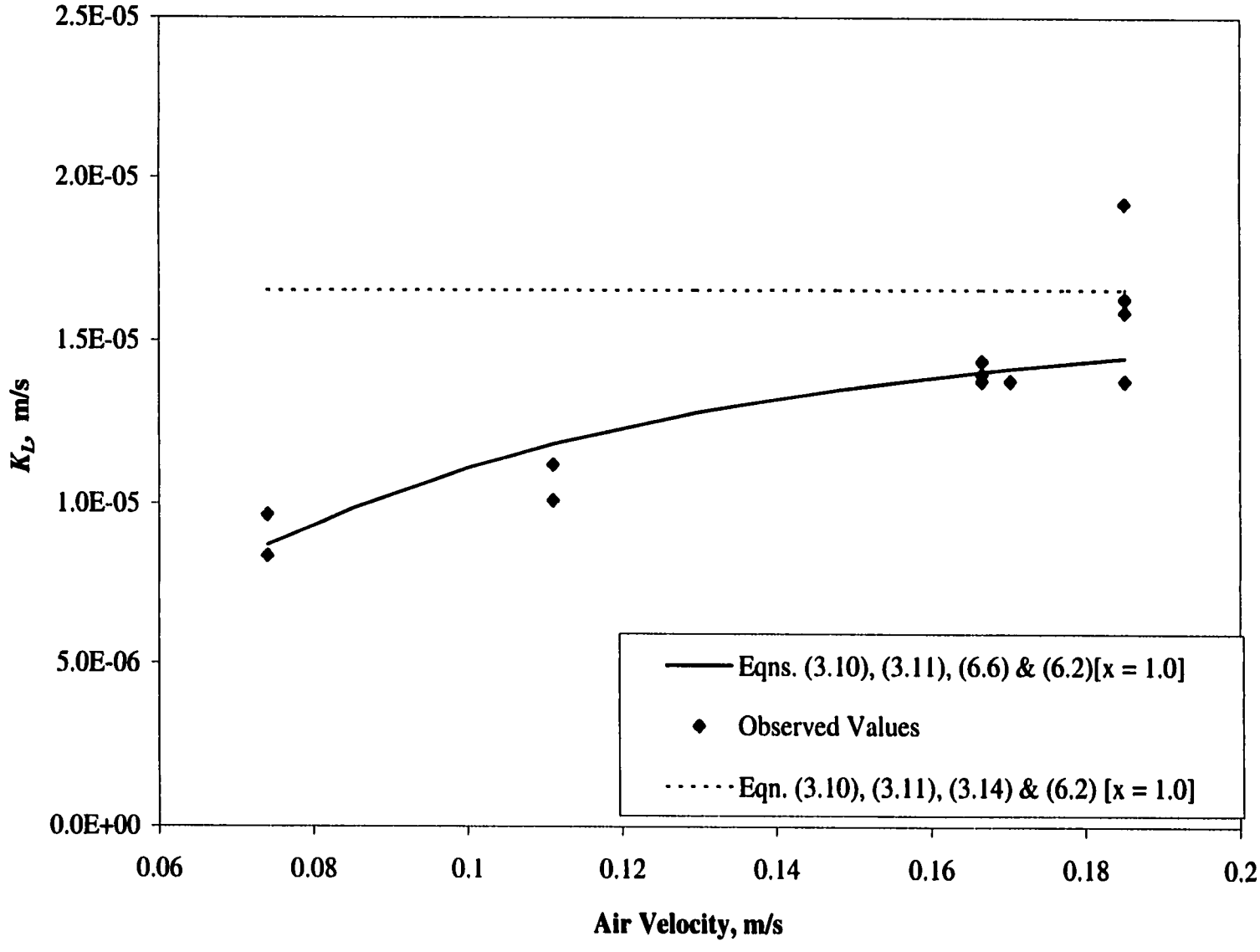

Figure 6.20 Comparison of Lévéque Equation and Modified Lévéque Equation with Experimental Data (Dry Tests)

order of magnitude higher than this study. A higher overall mass transfer coefficient of oxygen was also obtained by Sengupta et al. (1998) for modules with liquid cross-flow on the shell side as compared with liquid flow on the lumen side. From the above comparison, it is clear that the switch of the solution from lumen to shell side of the fibers does improve the VOC removal efficiency.

A comparison of the values of K_La obtained from this study with those reported for PTA in the literature is given in Table 6.12. Although the air to water ratio for this study and that for PTAs are much different, the K_La obtained from this study are higher than those reported for PTA. The K_La values are reported in h^{-1} for convenience.

Table 6.12 Comparison of K_La

	Dry[1]	Wet [2]	Zander et al.[3]	Cornwell [4]	Ball et al.[5]
Process	MAS[6]	MAS	PTA[7]	PTA	PTA
A/W ratio[8]	2.5 : 1	2.25 : 1	50 : 1	30 : 1	44:1
K_La, h^{-1}	146-203	84-93	29.7 - 32.4	17.9 - 30	21.3

[1] Obtained in this study for dry tests
[2] Obtained in this study for wet tests
[3] Reported by Zander et al., 1989a
[4] Reported by Cornwell, 1990
[5] Reported by Ball et al., 1984
[6] MAS = Membrane air stripping using microporous polypropylene hollow fiber
[7] PTA = Packed tower air stripping
[8] A/W ratio = air to water ratio

Due to the lack of facilities for the direct analysis of stripping air at the exit of the module, chloroform concentration in the stripping air was unknown. But, in a number of cases, exit air was passed through a cold trap immersed in liquid nitrogen to observe the condensed liquid. Although, a number of steps were required before final collection of the condensed liquid in a vial, the condensed liquid separated into chloroform and water

phases, the volume of the latter phase being negligibly small (less than 10% of the total volume). The samples were collected for a period of 10 minutes at the beginning of MAS tests with aqueous solutions having initial chloroform concentration of 680 ± 30 ppm. These results indicate that MAS can be a technically attractive process for recovery of almost pure organic solvents from dilute aqueous solutions. This may reduce the need for further purification of the recovered organics as is normally the case while using conventional extraction processes.

6.5 EFFECT OF CHLOROFORM CONCENTRATION ON ITS REMOVAL FROM AQUEOUS SOLUTIONS

The effect of initial feed chloroform concentration has been studied in a range from 81 to 908 ppm. The $ln(C_0/C_t)$ versus time plot such as shown in Fig. 6.9 should provide k as a slope of a linear regression line. It was found that the linear regressions for different feed concentrations fit the data very well as the values of R^2 were more than 0.99. The overall mass transfer coefficient, K_L, was calculated by eqn. (3.36) and the results are presented in Table 6.13 and in Fig 6.21.

From the figure, it is clear that there is no effect of the initial feed chloroform concentration on the overall mass transfer coefficient, hence this technology has potential for industrial wastewater application for removal/recovery of organics in a wide range of concentrations without facing any operational limitations. The values for K_La were further calculated and the results are also presented in Table 6.13. The following numerical values were used in these calculations: $u^w = 5.95 \times 10^{-3}$ m/s; $a = 2930$ m^2/m^3;

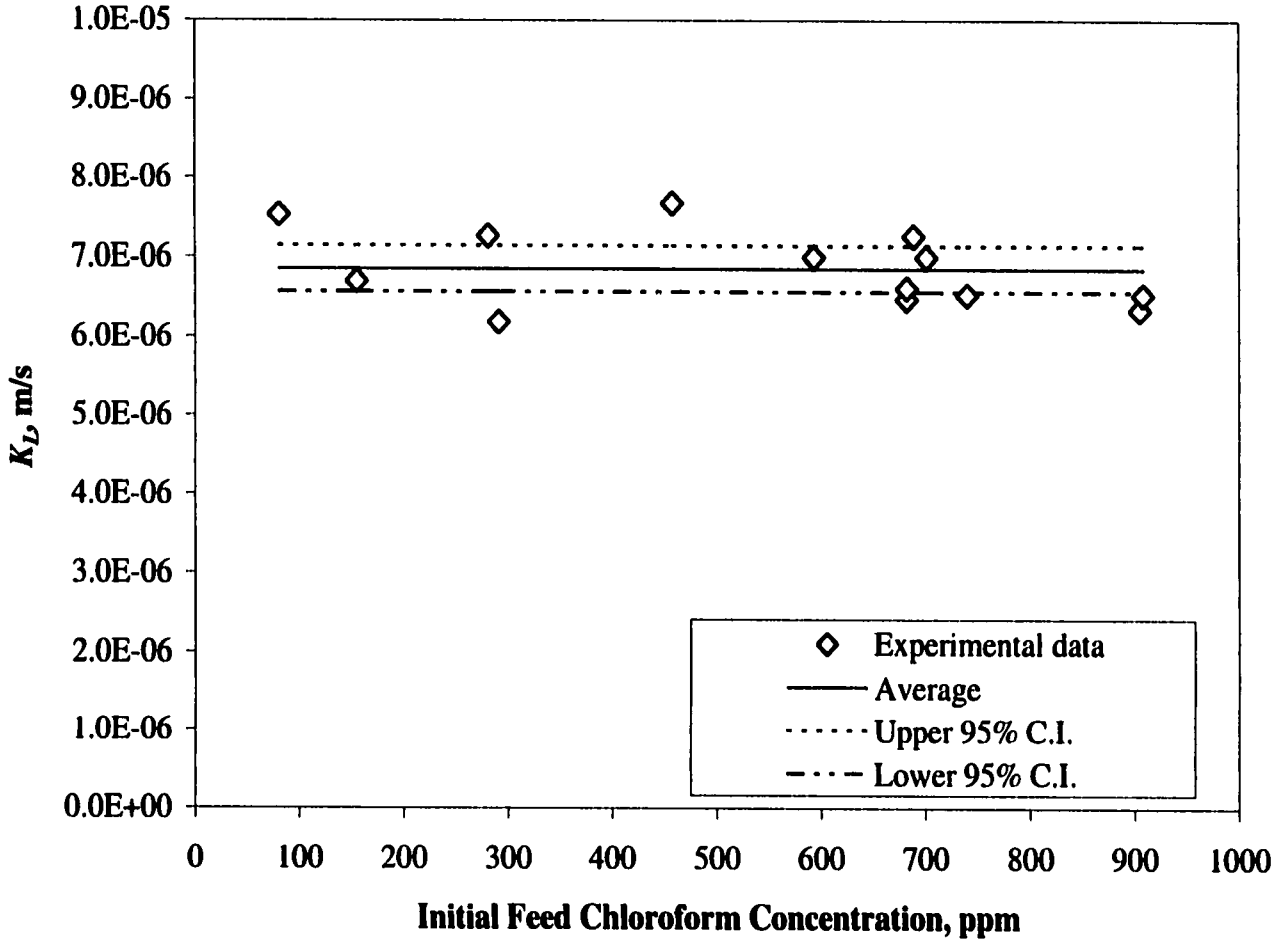

Figure 6.21 Effect of Initial Feed Chloroform Concentration on K_L

L= 0.15 m; R = 3.78; Q_w = 3.33x10^{-5} m^3/s; Q_a = 5.83x10^{-5} m^3/s and V_w = 6.675 x10^{-3}m^3.

Table 6. 13 Values of k, K_L and K_La (effect of initial feed $CHCl_3$ concentration)

Initial $CHCl_3$ Conc., ppm	k, min^{-1}	R^2	K_L, m/s*	K_La, h^{-1}
81	0.0661	0.9993	7.53E-06	79.38
155	0.0635	0.9946	6.70E-06	70.70
281	0.0653	0.9942	7.26E-06	76.53
291	0.0616	0.9986	6.19E-06	65.27
458	0.0665	0.9950	7.67E-06	80.88
593	0.0645	0.9935	7.00E-06	73.85
682	0.0627	0.9936	6.48E-06	68.33
682	0.0632	0.9902	6.62E-06	69.80
689	0.0653	0.9942	7.26E-06	76.53
701	0.0645	0.9978	7.00E-06	73.85
740	0.0629	0.9954	6.53E-06	68.91
905	0.0622	0.9929	6.34E-06	66.92
908	0.0629	0.9911	6.53E-06	68.91
Average	0.06394		6.85E-06	72.30
STDEV	0.00154		4.66E-07	4.92
Cv	0.02410		6.80E-02	0.068
Upper 95% C.I.			7.14E-06	
Lower 95% C.I.			6.57E-06	

* K_L calculated using eqn. (3.36)

6.6 REMOVAL OF TOLUENE FROM AQUEOUS SOLUTION

Experiments were conducted for MAS of toluene from aqueous solutions under wet conditions only. The samples from the toluene experiments were analyzed by TOC analyzer. The TC values were directly converted to toluene concentration by multiplying TC values by a factor of 1.10. For some MAS experiments, all the samples collected from the beginning to the end of the experiment were analyzed by GC6890 by direct injection of the aqueous sample as described in Section 4.6.4. It was found from the analyses conducted using GC6890 that the samples contained only toluene and no other

compounds. This might have been caused by the excess toluene used for solution preparation. As toluene is a good solvent, all the organic impurities in toluene as well as in water might have been partitioned in toluene floating above the solution. An overlapping view of the chromatographs of 8 samples from a single MAS experiment is shown in Fig. 6.22.

The rate constants obtained for toluene removal by plotting the $ln(C_0/C_t)$ versus time were lower than those observed for chloroform. A typical example is presented in Fig. 6.23, which shows a significantly lower rate constant (slower removal) for the toluene test than for the chloroform test under identical operating conditions. The diffusion coefficients for toluene in the air phase and in the water phase are lower than those of chloroform by 11.6 and 13.8%, respectively. Thus, the removal of toluene should be slightly lower than that of chloroform. The observed overall mass transfer coefficients, K_L (Appendix – J), were calculated from the rate constants using eqn. (3.36) for toluene and compared with the values predicted by using eqns. (3.10), (3.11), (3.14) and (6.2) with $x = 0.75$ in Fig. 6.24.

The overall mass transfer coefficients were further predicted using eqns. (3.10), (3.11), (6.5) and (6.2) with $x = 0.75$ and results are also shown in Fig. 6.24. It was found that the observed values of K_L are far smaller than those predicted. It is stated in section 6.3 that adsorption of toluene on the hydrophobic surface of the system including the membrane was very high. Toluene, when adsorbed onto hollow fibers, swelled the polymer matrix, resulting in the reduction of the pore size. Hence, the membrane transport resistance

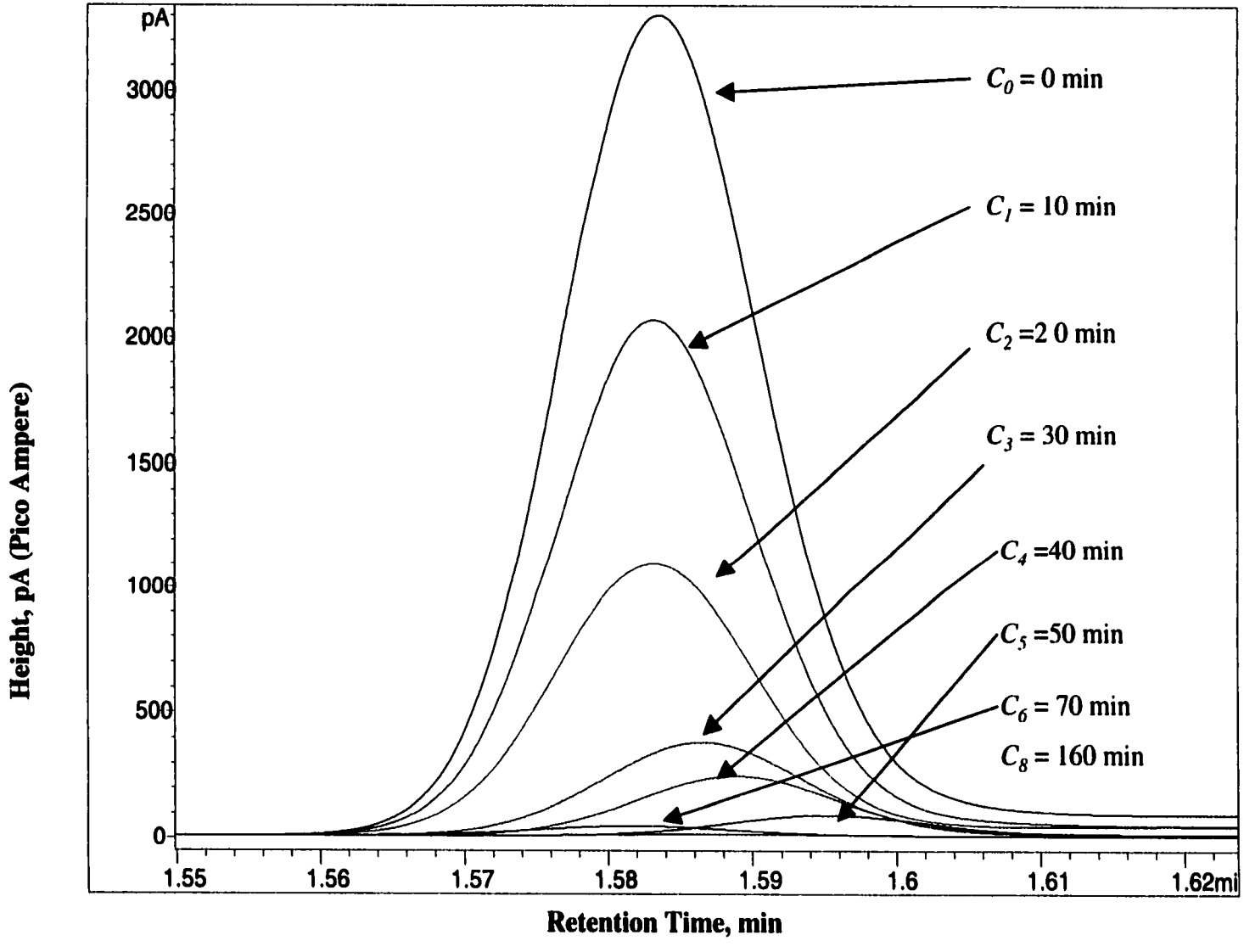

Figure 6.22 Overlapping View of Chromatographs of 8 Toluene Samples

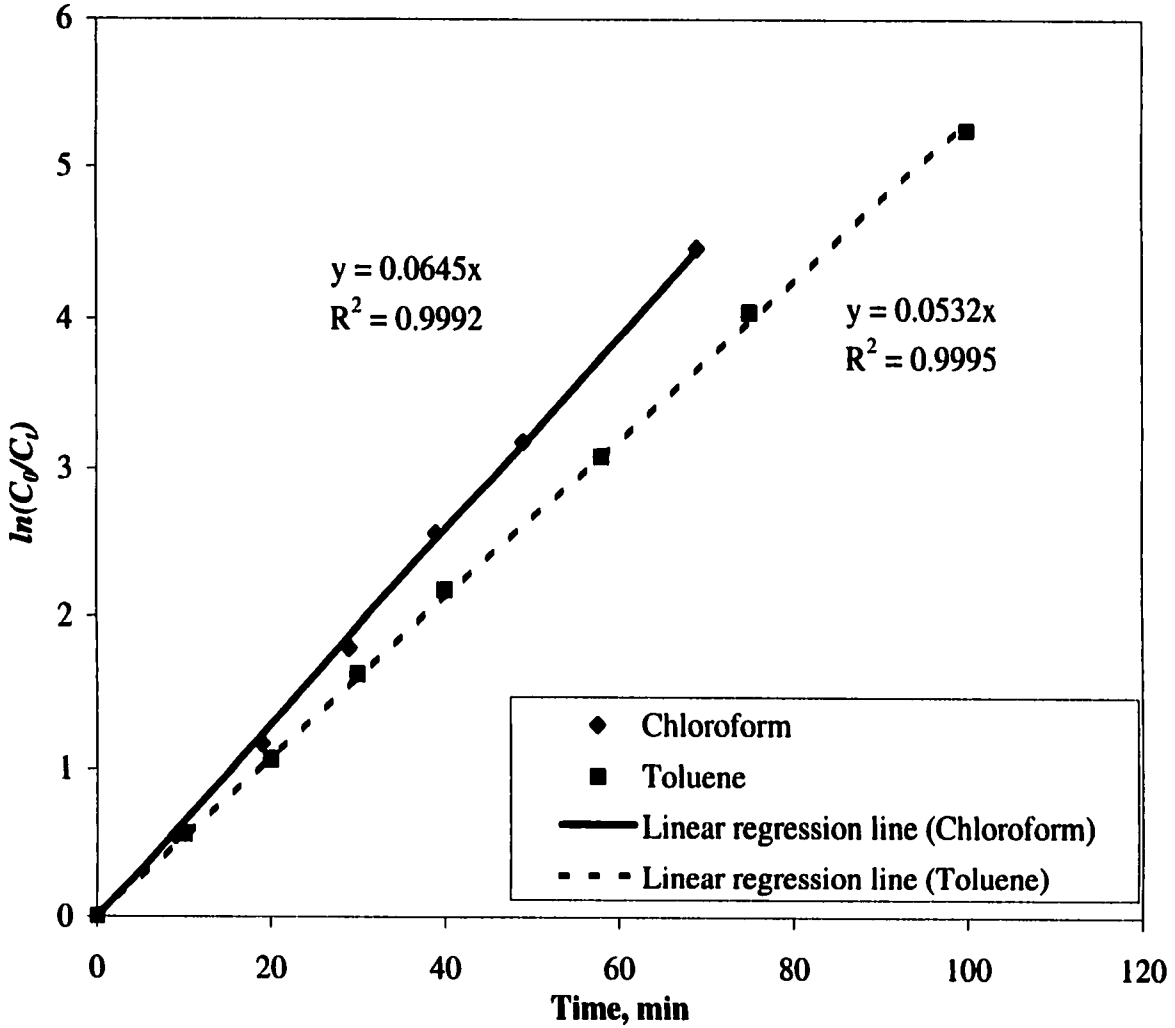

Figure 6.23 Comparison of Rate Constants of Chloroform and Toluene (Air Velocity = 0.13 m/s & Solution Velocity = 5.95 x 10-3 m/s)

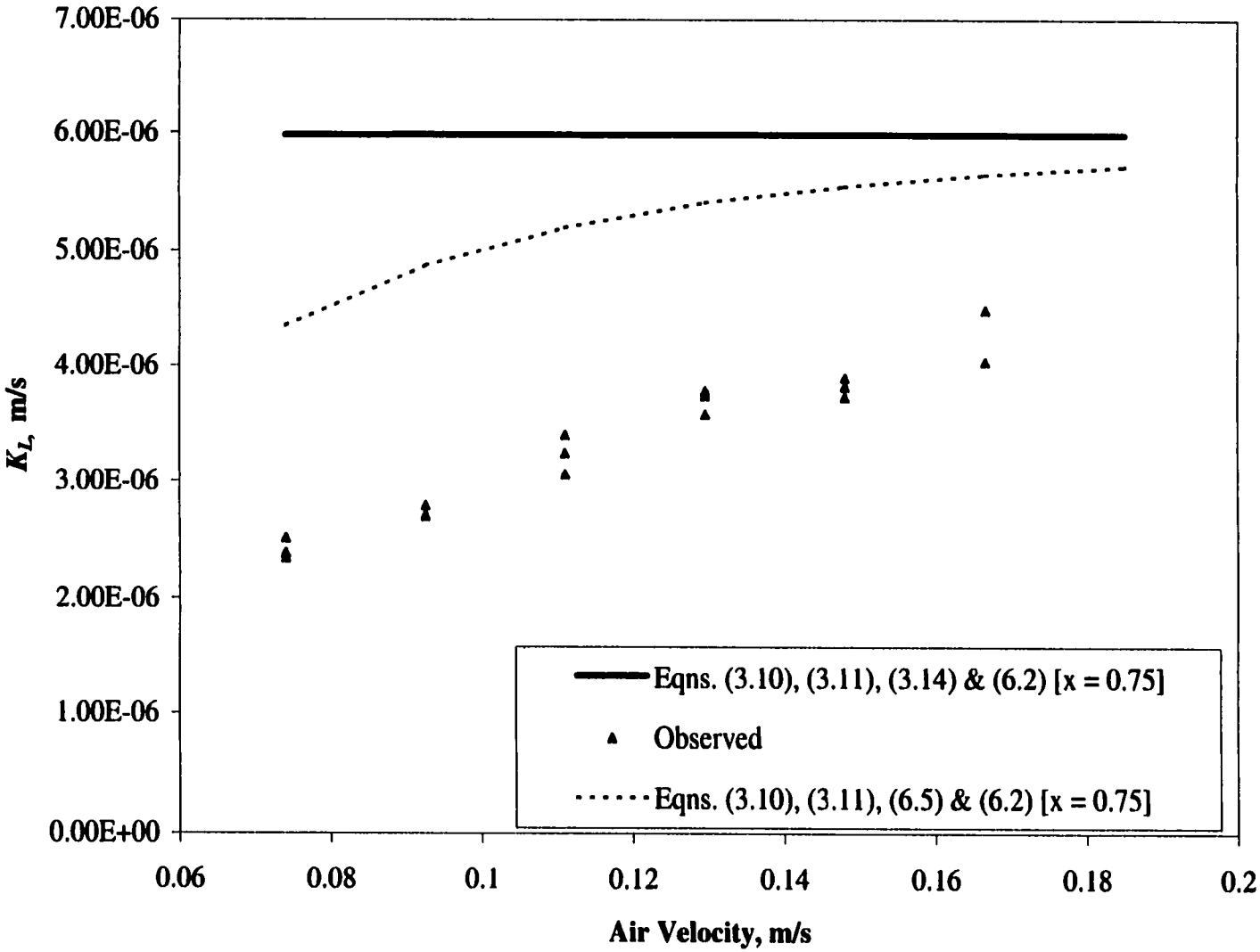

Figure 6.24 Predicted K_L Vs Observed K_L for Toluene

increased. Wang and Cussler (1993) reported that the results from their stripping experiments of toluene were not reliable. They have attributed it to the swelling effect of toluene on polypropylene hollow fibers. It was also reported that toluene increased the weight of polypropylene by 11% after a contact period of 10 days as a result of swelling (Kroschwitz, 1985). The gradual desorption of the adsorbed toluene at the later stage of experiments likely contributed to the decrease in the rate of toluene removal.

The main factor behind this deviation was likely the reduction of the effective pore diameter, which was directly related to the adsorption/swelling by toluene of the membrane. On the other hand, this adsorption was dependent on the toluene concentration in the solution. For the batch system used in this study, the toluene concentration decreased with time. Thus, it is difficult to account for the changes of the pore shape and size over the period of the experiment to model it properly for a batch system. Precise quantification of swelling effect by toluene is out of the scope of this study. A further investigation regarding this phenomenon is needed. It can be concluded that the interactions between the membrane and toluene played a very important role during mass transport of toluene and should be taken into account during design of MAS process for such VOCs.

6.7 REMOVAL OF MIXTURES OF CHLOROFORM AND TOLUENE FROM AQUEOUS SOLUTION

Experiments were conducted for MAS of mixtures of chloroform and toluene from aqueous solutions under wet conditions only. The samples from the experiments were analyzed by gas chromatography (GC6890) after extraction in n-pentane as described in

section 4.5.3. The rate constants were calculated separately for chloroform and toluene by plotting the $ln(C_0/C_t)$ versus time (Appendices - K and L). The rate constants for toluene were similar to those obtained from experiments with single toluene solute. But, the rate constants observed for the removal of chloroform were much lower than those observed from experiments with single chloroform solute. A typical example is presented in Fig. 6.25, which shows a lower rate constant (slower removal) for the test with chloroform/toluene mixture than that for single chloroform test under identical other operating conditions. K_L values were compared between single and mixed solute systems for chloroform and for toluene in Figs. 6.26 and 6.27, respectively. The decrease in K_L of chloroform in the presence of toluene might have been caused by the reduction of the pore size as a result of toluene adsorption/swelling. On the other hand, the slight increase in K_L values for toluene might have been caused by the competition of chloroform for adsorption sites, which inevitably reduces toluene adsorption/swelling and hence the degree of pore size reduction. This also reduces desorption of toluene at the later stages.

6.8 PRESSURE DROPS ON THE LUMEN AND SHELL SIDES OF THE HOLLOW FIBERS

The pressure drop caused by liquid flow on the shell side was studied experimentally. It was found that the pressure drops varied from 0.90 kPa for a flow of 0.4 $x10^{-3}$ m^3/min to 21.63 kPa for a flow of 4.0 $x10^{-3}$ m^3/min (Fig. 6.28).

The pressure drop caused by air flow on the lumen side was studied both experimentally and theoretically. The flows in the lumen of the fibers were in the laminar range.

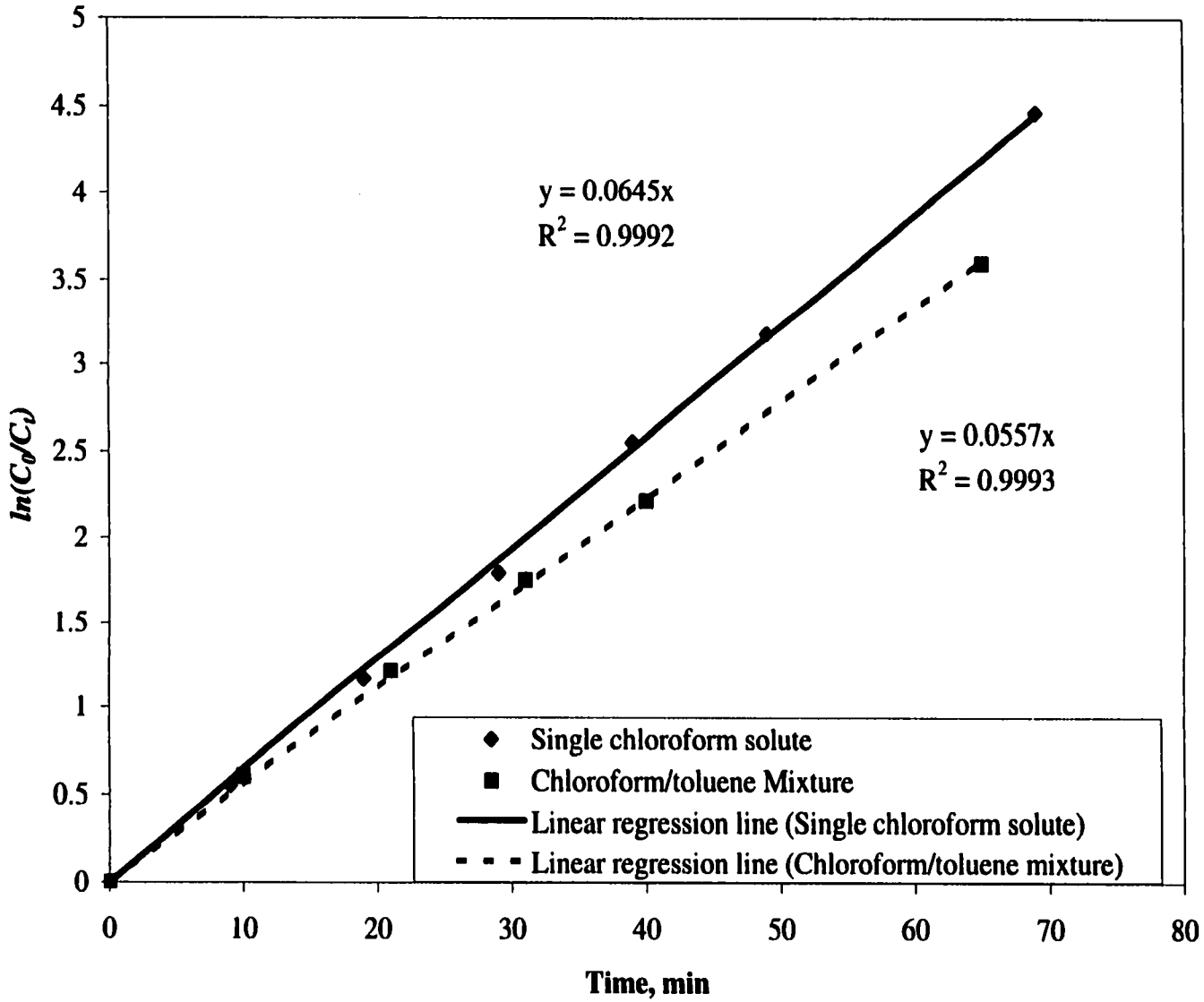

Figure 6.25 $Ln(C_0/C_t)$ Versus t Plot for Aqueous Solutions Involving Chloroform as a Single Solute or as Chloroform/Toluene Mixture (Air Velocity = 0.13 m/s & Solution Velocity = 5.95 x 10^{-3} m/s)

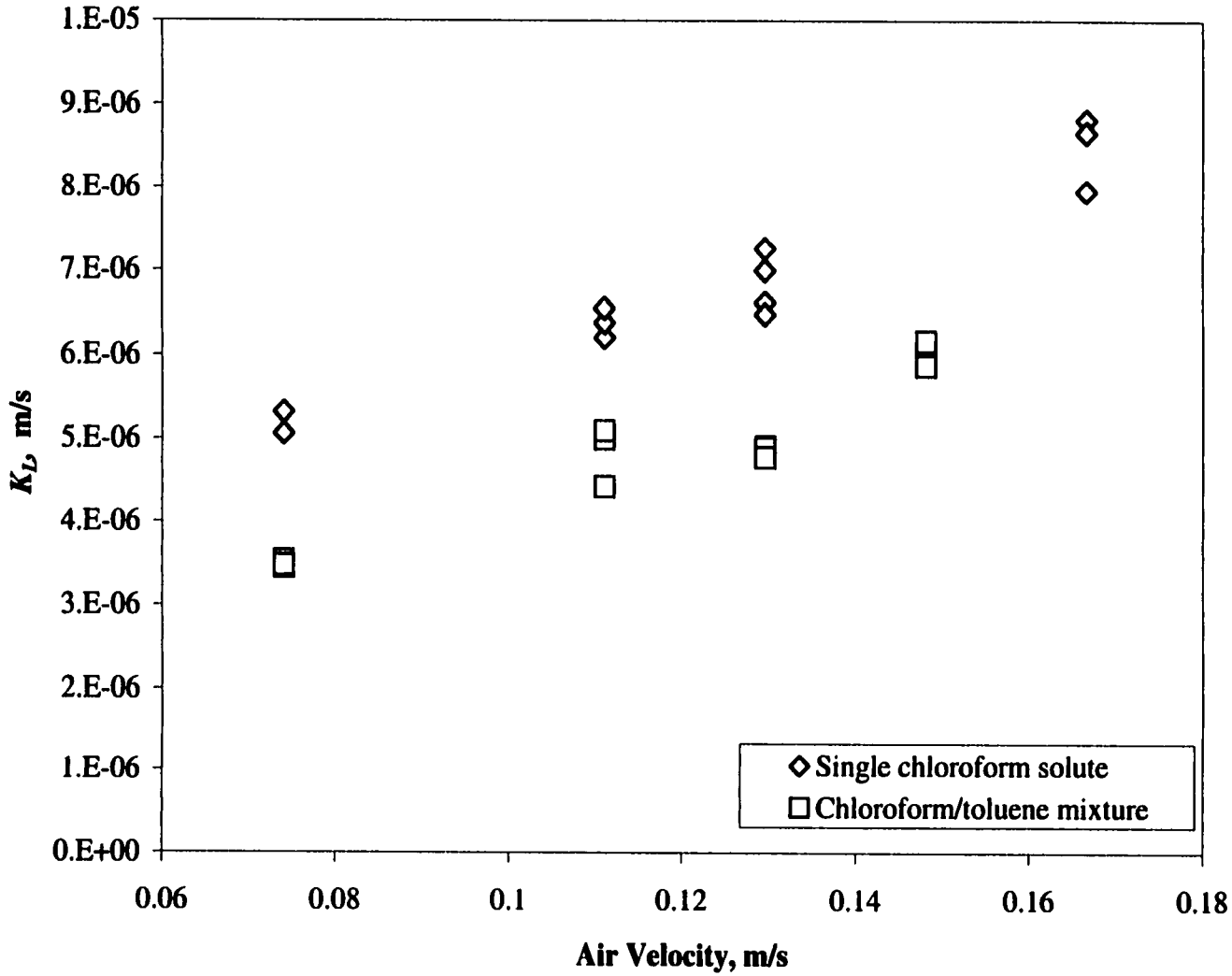

Figure 6.26 Comparison of K_L for MAS of Chloroform from Aqueous Solutions Involving Chloroform as a Single Solute or as Chloroform/Toluene Mixture (Solution Velocity = 5.95 x 10^{-3} m/s)

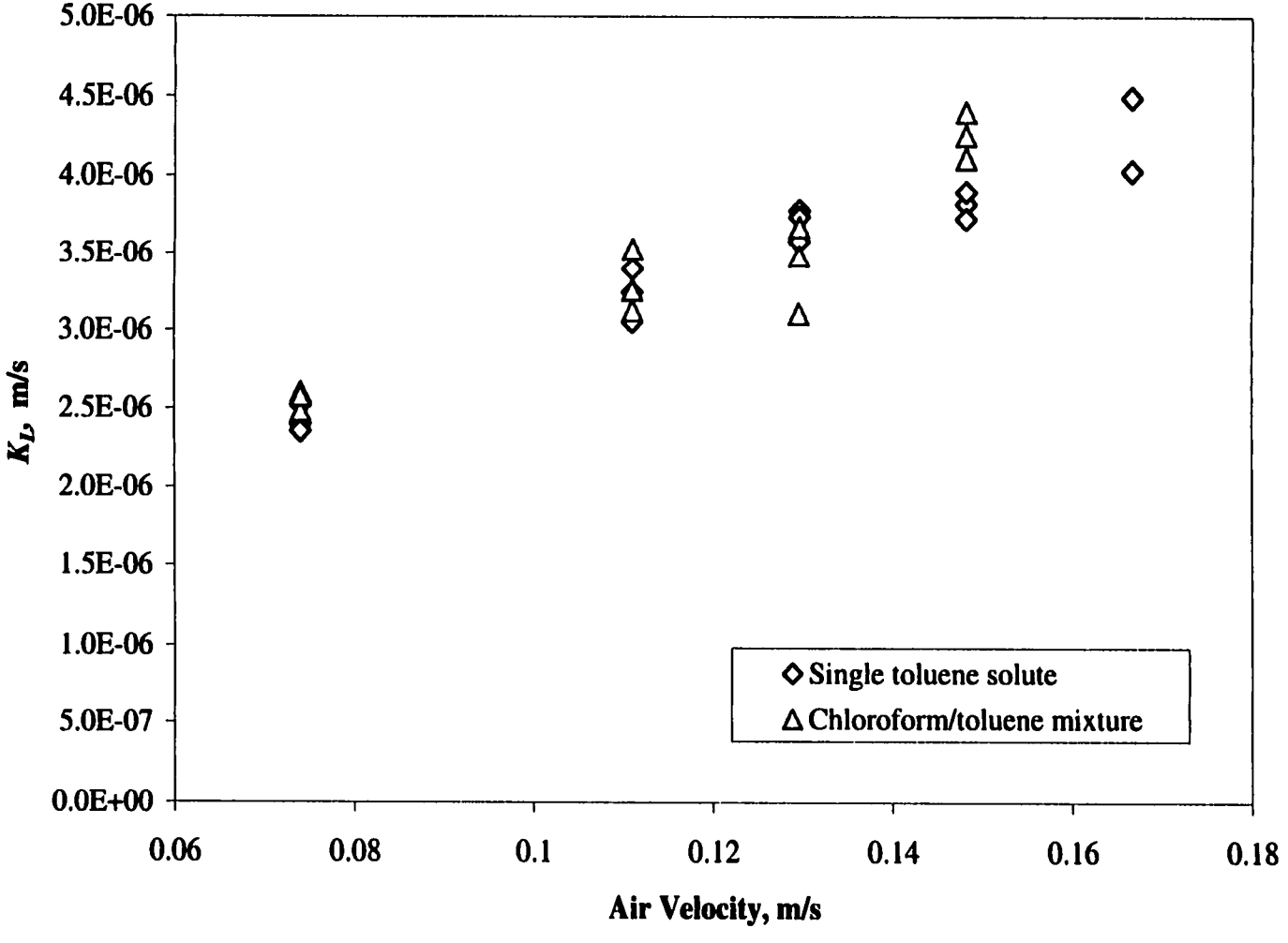

Figure 6.27 Comparison of K_L for MAS of Toluene from Aqueous Solutions Involving Toluene as a Single Solute or as Chloroform/Toluene Mixture (Solution Velocity = 5.95 x 10^{-3} m/s)

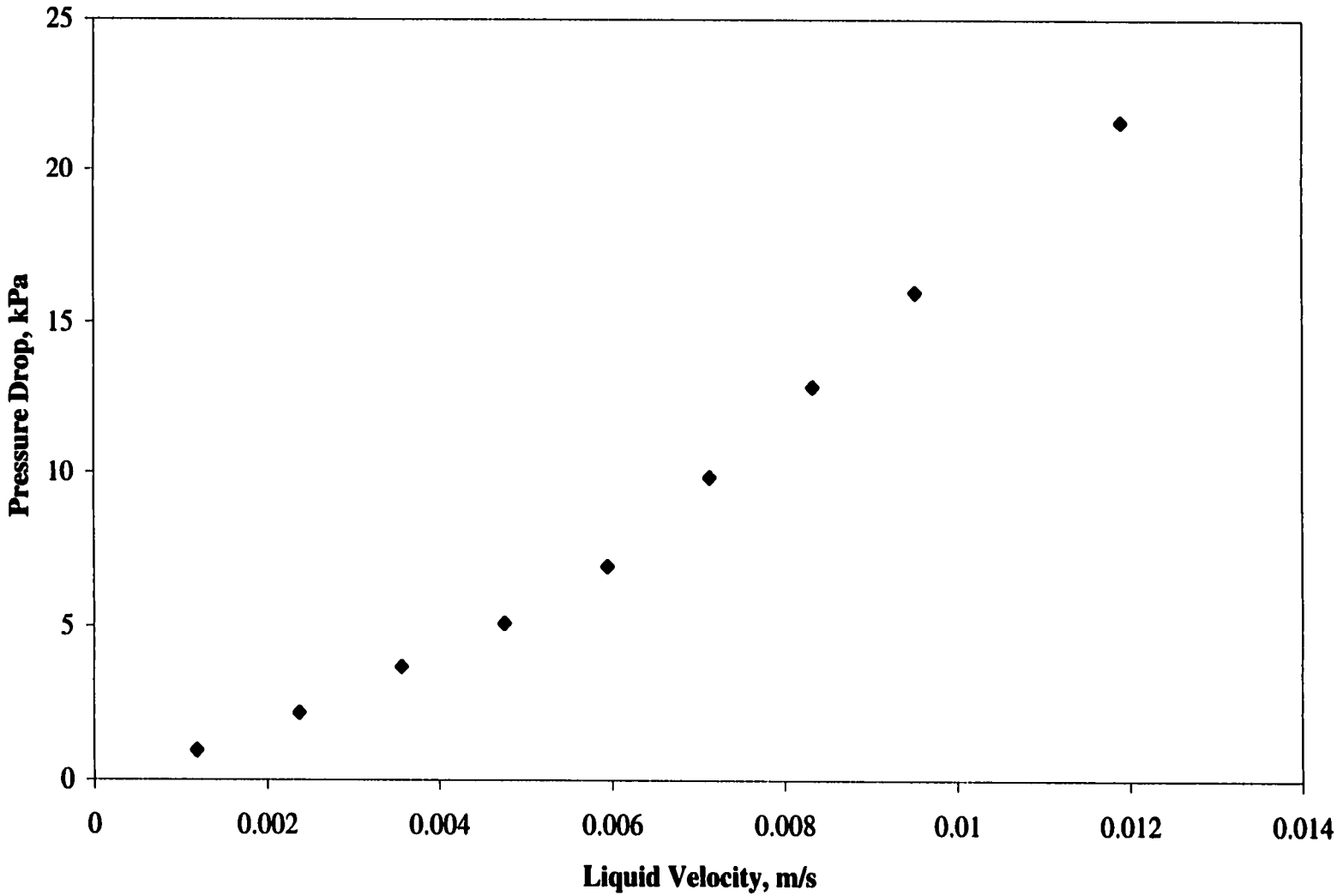

Figure 6.28 Observed Pressure Drops for the Liquid Flow on the Shell Side

Although many alternate forms of equations are available in the literature for theoretical calculation of the pressure drop in pipes (Crawford and Eckes, 1984; Govier and Aziz, 1972), in this study Hagen-Poiseuille equation was used. A stabilized steady-state laminar flow was assumed for the entire length of the fiber. As shown in Fig. 6.29, the experimental values were an order of magnitude higher than theoretical ones. Data provided by the manufacturer for air pressure drop on the lumen side had values four times higher than those predicted by Hagen-Poiseuille (Whisnant, 1999). It needs to be pointed out that this observed pressure drop was the combined effect of the pressure drop caused by the air flow in the lumen side, the entrance effect, exit effect as well as due to the changes of flow direction at the inlet and outlet of the module due to its shape. Although the predicted value took into account the pressure drop due to the entrance and exit effects, it did not take the pressure drop due to the shape of the inlet and outlet of the module into consideration. The experimental values for air side pressure drop in the lumen side of the fiber in this study were about five times higher than those reported for the shell side by Zander et al. (1989a). A higher pressure drop by a factor of four on the lumen side compared to that on the shell side for liquid flow was also reported by Sengupta et al. (1998). This indicates that the pressure drop mentioned by the manufacturer was not correct.

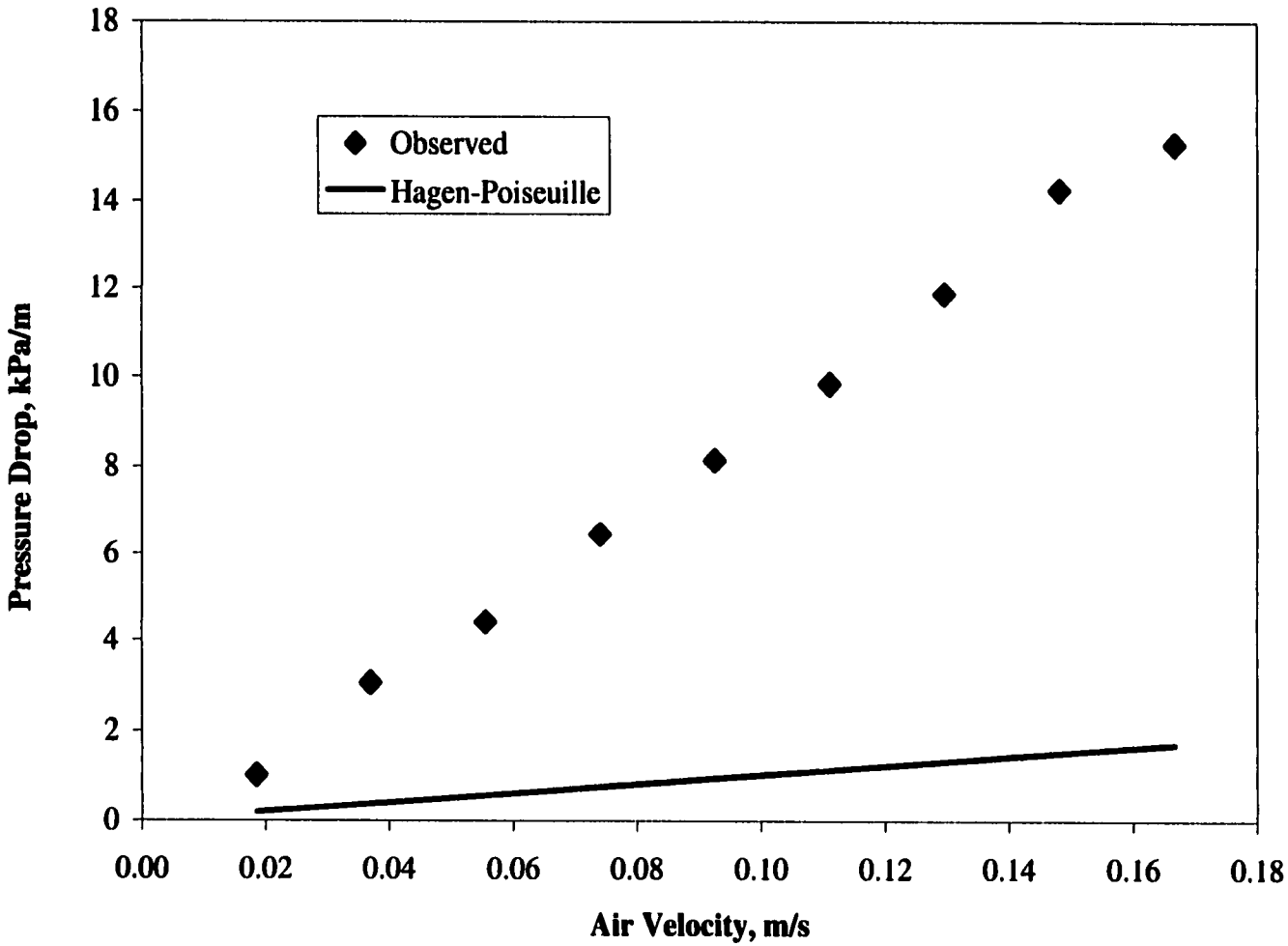

Figure 6.29 Air Pressure Drops on the Lumen Side of Hollow Fiber for Present Study

CHAPTER 7

Conclusions and Recommendations

7.1 CONCLUSIONS

The polypropylene hollow fiber membrane pores were almost completely air-filled for a short period of time after coming in contact with an aqueous phase. During this condition, the mass transport through these pores was simply diffusion through air and its contribution to the overall mass transfer resistance was negligible.

It was speculated that the pores became partially wetted or blocked by water due to their prolonged contact with water during the air-stripping operation. The deposition of water in the pores possibly created a liquid barrier and led to a higher membrane resistance. In this situation, to describe mass transfer within the membrane, one needs to consider diffusion through air as well as liquid in the pores.

A model that considers the membrane resistance to be composed of 1) a resistance for the fraction of pores that are air-filled plus, 2) a resistance for the fraction of pores that are liquid–filled has been proposed. The model predictions agree well with our experimental data as well as that from the literature. The model also explains the discrepancies in the values reported by Kreulen et al. (1993) and Qi and Cussler (1985c).

The mass transfer resistance created by the membrane when partially wetted was almost equal to liquid phase resistance and its contribution to the overall mass transfer resistance became significant.

The Kreith and Black (1980) correlation provides better predictions in these closely packed membrane modules having liquid cross-flow on the shell side compared to the correlations of Yang and Cussler (1986) and Reed et al. (1995).

Lévéque's (1928) correlation overestimated the local air phase mass transfer coefficient in the lumen of the fiber at low air velocities. The alternative correlations developed by Wickramasinghe et al. (1992) for predicting the local liquid phase mass transfer coefficient in the lumen of the fiber at low flow rates had some limitations in predicting the local air phase mass transfer coefficient in the lumen of the fiber at the range of air velocities studied. An alternative correlation has been proposed which successfully predicted the experimental data.

Although, liquid cross-flow on the shell side yielded a higher overall mass transfer coefficient than that for liquid flow in the lumen side, the air pressure drop on the lumen side was significantly higher than that of shell side.

It was possible to concentrate chloroform from ppm levels to more than 90% of chloroform from aqueous solution using MAS. The chloroform was relatively pure thereby reducing the need for further purification.

No effect of feed chloroform concentration was observed on the overall mass transfer coefficient within the range of concentration (81 – 908 ppm) studied in this work. Thus, MAS has great potential for removal/recovery of VOCs from VOCs laden industrial wastewater having a wide range of VOC concentrations.

The toluene adsorption/swelling on polypropylene membrane was very high and might have caused reduction of the effective pore diameter. As a result, the overall mass transfer coefficient obtained from MAS of toluene from aqueous solutions were much lower than expected according to its physicochemical properties.

The presence of toluene in the binary aqueous solution with chloroform significantly reduced the mass transport of chloroform, while removal rate of toluene was affected only marginally by the presence of chloroform.

There was no evidence of any effect of initial concentration of chloroform in the aqueous phase within the range of 21 to 851 ppm on the dimensionless Henry's law constant.

The dimensionless Henry's law constant of chloroform and toluene were not impacted by the presence of each other when present in liquid concentration of 809 and 255 ppm, respectively.

7.2 RECOMMENDATIONS

The removal/recovery of VOCs from an industrial VOCs laden wastewater needs to be studied to determine the necessary pretreatment requirements.

The present study should be continued with a half-industrial pilot plant to investigate MAS of organics from aqueous solution with continuous solution flow including VOC recovery from stripped-air.

Further study should explore technical and economical feasibility of hybrid system for treatment of VOC laden wastewater.

The kinetics of adsorption and desorption of toluene or alike compounds onto polypropylene membranes needs further detailed study.

The impact of adsorption on pore size needs to be studied in detail.

References:

Abraham, M. H., J. Andonian-Haftvan, G. S. Whiting, A. Leo and S. Taft, "Hydrogen Bonding. Part 34. The factors That Influence the Solubility of Gases and Vapors in Water at 298 K, and a New Method for its Determination", J. Chem. Soc. Perkin Trans., **2**, 1777-1791 (1994).

Al-Dhowalia, K. H., "Trace Volatile Organics Removal from Water and Wastewater by Air Stripping", Ph. D. Thesis, University of Colorado at Boulder, CO, USA (1982).

Altschuh, J., R. Brüggemann, H. Santl, G. Eichinger and O. G. Piringer, "Henry's Law Constants for a Diverse Set of Organic Chemicals: Experimental Determination and Comparison of Estimation Methods", Chemosphere, **39**, 11, 1871-1887 (1999).

Ashworth R. A., G. B. Howe, M. E. Mullins and T. N. Rogers, "Air-Water Partioning Coefficients of Organics in Dilute Aqueous Solutions", Presented at AIChE Summer National Meeting, Boston, MA, USA (1986).

Ball, W. P., M. D. Jones and M. C. Kavanaugh, "Mass Transfer of Volatile Organic Compounds in Packed-Tower Aeration", J. Water Pollution Control Federation, **56,** 2, 127-136 (1984).

Bhowmick, M. and M. J. Semmens, "Batch Studies on a Closed Loop Air Stripping Process", Water Res., **28**, 9, 2011-2019 (1994).

Bhowmick, M. and M. J. Semmens, "A Novel Closed Loop Air Stripping Process", in "Hazardous and Industrial Wastes - Proceedings of the Mid-Atlantic Industrial Waste Conf. 1993", Publ. by Technomic Publ Co Inc, Lancaster, PA, USA (1993), pp.136-145.

Bhowmick, M., "A Novel Closed Loop Air Stripping Process", Ph. D. Thesis, University of Minnesota, MN, USA (1992).

Boswell, S. T. and A. D. Vaccari, "Plate and Frame Membrane Air Stripping", in "Proceedings of the 21st Annual Conference on Water Policy and Proc. 21 Annu. Conf. Water Policy Management Solving Problem, 1994", Publ by ASCE, New York, NY, USA (1994), pp. 726-729.

Brennan, R. A. N. Nirmalakhandan and R. E. Speece, " Comparison of Predictive Methods for Henry's Law Coefficients of Organic Chemicals", Water Res., **32**, 6, 1901-1911 (1998).

Brewer, J., "Literature Reviews and Research Scooping Study on the Treatment of Volatile Organic Carbon Compounds in the Off-gas from Contaminated Groundwater and Soil

Remedial Technologies", National Groundwater and Soil Remediation Program, Environment Canada, Ottawa, ON, Canada (1991).
Burkhard L. P., D. E. Armstrong and A. W. Andren, "Henry's Law Constants for Polychlorinated Biphenyls", Environ. Sci. Technol., **19**, 590-596 (1985).

Castro, K. and A. K. Zander, "Membrane Air-Stripping: Effect of Pretreatment", J. Am. Water Works Assoc., **87**, 3, 50-61 (1995).

Clark, R. M., R. G. Eilers and J. A. Goodrich, "VOCs in Drinking Water: Cost of Removal", J. Environ. Eng.-Div, ASCE, **110**, 6, 1146-1162 (1984).

Collins, J., "Enhancing the Scrubbing of Chlorinated Compounds from Air Streams", A. Master of Engineering Thesis, Department of Civil and Environmental Engineering, Carleton University, Ottawa, ON, Canada (1998).

Cornwell, D. A., "Air Stripping and Aeration", in "Water Quality and Treatment, A Handbook of Community Water Supplies", Fourth Edition, F. W. Pontius, Ed., Am. Water Works Assoc., McGraw-Hill, Inc., New York, NY, USA (1990), pp. 229-268.

Côté, P., J. L. Bersillon and A. Huyard, "Bubble-Free Aeration Using Membranes: Mass Transfer Analysis", J. Membr. Sci., **47**, 91-106 (1989).

Crawford, H. B. and B. E. Eckes, Eds., "Perry's Chemical Engineers' Handbook", Sixth Edition, McGraw-Hill, Inc., New York, NY, USA (1984), pp. 5-20 – 5-68.

Cussler, E. L.,"Diffusion. Mass Transfer in Fluid Systems", Cambridge Univ. Press, London, UK (1984).

Dvorak, B. I., D. F. Lawler, G. E. Speitel, Jr., D. L. Jones and D. A. Boadway, "Selecting Among Physical/Chemical Processes for Removing Synthetic Organics from Water", Water Environ. Res., **65**, 7, 827-838 (1993).

Dyksen, J. E. and A. F. Hess, "Alternatives for Controlling Organics in Groundwater Supplies", J. Am. Water Works Assoc., **74**, 8, 394-403 (1982).

Ehrenfeld, J. R. and J. H. Ong, "Evaluation of Emission Control Technologies", in: Controlling Volatile Emissions at Hazardous Waste Sites, Ehrenfeld et. al., Eds., Noyes Publications, Park Ridge, NJ, USA (1986), pp. 1-156.

ESE (Environmental Science and Engineering, Inc.), "Trace Organics Removal by Air Stripping", Supplementary Report Prepared for the Am. Water Works Assoc. Res. Foundation, Denver, CO, USA, (1981).

Evans, R. B., G. M. Watson and E. A. Mason, "Gaseous Diffusion in Porous Media at Uniform Pressure", J. Chem. Phys., **35**, 6, 2076-2083 (1961).

Fox, H. W. and W. A. Zisman, " The Spreading of Liquids on Low-Energy Surfaces. I. Polytetrafluoroethylene", J. Colloid Sci., **5**, 514 (1950).

Freitas dos Santos, L. M., "Biological Treatment of VOC-Containing Wastewaters: Novel Extractive Membrane Bioreactors vs. Conventional Aerated Bioreactor", Trans Inst. Chem. Eng., **73**, Part B. 227-234 (1995).

Fuller, E. N., P. D. Schettler and J. C. Giddings, "A New Method for Prediction of Binary Gas-Phase Diffusion Coefficients", Ind. Eng. Chem., **58**, 2, 19-27, (1966).

Gabelman, A. and S. Hwang, "Hollow Fiber Membrane Contractors", J. Membr. Sci., **159**, 61-106, 1999.

Goethaert, S., C. Dotremont, M. Kuijpers, M. Michiels and C. Vandecasteele, "Coupling Phenomena in the Removal of Chlorinated Hydrocarbons by Means of Pervaporation", J. Membr. Sci., **78**, 135-145 (1993).

Gossett, J. M., "Measyrement of Henry's Law Constants for C_1 and C_2 Chlorinated Hysrocarbons", Environ. Sci. Technol., **21**, 2, 202-208 (1987).

Gossett, J. M., C. E. Cameron, B. P. Eckstrom, C. Goodman and A. H. Lincoff, "Mass Transfer Coefficients and Henry's Constants for Packed-Tower Air Stripping of Volatile Organics: Measurements and Correlations", Rept. No. ESL-TR-85-18, Engineering & Service Laboratory, U. S. Air Force Engineering and Services Center, Tyndall AFB, FL (1985).

Govier, G. W. and K. Aziz, " The Flow of Complex Mixtures in Pipes", Van Nostrand Reinhold Company, New York, NY, USA (1972).

Greenberg, A. E., L. S. Clesceri and A. D. Eaton, Eds., "Standard Methods for the Examination of Water and Wastewater", Am. Public Health Assoc., Washington, DC, USA (1992).

Greenwood, N. N. and A. Earnshaw, "Chemistry of Elements", 1st Edition, Pergamon Press, New York, NY, USA (1984).

Guha, A. K., P. V. Shanbhag, C. H. Yun, D. Trivedi, D. Vaccari and K. K. Sirkar, "Novel Membrane- Based Separation and Oxidation Technologies", Waste Manage., **13**, 395-401 (1993).

Hand, D. W., J. C. Crittenden and J. l. Gehin, "Design and Evaluation of an Air-Stripping Tower for Removing VOCs from Groundwater", J. Am. Water Works Assoc., **78**, 9, 87-97 (1986).

Hine, J. and P. K. Mookerjee, "The Intrinsic Hydrophilic Character of Organic Compounds. Correlation in Terms of Structural Contributions", J. Org. Chem., **40**, 292-298 (1975).

Howe, G. B., M. E. Mullins and T. N. Rogers, "Evaluation and Prediction of Henry's Law Constants and Aqueous Solubilities for Solvents and Hydrocarbons Fuel Components", NTIS Report, ELS-86-66 (1987).

Karoor, S. and K. K. Sirkar, "Gas Absorption Studies in Microporous Hollow Fiber Membrane Modules", Ind. Eng. Chem. Res., **32,** 674-684 (1993).

Kavanaugh, M. C. and R. R. Trussell, "Design of Aeration Towers to Strip Volatile Contaminants from Drinking Water", J. Am. Water Works Assoc., **72**, 12, 684-692 (1980).

Kesting, R. E., "Synthetic Polymeric Membrane", McGraw-Hill, New York, NY, USA (1971).

Keurentjes, J. T. F., J. G. Harbrecht, D. Brinkman, J. H. Hanemaaijer, M. A. Cohenstuart and K. van't Riet, "Hydrophobicity Measurements of Microfiltration and Ultrafiltration Membranes", J. Membr. Sci., **47**, 333-344 (1989).

Kiani, A., R. R. Bhave and K. K. Sirkar, "Solvent Extraction with Immobilized Interfaces in a Microporous Membrane", J. Membr. Sci., **20**, 125-145 (1984).

Kim, B. and P. Harriott, "Critical Entry Pressure for Liquids in Hydrophobic Membranes", J. Colloid. Sci., **115**, 1, 1-8 (1987).

Knudsen, J. G. and D. L. Katz, "Fluid Dynamics and Heat Transfer", McGraw-Hill Book Company, Inc, New York, NY, USA (1958).

Kosuko, M., M. E. Mullins, K. Ramanathan, and T. N. Rogers, "Catalytic Oxidation of Groundwater Stripping Emissions", Environ. Prog., **7**, 2, 136-142 (1988).

Kreith, F. and W. Z. Black, "Basic Heat Transfer", Harper and Row, New York, NY, USA (1980).

Kreulen, H., C. A. Smolders, G. F. Versteeg and W. P. M. Van Swaaij, "Determination of Mass Transfer Rates in Wetted and Non-Wetted Microporous Membranes", Chem. Eng. Sci., **48**, 11, 2093-2102 (1993).

Kroschwitz, J. I., Eds., "Encyclopedia of Polymer Science and Engineering", 2nd. ed., **13**, John Wiley & Sons, New York, NY, USA (1985), pp. 464-530.

Lalezary, S., M. Pirbazari, M. J. McGuire and S. W. Krasner, "Air Stripping of Taste and Odor Compounds from Water", J. Am. Water Works Assoc., **76**, 3, 83-87 (1984).

Lamarche, P., "Air Stripping Mass Transfer Correlations for Volatile Organics", M. A. Sc., Thesis, Department of Civil Engineering, The University of Ottawa, Ottawa, ON, Canada (1986).

Lamarche, P. and R. L. Droste, "Air-Stripping Mass Transfer Correlations for Volatile Organics", J. Am. Water Works Assoc., **81**, 1, 78-89 (1989).

Laurent, A. and J. C. Charpentier, "Aires Interfaciales et Coefficients de Transfert de Matiere dans les Divers Types D' Absorbeurs et de Reacteurs Gaz-Liquide", Chem. Eng. J., **8**, 85-101 (1974).

Leighton, D. T. Jr. and J. M. Calo, "Distribution Coefficients of Chlorinated Hydrocarbons in Dilute Air-Water Systems for Groundwater Contamination Applications", J. Chem. Eng. Data, Amer. Chem. Society, **26**, 4, 382-385 (1981).

Lévéque, J. A., "Les Lois de la Transmission de Chaleur par Convection", Annales de Mines, **12** (13-14), pp. 201- (1928).

Lipski, C. and P. Côté, "The Use of Pervaporation for the Removal of Organic Contaminants from Water", Environ. Prog., **9**, 254-261(1990).

Mackay, D. and W. Y. Shiu, "A Critical Review of Henry's Law Constants for Chemicals of Environmental Interest", J. Phys. Chem. Ref. Data, **10**, 4, 1175-1198 (1981).

Mackay, D., W. Y. Shiu and R. P. Sutherland, "Determination of Air-Water Henry's Law Constants for Hydrophobic Pollutants", Environ. Sci. Technol., **13**, 3, 333-337 (1979).

Mahmud, H., A. Kumar, R. M. Narbaitz and T. Matsuura, "A Study of Mass Transfer in the Membrane Air-Stripping Process Using Microporous Polypropylene Hollow Fibers", J. Membr. Sci., **179**, 1-2, 29-41. (2000).

Mahmud, H., A. Kumar, R. M. Narbaitz and T. Matsuura, "Hollow Fiber Membrane Air Stripping: A Process for Removal of Organics from Aqueous Solutions", Sep. Sci. Technol., **33**, 14, 2241-2255 (1998).

Malek, A., K. Li and W.K. Teo, "Modeling of Microporous Hollow Fiber Membrane Modules Operated under Partially Wetted Conditions", Ind. Eng. Chem. Res., **36**, 784-793 (1997).

Matson, S. L., "Method and System for Removing Radon from Radon Containing Water", U. S. Patent 510055 (1992).

Matson, S. L., J. Lopez and J. A. Quinn, "Separation of Gases with Synthetic Membranes", Chem. Eng. Sci., **38**, 503-524 (1983).

Matsuura, T., "Synthetic Membranes and Membrane Separation Processes", CRC Press, Boca Raton, FL, USA (1993).

McGregor, F. R., P. J. Piscaer and E. M. Aieta, "Economics of Treating Waste Gases from an Air Stripping Tower Using Photochemically Generated Ozone", Ozone Sci. & Eng., **10**, 339-352 (1988).

Meylan W. M. and P. H. Howard, " Bond Contribution Method for Estimating Henry's Law Constant", Environ. Toxicol. Chem., **10**, 1283-1293 (1991).

Munz, C. and P. V. Roberts, "Transfer of Volatile Organic Contaminants into a Gas Phase during Bubble Aeration", Technical Report No. 262, Department of Civil Engineering, Stanford University, Stanford, CA, USA (1982).

Nirmalakhandan, N. and R. E. Speece, "QSAR Model for Predicting Henry's Law Constant", Environ. Sci. Technol., **22**, 1349-1361 (1988).

Nirmalakhandan, N., R. A. Brennan and R. E. Speece, "Predicting Henry's Law Constant and the Effect of Temperature on Henry's Law Constant", Wat. Res., **31**, 6, 1471-1481 (1997).

Norris, R. H., M. Y. Schenectady and D. D. Streid, "Laminar-Flow Heat-Transfer Coefficents for Ducts", ASME Trans., **62**, 525-533 (1940).

Onda, K., H. Takeuchi and Y. Okumoto, "Mass Transfer Coefficients Between Gas and Liquid Phase in Packed Columns", J. Chem. Eng. Japan, **1**, 56-62 (1968).

Peters, M. S. and K. D. Timmerhaus, "Plant Design and Economics for Chemical Engineers", 3rd. Edition, McGraw-Hill Book Company, New York, NY, USA (1980).

Prasad, R. and K.K. Sirkar, "Dispersion-Free Solvent Extraction with Microporous Hollow-Fiber Modules", AIChE J., **34**, 2, 177-187 (1988).

Prasad, R. and K.K. Sirkar, "Hollow-Fiber Solvent Extraction: Performance and Design", J. Membr. Sci., **50**, 153-175 (1990).

Pollard, W. G. and R. D. Present, "On Gaseous Self-Diffusion in Long Capillary Tubes", Phys. Rev., **73**, 7, 762-774 (1948).

Qi, Z. and E. L. Cussler, "Microporous Hollow Fibers for Gas Absorption. I Mass Transfer in the Liquid", J. Membr. Sci., **23**, 321- 332 (1985a).

Qi, Z. and E. L. Cussler, "Microporous Hollow Fibers for Gas Absorption. II Mass Transfer Across the Membrane", J. Membr. Sci., **23**, 333- 345 (1985b).

Qi, Z. and E. L. Cussler, "Hollow Fibers Gas Membranes", AIChE J., **31**, 9, 1548-1553 (1985c).

Reed, B. W., M. J. Semmens and E. L. Cussler, "Membrane Contactors", in "Membrane Separations Technology, Principles and Applications", R. D. Noble and S. A. Stern, Eds., Elsevier Science Publishers, New York, NY, USA (1995) , pp. 143-211.

Robbins, G. A., S. Wang and J. D. Stuart, " Using Headspace Method to Determine Henry's Law Conatants", Anal. Chem., **65**, 3113-3118 (1993).

Roberts, P. V. and P. G. Dändliker, "Mass Transfer of Volatile Organic Contaminants from Aqueous Solution to the Atmosphere during Surface Aeration", Environ. Sci. Technol., **17**, 8, 484-489 (1983).

Roberts, P. V. and J. A. Levy, "Energy Requirements for Air Stripping Trihalomethanes", J. Am. Water Works Assoc., **77**, 4, 138-146 (1985).

Roberts, P. V., G. D. Hopkins, C. Munz and A. H. Riojas, "Evaluation Two-Resistance Models for Air Stripping of Volatile Organic Contaminants in a Countercurrent Packed-Column", Environ. Sci. and Technol., **19**, 2, 164-173 (1985).

Russell C. J., S. L. Dixon and P. C. Jurs, "Computer-Assisted Study of the Relationship Between Molecular Structure and Henry's Law Constant", Anal. Chem., **64**, 1350-1355 (1992).

Rutledge, F., (1990). Personal communication with Schwarz et. al. (1991).

Sanemasa, I., M. Araki, T. Deguchi and H. Nagai, "Solubility Measurements of Benzene and the Alkylbenzenes in Water by Making Use of Solute Vapor", Bull. Chem. Soc. Japan, **55**, 4, 1054, (1982).

Schöner, P., P. Plucinski, W. Nitsch and U. Daiminger, "Mass Transfer in the Shell Side of Cross Flow Hollow Fiber Modules", Chem. Eng. Sci., **53**, 13, 2319-2326 (1998).

Schwarz, S. E., M. J. Semmens and K. J. Froelich, "Membrane Air Stripping: Operating Problems and Cost Analysis", in "45th Purdue Industrial Waste Conference Proceedings", Lewis Publishers, Inc., Chelsea, MI, USA (1991), pp. 547-556.

Semmens, M. J., R. Qin and A. Zander, "Using a Microporous Hollow-Fiber Membrane to Separate VOCs from Water", J. Am. Water Works Assoc., **81**, 4, 162-167 (1989).

Sengupta, A., P. A. Peterson, B. D. Miller, J. Schneider and C. W. Fulk, Jr., "Large-Scale Application of Membrane Contactors for Gas Transfer from or to Ultrapure Water", Sep. Purif. Technol., **14**, 189-200, (1998).

Sherwood, T. K., R. L. Pigford and C. R. Wilke, "Mass Transfer", McGraw-Hill, Inc., New York, NY, USA (1975).

Sieder, E. N. and G. E. Tate, "Heat Transfer and Pressure Drop of Liquids in Tubes", Ind. Eng. Chem., **28**, 12, 1429-1435 (1936).

Singley, J. E., A. L. Ervin, M. A. Mangone, J. M. Allan and H. H. Land, "Trace Organics Removal by Air Stripping", Am. Water Works Assoc., Rept. ESE No. 79-227-001, Denver, CO, USA (1980).

Sirkar, K. K., "Other New Membrane Processes", in "Membrane Handbook", Ho., W. S. Winston, Sirkar, K. K., Eds., Van Nostrand Reinhold, New York, NY(1992), pp. 885-899.

Smith, J. H., D. C. Bomberger and D. L. Haynes, "Prediction of the Volatilization Rates of High-Volatility Chemicals from Natural Water Bodies", Environ. Sci. Technol., **14**, 11, 1332-1337 (1980).

Tirmizi, N. P., B. Raghuraman, and J. Wiencek, "Demulsification of Water/Oil/Solid Emulsions by Hollow-Fiber Membranes", AIChE J., **42**, 5, 1263-1275 (1996).

Treybal, R. E., "Mass-Transfer Operations", 3rd Edition, McGraw-Hill Book Company, New York, NY, USA (1980).

Turner, L. H., Y. C. Chiew, R. C. Ahlert and D. S. Kosson, "Measuring Vapor-Liquid Equilibrium for Aqueous Organic Systems: Review and a New Technique", AIChE J., **42**, 6, 1772-1788 (1996).

Wang, K. L. and E. L. Cussler, "Baffled Membrane Modules Made with Hollow Fiber Fabric", J. Membr. Sci., **85**, 265-278 (1993).

Whisnant, J. T., Sales Representative, Hoechst Celanese, Personal Communication, 1999

Wickramasinghe, S. R., M. J. Semmens and E. L. Cussler, "Mass Transfer in Various Hollow Fiber Geometries", J. Membr. Sci., **69**, 235-250 (1992).

Wilke, C. R. and P. Chang, " Correlation of Diffusion Coefficients in Dilute Solutions", AIChE J., **1**, 2, 264-270 (1955).

USEPA, Fact Sheet, Drinking Water Regulations Under the Safe Drinking Water Act, USEPA, Office of Drinking Water, Washington, DC, USA (1990).

Yang, M. C. and E. L. Cussler, "Designing Hollow-Fiber Contactors", AIChE J., **32**, 11, 1910-1916 (1986).

Zander, A. K., M. J. Semmens and R. M. Narbaitz, "Removing VOCs by Membrane Stripping", J. Am. Water Works Assoc., **81**, 11, 76-81 (1989a).

Zander, A. K., R. Qin and Semmens, M. J. "Membrane/Oil Stripping of VOCs from Water in Hollow-Fiber Contactor", J. Environ. Eng., **115**, 4, 768-784 (1989b).

Zisman, W. A., "Relation of the Equilibrium Contact Angle to Liquid and Solid Constitution", Adv. Chem. Ser., **43**, 1, (1964).

APPENDIX – A

GC (PURGE AND TRAP) CALIBRATION

The standard solution was prepared in a teflon bag. The mixing in the bag was provided by magnetic stirrer. The empty weight (bag + stirring bar) was determined. The bag was filled with water and the quantity of water was determined from the difference in the total weight (bag + stirring bar + water) and the empty weight. Chloroform was measured by a 10 µl micro syringe and injected into the bag via septa. The solution was mixed for six hours and kept in a refrigerator at about 5°C. Table A1 shows the calculation of the chloroform stock solution's concentration.

Table A1. Preparation of chloroform stock solution

T. bag + st. bar	=	32.3866	g
T. bag + st. bar + water	=	893.13	g
water	=	860.7434	g
Target $CHCL_3$ conc.	=	10	ppm
Mass of $CHCl_3$ needed	=	8.607434	mg
Volume of $CHCl_3$ needed	=	5.815834	µl
Volume of $CHCl_3$ added	=	6	µl
Calculated $CHCl_3$ conc.	=	10.31666	ppm

Samples of this stock solution, which had chloroform concentration of 10.32 ppm were diluted in vials to prepare different concentration standards as shown in Table A2. Gas tight syringes [Hamilton Co., Reno, NV] and a 30 ml hypodermic syringe [Becton Dickinson and Company, Franklin Lakes, NJ] were used to transfer samples of stock solution into the vials. The solution was mixed for an hour using a magnetic stirrer and

kept in a refrigerator at about 5°C until analysis. The concentrations in the vials were calculated using eqn. A1.

$$Chl.conc. = \frac{W_{SS} * C_{ss} + W_{wat} * C_{wat}}{W_{SS} + W_{wat}} \quad \text{(A1)}$$

Where:
W_{ss} = weight of stock solution, g
C_{ss} = conc. of stock solution, ppm
W_{wat} = weight of water
C_{wat} = conc. of water, 0 ppm

Table A2. Chloroform standards and the GC (P&T) area

	Weight A[1]	Weight B[2]	Water[3]	Total[4]	Stock Solution[5]	$CHCl_3$ conc.	GC area	GC area
	g	G	G	g	g	ppm	µVolts.s	Volts.s
Direct						10.31666	45523673	45.52
Direct						10.31666	46578439	46.58
Direct						10.31666	47325371	47.33
Vial 1	44.934	53.845	8.911	82.517	28.672	7.870563	33234175	33.23
Vial 2	44.9402	55.7696	10.8294	82.5798	26.8102	7.348426	33023426	33.02
Vial 3	44.7097	58.5946	13.8849	82.5835	23.9889	6.534475	28442845	28.44
Vial 4	46.1887	62.7764	16.5877	83.5326	20.7562	5.734129	26012743	26.01
Vial 5	45.5313	64.3334	18.8021	82.3768	18.0434	5.052115	21573420	21.57
Vial 6	44.9487	65.4472	20.4985	82.7132	17.266	4.716798	22092341	22.09
Vial 7	45.0452	67.4529	22.4077	82.7642	15.3113	4.18785	18987569	18.99
Vial 8	45.5639	69.4382	23.8743	83.3426	13.9044	3.797034	18270544	18.27
Vial 9	44.9764	70.8821	25.9057	82.6438	11.7617	3.221393	14098755	14.10
Vial 10	45.1653	72.9658	27.8005	82.8732	9.9074	2.710607	11239674	11.24
Vial 11	45.0458	74.5693	29.5235	83.0472	8.4779	2.30159	10097653	10.10
Vial 12	44.9824	78.8471	33.8647	82.6485	3.8014	1.041195	4075430	4.08
Vial 13	44.9436	80.8254	35.8818	82.5341	1.7087	0.46895	2007615	2.01

[1] Weight A = Vial + cap + septa + st. bar
[2] Weight B = Weight A + Water
[3] Water = Weight B – Weight A
[4] Total = Weight B + Std. Solution
[5] Std. Solution = Total – Weight B

The analysis was conducted on the same day. The standard solutions with different concentrations and the corresponding GC (P&T) responses are given in Table A2 and the

calibration curve is shown in Fig A1. The summary of the linear regression statistics is given in Table A3.

Table A3. Summary of the linear regression statistics

Regression Statistics						
Multiple R	0.9981709					
R Square	0.9963451					
Adjusted R Square	0.996084					
Standard Error	0.2000708					
Observations	16					
ANOVA						
	df	*SS*	*MS*	*F*	*Significance F*	
Regression	1	152.7658865	152.7659	3816.443	1.828E-18	
Residual	14	0.560396762	0.040028			
Total	15	153.3262832				
	Coefficients	*Standard Error*	*t Stat*	*P-value*	*Lower 95%*	*Upper 95%*
Intercept	0.071178	0.09930448	0.716765	0.485306	-0.1418091	0.284165
X Variable 1	0.2216411	0.00358774	61.77737	1.83E-18	0.2139462	0.229336

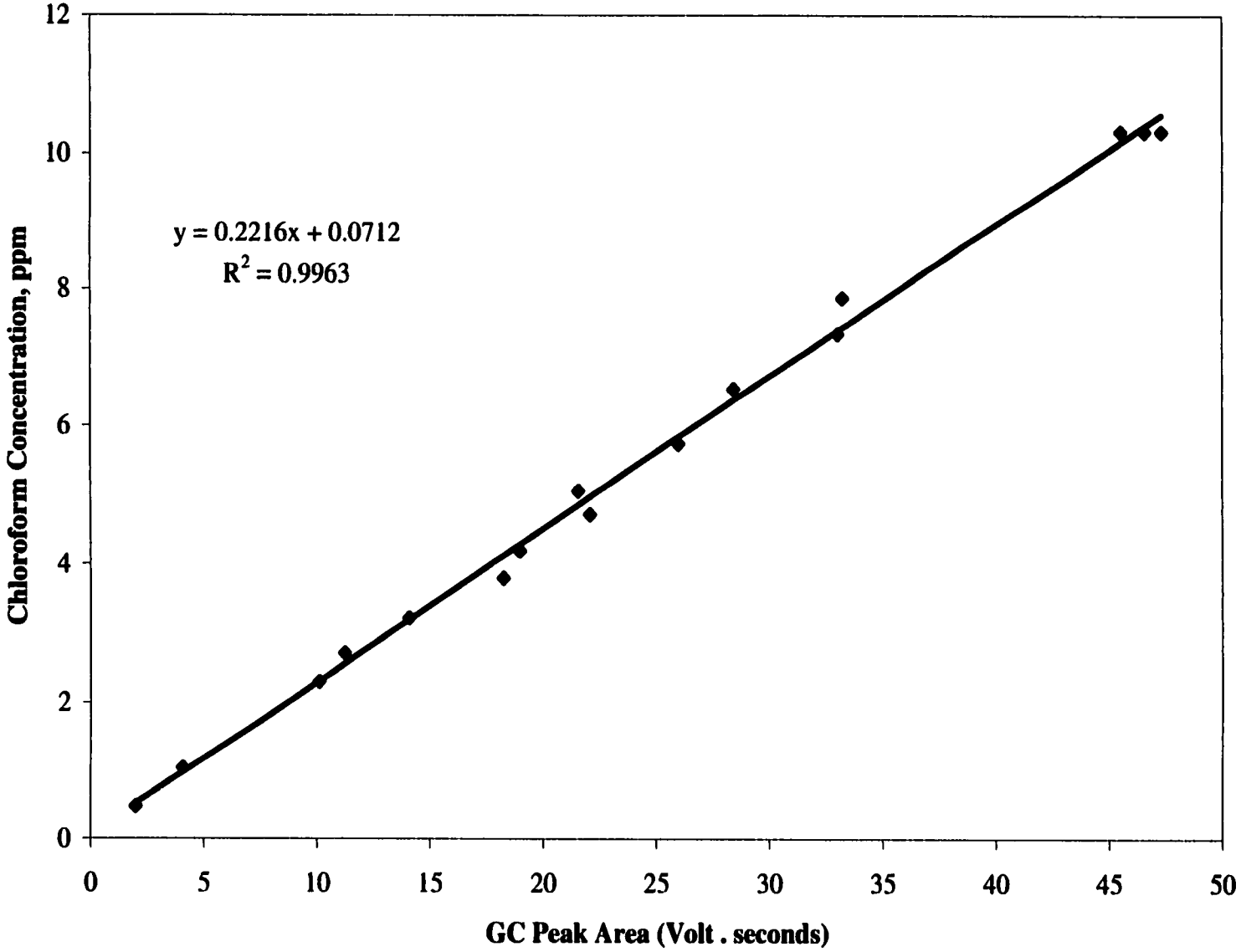

Figure A1 Gas Chromatograph (Purge & Trap) Calibration Curve for Chloroform

APPENDIX - B

GC6890 CALIBRATION

The calibration was done preparing binary standard solutions of chloroform and toluene in vials and n-pentane was used as solvent. The weight of n-pentane was determined by weighing the vials including cap, septa and stirring bar before and after the addition of n-pentane. VOCs were measured using 10, 50 and 100 µl micro syringes [Hamilton Co., Reno, NV] and injected into the vials through the septa. The volumes of VOCs were then converted to weights for calculations. Two stock solutions of different sizes were prepared at different dates. Two stock solutions were prepared to compare and to evaluate error. The stock solutions were mixed using a magnetic stirrer for 4 h. After the mixing, stock solutions were transferred without dilution into 2ml GC vials. At the same time, stock solutions were diluted into 2ml GC vials as given in Table B1. For transfer and dilution, adjustable micro pipettors were used for n-pentane measurements as well as for measurements of standard solution above 500 µl and 50, 100 and 500 µl micro syringes [Hamilton Co., Reno, NV] were used for measurements of standard solution below 500 µl. The concentrations of the VOCs in the standard solutions and the GC responses are given in Table B1 and shown in Fig. B1.

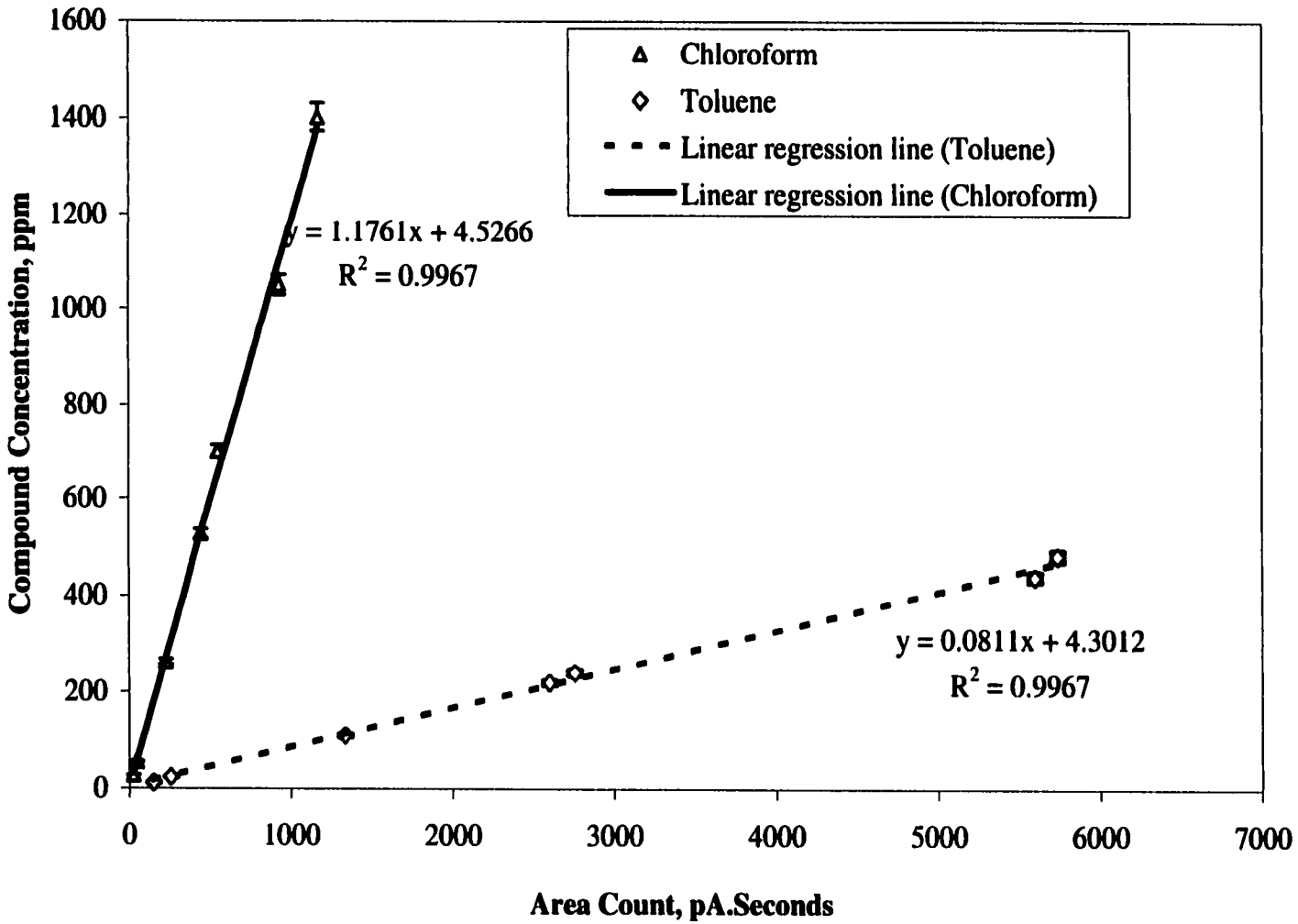

Figure B1 GC6890 Calibration for Toluene and Chloroform Extraxted in n-Pentane

Table B1. Data from GC6890 calibration in n-pentane

Std. Solution ID	Std. Solution Microliter	n-pentane Microliter	$CHCl_3$ Conc ppm	GC Area pA.s[1,2]	C_7H_8 Conc ppm	GC Area pA.s[1,2]
A1	Full	nil	1401.37	1169.93	480.67	5737.13
A2	950.00	950.00	700.68	551.71	240.34	2755.65
B1	Full	nil	1049.71	931.07	439.08	5596.46
B2	950.00	950.00	524.85	446.08	219.54	2598.17
B3	475.00	1426.00	262.29	227.16	109.71	1335.04
B4	100.00	1800.00	55.25	44.02	23.11	255.74
B5	50.00	1850.00	27.62	22.75	11.55	147.60

[1]pico Ampere*second
[2]Average of three injections. Error 2%.

The summary of the linear regression statistics for chloroform and toluene are given in Table B2 and Table B3, respectively.

Table B2. Summary of the linear regression statistics for chloroform

Regression Statistics	
Multiple R	0.998342861
R Square	0.996688469
Adjusted R Square	0.996026163
Standard Error	32.49272852
Observations	7

ANOVA

	df	*SS*	*MS*	*F*	*Significance F*
Regression	1	1588813.6	1588813.6	1504.8755	2.14519E-07
Residual	5	5278.88703	1055.7774		
Total	6	1594092.49			

	Coefficients	*Standard Error*	*t Stat*	*P-value*	*Lower 95%*	*Upper 95%*
Intercept	4.526634388	19.1502845	0.2363743	0.8225203	-44.70065878	53.7539
X Variable 1	1.176074235	0.03031688	38.792725	2.145E-07	1.098142353	1.25401

Table B3. Summary of the linear regression statistics for toluene

Regression Statistics	
Multiple R	0.998338731
R Square	0.996680223
Adjusted R Square	0.996016267
Standard Error	11.82780817
Observations	7

ANOVA

	df	*SS*	*MS*	*F*	*Significance F*
Regression	1	210002.9626	210002.96	1501.1251	2.15857E-07
Residual	5	699.4852308	139.89705		
Total	6	210702.4478			

	Coefficients	*Standard Error*	*t Stat*	*P-value*	*Lower 95%*	*Upper 95%*
Intercept	4.301166885	7.094109255	0.6063012	0.5707852	-13.93479171	22.53712
X Variable 1	0.081076684	0.002092606	38.744355	2.159E-07	0.075697477	0.08645

APPENDIX - C

EFFECT OF HEADSPACE

As stated in the experimental section, these tests were carried out to determine the magnitude of the transfer of chloroform from the liquid phase into the air phase in the headspace of the reservoir. Results of these tests are presented in the following Table C1.

Table C1. Results from the effect of headspace tests

Levels	V_L $m^3 \times 10^3$	Headspace $m^3 \times 10^3$	Ccal ppm	Cmeas ppm	Difference ppm	Difference %	Difference -error[1]
D	6.675	0.000	1006.27	993.21	13.06	1.30	0.01
D	6.675	0.000	1002.02	989.12	12.90	1.29	0.00
C	6.000	0.675	745.99	715.31	30.68	4.11	2.82
C	6.000	0.675	760.44	717.23	43.21	5.68	4.39
B	5.000	1.675	753.66	695.42	58.24	7.73	6.44
B	5.000	1.675	749.41	699.54	49.87	6.65	5.36
A	4.000	2.675	745.56	662.50	83.06	11.14	9.85
A	4.000	2.675	746.74	656.73	90.01	12.05	10.76

[1]When the reservoir was completely filled with water, the difference between the calculated and the measured value might be experimental error or adsorption on the container. So, this value is deducted from all the values to take into account the error.

It was observed that the volume of headspace had a significant effect on amount of chloroform transferred from the liquid phase to air phase. The degree of this transfer varied with the volume of headspace. The total reduction in chloroform concentrations of the solution varied from 4.11% at solution level C to 12.05 % at solution level A. At level D, the difference between calculated and measured concentrations were about 1%, which might be due to analytical errors or adsorption and this difference was subtracted from all the values. Thus, the loss of chloroform due to partitioning into the headspace varied

from 2.82% at solution level C to 10.76% at solution level A. The transfer of chloroform to the headspace would lead to an erroneous result in the membrane transport calculation. Therefore, the level D should be maintained during the air-stripping experiments.

APPENDIX - D

REVERSE STRIPPING TESTS

The results from the reverse stripping tests are given are presented in table below. The TC concentration in the reservoir did not change much during the test. The changes observed were with in limit of error of the TOC analyzer. It was concluded that reverse stripping did not occur during the test.

Change of TC Concentration in Reservoir during Reverse Stripping Tests

Time, min	1st. Test, ppm TC	2nd. Test, ppm TC
R.O	0.45	0.41
0	0.52	0.53
10	0.51	0.51
20	0.51	0.55
30	0.54	0.56
40	0.52	0.51
50	0.50	0.52
60	0.53	0.49
80	0.55	0.56
100	0.51	0.53
120	0.53	0.50
140	0.50	0.53

APPENDIX - E

Numerical X_L^w Values from Water Tests (Preliminary Experiments)

Data from preliminary water tests with and without controlling membranes contact period with water at water and air flow rates of 6.33 x 10^{-5} m^3/s and 3.33 x 10^{-5} m^3/s, respectively at 21°C.

Contact period not controlled		Contact period controlled			
Samples[1]		Period	Continuous[2]	Time to time[3]	After 48 h[4]
	X_L^w, ppm	h	X_L^w, ppm	X_L^w, ppm	X_L^w, ppm
1	15946.43	0.50		15213.71	
2	9998.61	1.50	15276.85		
3	10689.70	2.50	15239.38		
4	9684.29	3.80	15265.06		
5	10897.17	4.00		15013.18	
6	10657.09	5.33	15043.02		
7	10263.88	6.00		14919.51	
8	10480.85	9.50		14068.14	
9	16420.34	9.90	14744.66		
10	15052.73	11.45	14592.01		
11	14542.74	11.50		13863.45	
12	11219.82	14.00	13738.55		
13	11087.98	24.33	12524.29		
15	12647.79	25.50	12822.65		
16	10872.88	26.50	12569.39		
17	11872.82	27.50	12669.30		
18	12038.58	29.00		12599.92	
19	11205.94	29.50	12674.85		
20	15611.99	31.00		12638.77	
21	14932.00	33.00	12572.16		
22	14696.09	38.50	12613.10		
		45.50		12497.22	
		48.50			12568.69
		49.50	12557.59		
		50.00			12574.94
		51.00		12592.98	
		52.00			12596.45
		52.50	12683.87		
		57.50	12549.96		
		59.00		12615.88	
		70.00	12548.57	12574.24	

[1] Random sampling.

[2] X_L^w values from experiment with continuous air flow from the start of the test.

[3] X_L^w values from experiment without continuous air flow from the starting of the test. The air flow was resumed time to time.

[4] X_L^w values from experiment, in which air flow was started after 48 hours of the membrane/water contact.

APPENDIX – F

Numerical X_L^w Values from Water Tests (Dry)

Water flow rate	Air flow rate	Air velocity	X_L^w
m^3/s	m^3/s	m/s	ppm
6.33E-05	1.67E-05	3.68E-02	15228
6.33E-05	1.67E-05	3.68E-02	15223
6.33E-05	1.67E-05	3.68E-02	15140
6.33E-05	3.33E-05	7.37E-02	14752
6.33E-05	3.33E-05	7.37E-02	14849
6.33E-05	3.33E-05	7.37E-02	14564
6.33E-05	5.00E-05	1.11E-01	14127
6.33E-05	5.00E-05	1.11E-01	14127
6.33E-05	5.00E-05	1.11E-01	14331
6.33E-05	5.00E-05	1.11E-01	14960
6.33E-05	5.00E-05	1.11E-01	13628
6.33E-05	5.00E-05	1.11E-01	13988
6.33E-05	5.00E-05	1.11E-01	13896
6.33E-05	5.00E-05	1.11E-01	13942

APPENDIX – G

Numerical X_L^w Values from Water Tests (Wet)

Water flow rates	Air flow rates	X_L^w
m^3/s	m^3/s	Ppm
6.33E-05	1.75E-05	13988
6.33E-05	1.75E-05	13590
6.33E-05	1.75E-05	13230
6.33E-05	1.75E-05	13283
6.33E-05	1.83E-05	13095
6.33E-05	2.50E-05	12587
6.33E-05	2.50E-05	12717
6.33E-05	2.50E-05	12508
6.33E-05	2.50E-05	12512
6.33E-05	2.55E-05	12517
6.33E-05	3.33E-05	11927
6.33E-05	3.33E-05	11895
6.33E-05	3.33E-05	12018
6.33E-05	3.33E-05	11990
6.33E-05	4.17E-05	11168
6.33E-05	4.17E-05	11202
6.33E-05	4.17E-05	11202
6.33E-05	5.00E-05	10103
6.33E-05	5.00E-05	11707
6.33E-05	5.00E-05	11379
6.33E-05	5.00E-05	11972

APPENDIX – H

Observed k and K_L Values Obtained from MAS of Chloroform (Dry Tests)

Q_w	u^w	Q_a	v^a	$CHCl_3$ conc	k	R^2	$R=Q_w/(Q_a.H)$	K_L
m^3/s	m/s	m^3/s	m/s	ppm	min^{-1}			m/s
3.3E-05	5.95E-03	8.33E-05	0.185	707	0.1030	0.9956	2.65	1.63E-05
3.3E-05	5.95E-03	8.33E-05	0.185	705	0.1025	0.9945	2.65	1.59E-05
3.3E-05	5.95E-03	8.33E-05	0.185	701	0.1062	0.9969	2.65	1.92E-05
3.3E-05	5.95E-03	8.33E-05	0.185	700	0.0991	0.9990	2.65	1.38E-05
3.3E-05	5.95E-03	7.50E-05	0.167	650	0.0922	0.9961	2.94	1.38E-05
3.3E-05	5.95E-03	7.50E-05	0.167	683	0.0925	0.9946	2.94	1.40E-05
3.3E-05	5.95E-03	7.50E-05	0.167	693	0.0930	0.9986	2.94	1.44E-05
3.3E-05	5.95E-03	5.00E-05	0.111	678	0.0648	0.9999	4.41	1.12E-05
3.3E-05	5.95E-03	5.00E-05	0.111	701	0.0638	0.9963	4.41	1.01E-05
3.3E-05	5.95E-03	3.33E-05	0.074	669	0.0446	0.9904	6.61	9.66E-06
3.3E-05	5.95E-03	3.33E-05	0.074	695	0.0441	0.9982	6.61	8.37E-06

Observed k and K_L Values Obtained from MAS of Chloroform (Wet Tests)

Q_w	u^w	Q_a	v^a	$CHCl_3$ conc	k	R^2	$R=Q_w/(Q_a.H)$	K_L
m^3/s	m/s	m^3/s	m/s	ppm	min^{-1}			m/s
3.3E-05	5.95E-03	7.50E-05	0.167	710	0.0809	0.9981	2.93945	8.82E-06
3.3E-05	5.95E-03	7.50E-05	0.167	708	0.0778	0.9980	2.93945	7.96E-06
3.3E-05	5.95E-03	7.50E-05	0.167	705	0.0804	0.9954	2.93945	8.67E-06
3.3E-05	5.95E-03	5.83E-05	0.130	689	0.0653	0.9942	3.77929	7.26E-06
3.3E-05	5.95E-03	5.83E-05	0.130	701	0.0645	0.9978	3.77929	7.00E-06
3.3E-05	5.95E-03	5.83E-05	0.130	682	0.0632	0.9902	3.77929	6.62E-06
3.3E-05	5.95E-03	5.83E-05	0.130	682	0.0627	0.9936	3.77929	6.48E-06
3.3E-05	5.95E-03	5.00E-05	0.111	698	0.0564	0.9974	4.40917	6.21E-06
3.3E-05	5.95E-03	5.00E-05	0.111	704	0.0569	0.9984	4.40917	6.38E-06
3.3E-05	5.95E-03	5.00E-05	0.111	681	0.0574	0.9996	4.40917	6.55E-06
3.3E-05	5.95E-03	5.00E-05	0.111	704	0.0570	0.9986	4.40917	6.41E-06
3.3E-05	5.95E-03	3.33E-05	0.074	709	0.0410	0.9926	6.61376	5.32E-06
3.3E-05	5.95E-03	3.33E-05	0.074	693	0.0405	0.9962	6.61376	5.06E-06

APPENDIX – J

Observed k and K_L Values Obtained from MAS of Toluene

Q_w	u^w	Q_a	v^a	C_7H_8 conc.	k	R^2	$R=Q_w/(Q_a.H)$	K_L
m^3/s	m/s	m^3/s	m/s	ppm	min^{-1}			m/s
3.33E-05	5.95E-03	7.50E-05	0.167	183	0.0666	0.9981	1.928	4.50E-06
3.33E-05	5.95E-03	7.50E-05	0.167	162	0.0619	0.996	1.928	4.04E-06
3.33E-05	5.95E-03	6.67E-05	0.148	165	0.0581	0.9988	2.169	3.82E-06
3.33E-05	5.95E-03	6.67E-05	0.148	186	0.0589	0.9902	2.169	3.90E-06
3.33E-05	5.95E-03	6.67E-05	0.148	153	0.0571	0.9994	2.169	3.73E-06
3.33E-05	5.95E-03	5.83E-05	0.130	166	0.0558	0.9967	2.479	3.78E-06
3.33E-05	5.95E-03	5.83E-05	0.130	143	0.0538	0.9998	2.479	3.58E-06
3.33E-05	5.95E-03	5.83E-05	0.130	162	0.0554	0.9985	2.479	3.74E-06
3.33E-05	5.95E-03	5.00E-05	0.111	170	0.0499	0.9989	2.892	3.40E-06
3.33E-05	5.95E-03	5.00E-05	0.111	148	0.0465	0.9985	2.892	3.06E-06
3.33E-05	5.95E-03	5.00E-05	0.111	196	0.0484	0.9999	2.892	3.24E-06
3.33E-05	5.95E-03	4.17E-05	0.093	181	0.0408	0.9999	3.471	2.70E-06
3.33E-05	5.95E-03	4.17E-05	0.093	164	0.0409	0.9992	3.471	2.71E-06
3.33E-05	5.95E-03	4.17E-05	0.093	169	0.0417	0.9991	3.471	2.79E-06
3.33E-05	5.95E-03	3.33E-05	0.074	172	0.0353	0.9998	4.338	2.39E-06
3.33E-05	5.95E-03	3.33E-05	0.074	147	0.0349	0.9992	4.338	2.35E-06
3.33E-05	5.95E-03	3.33E-05	0.074	179	0.0365	0.9991	4.338	2.52E-06

APPENDIX – K

Observed k and K_L Values Obtained from MAS of Chloroform from Mixture of Chloroform/Toluene

Q_w	u^w	Q_a	v^a	$CHCl_3$ conc.	k	R^2	$R=Q_w/(Q_a.H)$	K_L
m^3/s	m/s	m^3/s	m/s	ppm	min^{-1}			m/s
3.33E-05	5.95E-03	6.67E-05	0.148	1520	0.0650	0.9968	3.307	5.98E-06
3.33E-05	5.95E-03	6.67E-05	0.148	907	0.0645	0.9986	3.307	5.88E-06
3.33E-05	5.95E-03	6.67E-05	0.148	931	0.0659	0.9991	3.307	6.17E-06
3.33E-05	5.95E-03	5.83E-05	0.130	1068	0.0557	0.9993	3.779	4.90E-06
3.33E-05	5.95E-03	5.83E-05	0.130	952	0.0556	0.9994	3.779	4.89E-06
3.33E-05	5.95E-03	5.83E-05	0.130	764	0.0550	0.9975	3.779	4.78E-06
3.33E-05	5.95E-03	5.00E-05	0.111	797	0.0520	0.9955	4.409	5.00E-06
3.33E-05	5.95E-03	5.00E-05	0.111	921	0.0493	0.9964	4.409	4.42E-06
3.33E-05	5.95E-03	5.00E-05	0.111	930	0.0524	0.9959	4.409	5.09E-06
3.33E-05	5.95E-03	3.33E-05	0.074	965	0.0358	0.9993	6.614	3.46E-06
3.33E-05	5.95E-03	3.33E-05	0.074	1036	0.0361	0.999	6.614	3.53E-06
3.33E-05	5.95E-03	3.33E-05	0.074	1206	0.0359	0.9903	6.614	3.48E-06

APPENDIX - L

Observed k and K_L Values Obtained from MAS of Toluene from Mixture of Chloroform/Toluene

Q_w	u^w	Q_a	v^a	C_7H_8 conc.	k	R^2	$R=Q_w/(Q_a.H)$	K_L
m^3/s	m/s	m^3/s	m/s	ppm	min^{-1}			m/s
3.33E-05	5.95E-03	6.67E-05	0.148	221	0.0638	0.9997	2.169	4.40E-06
3.33E-05	5.95E-03	6.67E-05	0.148	202	0.061	0.9985	2.169	4.11E-06
3.33E-05	5.95E-03	6.67E-05	0.148	212	0.0624	0.9993	2.169	4.26E-06
3.33E-05	5.95E-03	5.83E-05	0.130	192	0.0488	0.9986	2.479	3.11E-06
3.33E-05	5.95E-03	5.83E-05	0.130	179	0.0528	0.9971	2.479	3.48E-06
3.33E-05	5.95E-03	5.83E-05	0.130	194	0.0547	0.9991	2.479	3.67E-06
3.33E-05	5.95E-03	5.00E-05	0.111	159	0.0511	0.9907	2.892	3.53E-06
3.33E-05	5.95E-03	5.00E-05	0.111	159	0.0485	0.999	2.892	3.25E-06
3.33E-05	5.95E-03	5.00E-05	0.111	167	0.0472	0.9951	2.892	3.12E-06
3.33E-05	5.95E-03	3.33E-05	0.074	195	0.0361	0.9977	4.338	2.48E-06
3.33E-05	5.95E-03	3.33E-05	0.074	185	0.0372	0.9997	4.338	2.60E-06
3.33E-05	5.95E-03	3.33E-05	0.074	175	0.037	0.9937	4.338	2.58E-06